AMBIENT ENERGY MATRIX ISOLATION SPECTROSCOPY

A Molecular Study of p-Toluenesulfonic Acid Solvation

A Senior Honors Thesis

submitted by

Thien Khuu

With Computations Contributed by

David J. Anick, M.D./Ph. D

Advisor: Professor Mary Jane Shultz, Ph. D

April 30, 2018

Shultz Laboratory for Aqueous and Surface Studies

Tufts University, Pearson Building, Medford, MA 02155, United States

Contents

Acknowledgements

I would first like to thank my Advisor Prof. Mary Shultz for her patience and “bravery” in giving me an opportunity to do research with her. It takes courage to let a freshman undergraduate with only two classes of general chemistry in charge of expensive equipment and chemicals. Mary, from your trust and encouragement, I was able to grow more independent as a scientist, recognize my potential, and be more confident in myself. Thank you for teaching me so much about chemistry and spectroscopy, your advice were invaluable.

I would also like to thank the rest of my committee members, Dr. David Anick and Prof. Jonathan Kenny. David, this project would not have gotten where it is now without your computational expertise. What perfect timing that we met! You have taught me so much about computational chemistry and given me lots of advice about graduate school and science in general. I love talking about science with you, so thank you! Jon, you have not only taught me the principles of quantum mechanics, but about how to become a better teacher as well. Your innovative teaching methods inspire me and will continue to do so in my future careers. I enjoyed our occasional lunches where we shared our interests in chemistry, literature, and personal life. I never thought I could be friends with my professor, but you proved me wrong. For that, I thank you.

I also want to thank the graduate students and our post-doctoral fellow, Dr. Patrick Bisson, for making P-100 an on-campus home for me. I’ve always felt comfortable and welcomed every time I swiped my ID to enter the lab, knowing I will see familiar and friendly faces behind the door full of playful chemistry puns, puns only we would understand. Patrick,

you have taught me so much about experimental methods and fixed so many of my broken things. Thank you for always listening and always being there to help whenever I needed it.

I would like to offer a special thanks my boyfriend, Adam Zoll, a fellow chemist who shared many classes and unforgettable memories with me in Pearson Hall. We both share a deep love for chemistry, albeit in different sub-fields. We met when we were being trained in laboratory safety prior to our start in our undergraduate research career. Our first "movie" together was a badly-made lab safety video about how things could turn bad in the lab if one does not follow the safety protocol – a truly romantic experience! You have listened to too many of my rants about broken equipment, bad data, good data, and about my mess of a life in general. Thank you for always being there to listen. You have made my time here truly special.

Finally, I like to thank Tufts Summer Scholars for the financial support of this project; the Tufts Chemistry Department for hosting the project; and the front office secretaries, Debbie, Elizabeth, and Karen for making sure everything goes where it supposed to be.

Abstract

Clathrate hydrates are water cages that incase hydrophobic gases, such as methane and CO_2. They form under extreme conditions (pressure ranging from 9 to several thousand atm, and at cryogenic temperature). They occur naturally in the permafrost and on the continental shelf of the seabed (700 m) where the pressure is about 70 atm. Clathrates are estimated to contain a substantial amount of energy. Extraction of this energy is dangerous and not environmentally favorable, since clathrate hydrates are not stable without its guest gas and at lower pressure environment. Careless extractions could release all the trapped hydrocarbon at once, thus accelerate global warming. Nonetheless, they have the potential to be a good system for cleaning greenhouse gases such as CO_2 and as a gas storage and transfer media. To produce these gas hydrate cost-effectively, promoters, such as the hydrotrope pToluenesulfonic acid (pTSA), are used. The molecular mechanism of how promoters interact with water and the guest gas molecule is studied here using a method called Ambient Energy Matrix Isolation Spectroscopy, or AE-MIS.

AE-MIS uses carbon tetrachloride (CCl_4) matrix to simplify the water spectrum in the mid-IR region. The vibrational signatures of water in CCl_4 – the symmetric stretch, asymmetric stretch, and rotation about the symmetry axis – are present because water exists as monomers in CCl_4 with quenched rotation about the axes perpendicular to the symmetry axis. Monitoring and interpreting changes of these features when studying water interaction with other molecules can give a molecular insight to puzzling mechanisms of bigger systems. Herein, experimental spectra of small (pTSA)•$(H2O)_n$ clusters ($n \leq 10$) and large clusters ($n \geq 20$) are presented. Peak assignments and a proposed bimodal distribution model are aided by Density Functional Theory (DFT) calculations.

1. Introduction:

1.1 Motivation: Clathrate Hydrates

Clathrate hydrates are water cages that encapsulate hydrophobic gases, such as methane (CH_4) or carbon dioxide (CO_2), inside. Gas-hydrates deposits (GHDs) occur naturally at the continental shelf of the seabed and in the permafrost due to its extreme formation conditions. For example, methane hydrates are stable from 20 MPa to 2 GPa (~9-20,000 atm) at temperature 70 K to 350 K.[2] It was estimated by Kwenvolden[3] and Makogon[4] in 1988 that the amount of gas stored in clathrate hydrates contained twice the energy of fossil fuel reserves. Indeed, Makogon estimated in 2007 that with modern energy consumption rate, if just 15% of the amount of energy available in natural GHDs could be produced, the world would have enough energy for 200 years.[2] Unfortunately, extraction of the natural gases in naturally occurring clathrate hydrates is dangerous, for these gas hydrates are unstable at lower pressure environment. The extraction process may alter the pressurized environment. If done recklessly, a large amount of methane could be released at once. Given that methane is more effective at absorbing infrared radiation than is CO_2,[5] a sudden increase in methane concentration in the atmosphere could worsen the greenhouse gas effect and accelerate global warming. Furthermore, such an event, or the existence of a "mining" facility at the location of these gas-hydrates deposits, could greatly alter the marine environment around it. Thus, extraction of the gases from naturally occurring clathrate hydrates is not environmentally favorable.

Clathrates also have the potential to be a green energy source by being the gas carrier and storage medium as well as an atmospheric cleanser by trapping CO_2. A method of reducing CO_2 concentration in the atmosphere is by a process called sequestration, which is performed by releasing the CO_2 in the ocean from 400-2000 m, where they are trapped by dissolution in water.[6-8] The pressure and temperature environment fitting for CO_2 hydrates to start appearing is

at 500 m, where they sink due to density and stabilize in the long term on the seabed.[8,9] CO_2 hydrates density depends on the amount of CO_2 dissolve in the water cage. For CO_2 hydrate to sink in ambient water, the mole ratio threshold of CO_2/water at 128.3 atm and 4 °C (1.3 km deep in the ocean) is 0.145.[9] Note that this is relative density, as many other parameters factor into CO_2 hydrate density, such as the pressure and temperature of formation. Thus, many aspects of CO_2 marine sequestration, such as CO_2 solubility, CO_2-hydrate formation mechanism, and CO_2-hydrate stability in different environment need to be studied further before putting it to practical use.

The gas storage of natural gas hydrate, specifically methane hydrate, can be achieved by mixing gas and water under hydrate forming condition: 275-283 K and 8-10 MPa (~79-99 atm).[10] Natural gas hydrate is more ideal than liquefied natural gas as a transportation medium since it was found that hydrates can store a large quantity of gas (180 SM^3 per M^3 of hydrate) and could be stored for 15 days at atmospheric pressure and just below freezing temperature at -15 °C.[11] It is estimated that using clathrate hydrates to transport natural gases from the North Sea to Central Europe could save up to 24% in cost compare to liquefied natural gases.[12] In reality, slow hydrate formation rate affects the cost-effectiveness of the formation process, since it requires keeping a cold bath at relatively high pressure. To increase the rate of hydrate formation and storage capacity of the gas hydrates, thereby increasing cost efficiency, promoters could be added to the solution.[11,13,14]

Several clathrate hydrate promoters have been studied. Tetrahydrofuran (THF), for example, is known to have successfully separate a large quantity CO_2 (more than 99 mol%) from flue gas exhaust at 273-283 K by lowering the equilibrium hydrate formation pressure in a process called hydrate base gas separation.[15] Surfactants such as sodium dodecyl sulfate (SDS)

and dodecyl polysaccharide glycoside (DPG) have also been studied to test their potential in increasing storage capacity of clathrate hydrates[11] with the conclusion that anionic surfactant (SDS) is more efficient than nonionic surfactant (DPG).

Another study has been done on similar organic compounds with properties comparable to surfactants called hydrotropes. Surfactants are amphipathic molecule with a long hydrophobic hydrocarbon chain and a hydrophilic end. They are known to self-assemble into micelles in aqueous solutions. Hydrotropes are similarly amphipathic, but instead of a long hydrocarbon chain, they contain a short and bulky hydrophobic end, usually an aromatic group. Gnanendran and Amin studied a common hydrotrope's, para-Toluenesulfonic acid (pTSA), effect on gas hydrate formation and compared it to surfactants.[16,17] They concluded that pTSA is a better promoter than surfactants due to higher solubility of hydrate forming gases achieved in water.

Although the aforementioned studies have shown that THF and the hydrotrope pTSA have the potential to improve clathrate hydrate formation efficiency, they were all done at a macroscopic level. A main area of interest in clathrate hydrate studies, the study of clathrate hydrate formation mechanism with a promoter, remains largely unexplored. Understanding how the hydrate promoters help gas hydrate formation could provide substantial insights into improving gas hydrate formation rate and efficiency while providing fundamental understanding of molecular-level water-gas-promoters interaction. This potential insight, therefore, could have a large impact in industry and environmental research as well as in fundamental research. This project focuses on pTSA's interaction with water on a molecular level using the CCl_4 matrix, since the same matrix have been used to study THF.[18]

1.2 Ambient Energy Matrix Isolation Spectroscopy

Clathrate hydrates, surfactants-water, and hydrotropes-water systems can all be classified as water clusters. Water clusters have been studied in the IR region since the 1970s[19-23] and are important in many biological systems,[24] organic chemistry mechanisms,[25,26] ice,[27,28] and clathrate hydrate nucleation.[29] Water clusters are stabilized through hydrogen bond networks. Infrared absorption spectroscopy (IR) is perhaps the most useful method to study hydrogen bonded (H-bonded) water systems due to the high sensitivity of the OH stretch to the local chemical environment. Unfortunately, broadening in the H-bonded region, which extends hundreds to thousands of wavenumbers, is a major limitation for assigning stretch resonances and diagnosing interactions. Despite the challenges, there have been pioneering theoretical[30-34] and experimental[34-38] works providing glimpses into H-bonded network structures in the mid-IR region. Among these pioneering works is a method developed by Kuo and Shultz[1] called Ambient Energy Matrix Isolation Spectroscopy (AE-MIS). AE-MIS uses a carbon tetrachloride (CCl_4) matrix, which operates at in the temperature range of CCl_4's liquid phase (-22.96°C – 76.72°C) and atmospheric pressure. It simplifies the rotational activity of water in the mid-IR region by restricting certain water's rotational modes as well as preventing hydrogen bonding between water molecules. The more specific molecular picture is explored further below.

a) Water Rotational and Vibrational Signatures in AE-MIS

Water has three rotational modes: about its symmetry axis (z-axis) and perpendicular to its symmetry axis (y-axis and x-axis). Water also as three fundamental vibrational modes: symmetric stretch (3650 cm^{-1}), asymmetric stretch (3760 cm^{-1}), and bend (1600 cm^{-1}).[39] Note that the frequencies given above are for water vibrations in gas phase. The symmetric stretch of water in CCl_4 is 3615.5±1 and the asymmetric stretch is 3708.5±0.5, redshifted due to CCl_4's dielectric constant (2.2379).[1] The bending mode of water cannot be observed because its

absorption frequency overlaps with CCl_4's own absorption, and since there are more CCl_4 than water molecules in the sample, the bending mode is swallowed. In IR spectroscopy, a molecule's vibration transition is coupled with a rotational transition. Additionally, water is an asymmetrical top, thus has a complex rotational spectrum extending for hundreds of wavenumbers.[39] These complex rotational lines, in CCl_4 matrix, collapse and only the rotational features that are associated with the asymmetric stretch is observed (Figure 1.1). This rotational feature can be identified using symmetry.

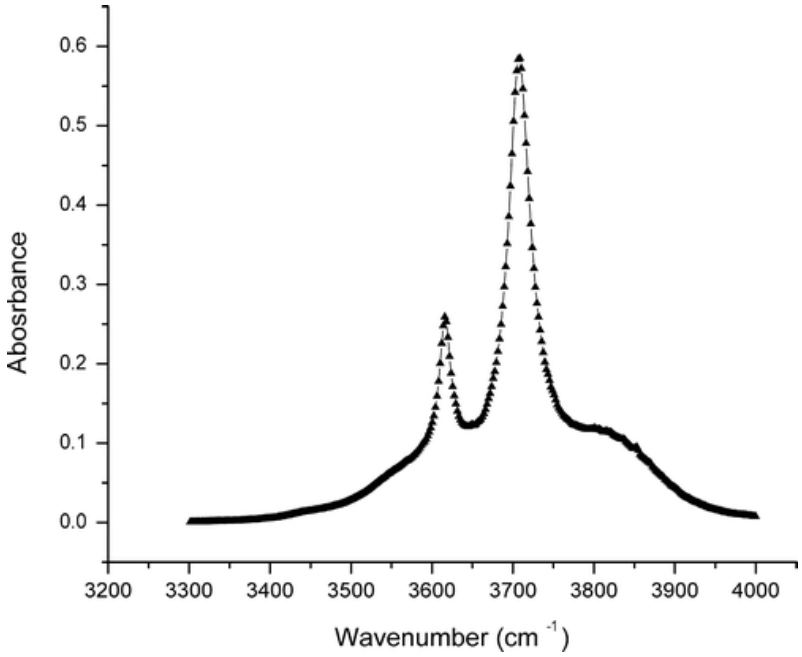

Figure 1.1. FTIR spectrum of water in CCl4. The concentration of water is 7.5 mM. Reproduced from reference 1.

A single water molecule has C_{2v} symmetry. The IR active Γ_{vib} of a C_{2v} point group contains the 2 A_1 and B_2 representations.[40] Since the A_1 representation is symmetric with respect to the rotation principle axis (z-axis), one must be the symmetric stretch for water and the other the bending mode. The B_2 representations are asymmetric with respect to rotation of the principle axis with subscript 2 denoting the asymmetric mode with respect to the C_n principle

axis, thus is the asymmetric stretch of water. The bending mode (A_1) is irrelevant in this context because it cannot be observed due to CCl_4 absorption below 1650 cm^{-1} as mentioned above.

Table 1.1 – C_{2v} character table.

C_{2v}	E	C_2 (z)	σ_v (xz)	σ_v (xz)	Linear functions, rotations	Quadratic functions	Cubic functions
A_1	+1	+1	+1	+1	z	x^2, y^2, z^2	z^3, x^2z, y^2z
A_2	+1	+1	-1	-1	R_z	xy	xyz
B_1	+1	-1	+1	-1	x, R_y	xz	xz^2, x^3, xy^2
B_2	+1	-1	-1	+1	y, R_x	yz	yz^2, y^3, x^2y

Looking at a C_{2v} character table (Table 1.1), the symmetric stretch (A_1) must be coupled with the rotations around the x (B_1) and y (B_2) axes. The absence of rotational wings around the symmetric stretch means that the rotation about the x and y axes must be restricted. The asymmetric stretch (B_2) couples with rotation about the y and z axis. Since the rotation about the y-axis is quenched, the rotational wings associated with the asymmetric stretch must be the rotation about the z-axis, or the symmetry axis. The absence of the broad band from 3000-3500 cm^{-1}, generally referred to as the hydrogen-bonded region, also suggests that water monomers, and not hydrogen-bonded water, exists in CCl_4. A possible model that fits these observations is that the slightly negatively charge oxygen atom of the water molecule interacts with the slightly positively charged carbon atom of CCl_4, the conclusion that Shultz and Kuo came to in reference 1. The electromagnetic potential map of water-CCl_4 modeling their interaction is shown in Figure 1.2.

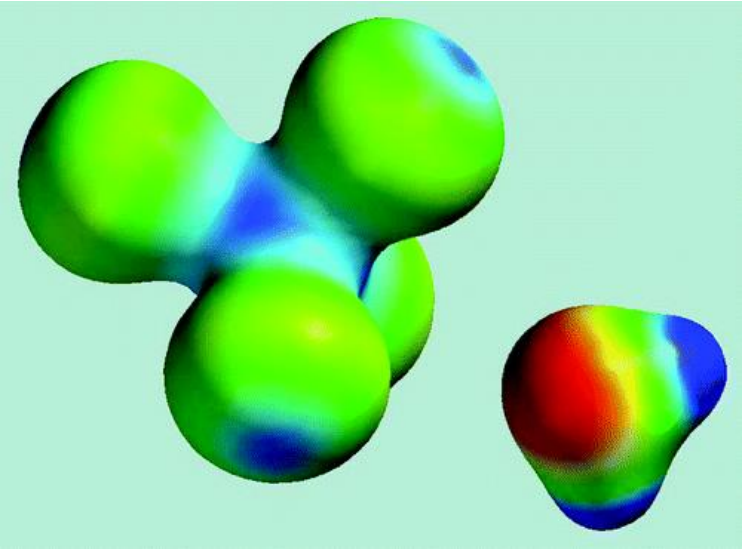

Figure 1.2 A molecular picture of water's interaction with CCl4. Density-potential surface for a water–carbon tetrachloride complex calculated at the DFT- B3LYP 6-31G level of theory. Reproduced from reference 1.*

b) Water as a Pseudo Prolate Top

To confirm the interaction above, water was treated as a near pseudo prolate top for calculation and modeling.[1] Here, we define the rotational constant of the rotation about the z-axis as A, x-axis as B, and y-axis as C. If the oxygen is weakly interacting with the carbon in CCl_4, then it has only one rotation (about its symmetry axis). The other two rotations are restricted (rotational constants equal zero), thus we have $A > B = C = 0$. Since the rotational constants and their principal moments of inertia have an inverse relationship, I_B and I_C are infinite while I_A is a finite number. Therefore, $I_A < I_B = I_C = \infty$, which is the definition of a prolate top. Quantum mechanics calculations of a prolate top[39] were applied to the system and detailed in reference 1. From this model, it is concluded that the vibrational origin is composed of $\Delta J = 0$, $\Delta K = 0$ transitions and $\Delta J = \pm 1$, $\Delta K = 0$ transitions. The former is associated with the vibration origin with no rotational excitation. As a near pseudo prolate top model, the symmetric stretch is a parallel mode, thus has no Q band. Due to the short-lived rotation in the x and y axis, their

rotational signals contributed to make a Q-like band. The latter results in a P-Q-R type structure (P when $\Delta J = -1$, R when $\Delta J = +1$, Q when $\Delta J = 0$, and $\Delta K = 0$ for all). This approximation results in an excellent fit for the spectrum of water in CCl_4 (Figure 1.1) and a calculated rotational constant of 14.8 cm^{-1} which is the same as water's rotational constant in the gas phase of 14.504 cm^{-1} (within experimental error).[1]

Kuo also reported the upper limit on the rotational lifetime of 0.83 ps, compare to 0.7-1.3 ps in liquid water,[1] which results in rotational bands rather than sharp lines. In the liquid state, water molecules are hydrogen-bonded to each other, thus restricting rotational motions and resulting in a short rotational lifetime. Since water exists as monomers in CCl_4, the only molecule that interacts with water to cause the short rotational life time is CCl_4.

Table 1.2. Ia/Is of water interaction with different cations. Reproduced from reference 1.

	in CCl_4	gas phase (ref 37)	Li^+ (ref 15)	Na^+ (ref 14)	K^+ (ref 14)	Cs^+ (ref 13)
A_0 (cm^{-1})	14.8 (±0.2)	14.5074	13.9	14.3	14.1	14.0
ν_{sym} (cm^{-1})	3615.5 (±1)	3657	3629	3634	3636	3635
ν_{asym} (cm^{-1})	3708.5 (±0.5)	3756	3691	3707	3710	3711
I_a/I_s	14.8	18	1.53	1.57	2.44	2.04

Furthermore, Kuo included a table comparing the ratio of the intensities between the asymmetric and symmetric stretch (I_a/I_s) in systems where water is coupled with different cations (Table 1.2).[1] It is observed that the above ratio decreases with the more positive cation, meaning that the symmetric stretch signal increases with increasing ionic strength. This enhancement makes sense because in cation-water complex, the slightly negative oxygen interacts strongly with the positively charged cation. The oxygen is "pinned down," increasing the oscillator strength of the symmetric stretch. In water-CCl_4 complex, the symmetric stretch is slightly

enhanced compare to the symmetric stretch of gas phase water (ratio I_a/I_s of 14.8 compare to 18, respectively), though not as much as the positive cation-water complex (ratios around 1.5-2.5). This behavior is consistent with the interaction of the oxygen in water with the carbon in CCl_4. Only a slight enhancement is observed because the carbon in CCl_4 is not a full positive charge. All three results: the rotational constant calculated from the near pseudo prolate top approximation, the short rotational lifetime, and the slight enhancement of the symmetric stretch are consistent with the oxygen-carbon interaction model.

Using this simple picture, the rest of this report is organized as follows: chapter 2contains a discussion of experimental and theoretical methods, chapter 3 results from these methods of (pTSA)•$(H_2O)_n$ for small clusters ($n \leq 10$) and chapter 4 for large clusters ($n \geq 20$). Chapter 5 focuses the hydrocarbon impurities and their implications in this system, and chapter 6 outlines future works and summary.

2. Experimental Methods

2.1 Preparing dried CCl_4

Anhydrous carbon tetrachloride (CCl_4, Sigma-Aldrich, ≥99.5% anhydrous) is dried further with silica gel for at least 2 days prior to use. The dried silica gel is held in a round bottom flask connected to a vacuum line with 1/4 inch stainless steel tubing (Figure 2.1). The flask is sealed with a greased rubber septum. CCl_4 comes from a bottle with a septum cap, and is removed using a 60 mL syringe and long needle. When not in use, the syringe is kept in a desiccator to prevent moisture absorption from the atmosphere.

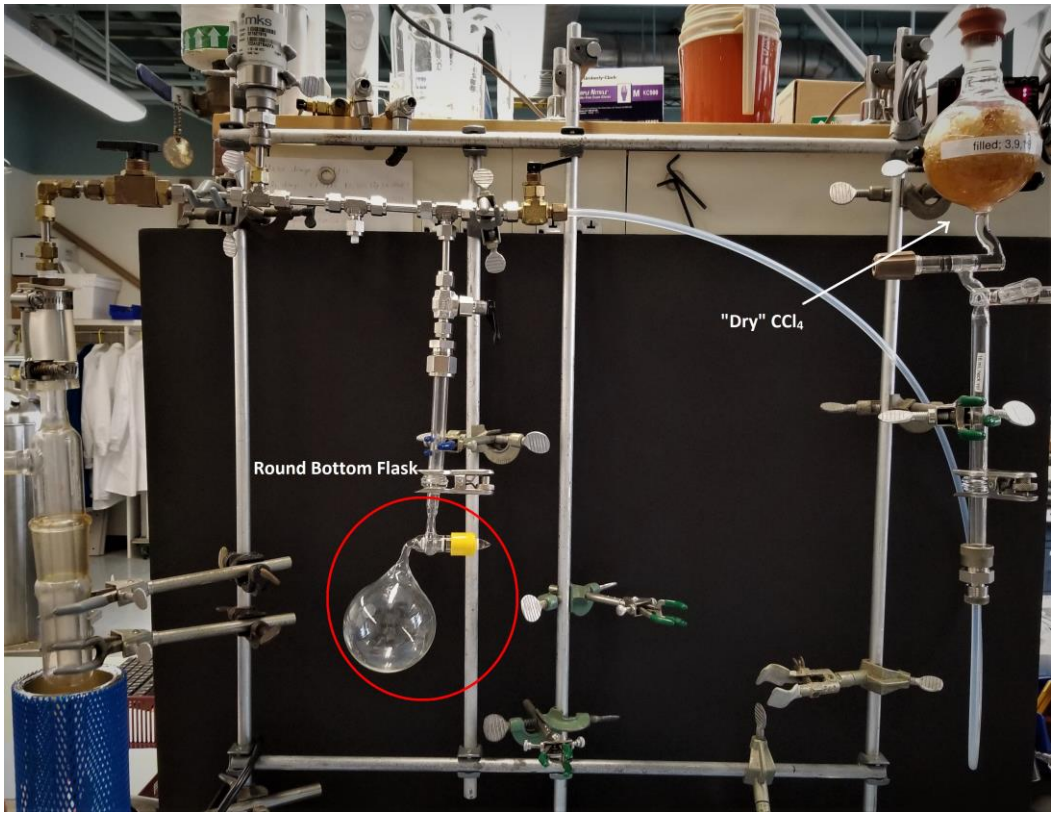

Figure 2.1 – Experimental setup: vacuum line, "dried" CCl_4 in silica gel, and a round bottom flask for sample addition.

2.2 Glass Cell

The glass cell that is used to contain the CCl_4 and acid sample has 25 cm path length and 30 cm diameter. Calcium fluoride (CaF_2) IR windows with 40 cm diameter are used. The windows and cell are held together via Torr Seal epoxy (Torr Seal base resin, 82 grams, Agilent Technologies) to withstand the cold (-20°C) temperature since the temperature range of Torr Seal is -45°C to 120°C (Figure 2.2).

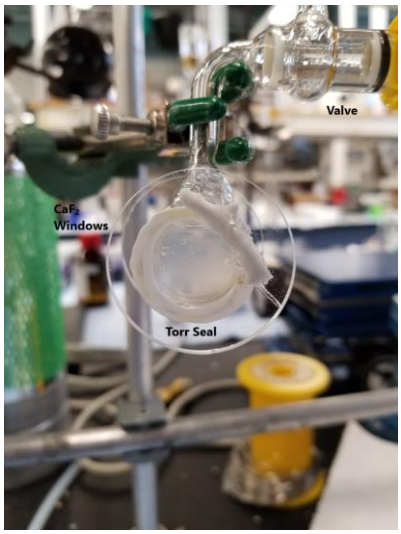

Figure 2.2 – A typical glass cell with CaF_2 windows attached by Torr Seal Expoxy.

2.3 Sample Preparation

a) Aqueous Stock pTSA Solutions

Aqueous stock solutions of different p-toluenesulfonic acid monohydrate (pTSA•H_2O, Sigma-Aldrich, ≥98.5%, ACS reagent) are prepared by mixing the solid pTSA•H_2O crystals with Nanopure water (18 MΩ, Barnsted GenPure Pro with UV). The acid:water ratios are determine by first measure about 0.50 grams of acid monohydrate, then convert that amount to mole, then decide the desired acid:water mole ratio (1:6, 1:8, 1:10, 1:26, 1:51), and finally convert the desired mole of water to mL by using water density of approximately 1 g/mL. The same process was used to make (pTSA)•$(D_2O)_n$ (D_2O, Signma-Aldrich, 99.9 atom % D) and (pTS^-Na^+)•$(H_2O)_n$ (pTS^-Na^+, Sigma-Aldrich, 95%) samples.

b) Experimental Procedure

The cell with windows glued on with epoxy are kept in a desiccator overnight prior to sample addition. The empty cell is first evacuated and weighted. A spectrum of the empty cell is acquired using a Nicolet Magna-IR 760 spectrometer with DTGS KBr detector at 64 scans and 1

cm^{-1} resolution. The spectrometer is purged with nitrogen gas overnight to remove atmospheric moisture prior to use. All FTIR spectra were taken using the same instrument and parameters. Then, dried CCl_4 is added to the cell. Residual CCl_4 usually remains on top of the cell valve after the cell is closed. Thus, the closed cell is evacuated to remove any residual CCl_4 in the valve.

The now filled cell is weighted, and its background spectrum at room temperature is taken. A difference spectrum of dried CCl_4 sample against the empty cell spectrum is also taken. The prepared pTSA solutions can now be added to the CCl_4-filled cell. Microliters are taken from the stock solutions prepared as described above using a 100-microliter syringe. The CCl_4 and acid sample are mixed in an evacuated round bottom flask (the flask is kept in a desiccator when not in use) and is sonicated for thirty minutes to ensure mixing before transferring it back to the cell. The sample is then allowed to equilibrate for 2 days at room temperature.

After 2 days, a difference spectrum of the acid sample in CCl_4 is taken against the CCl_4 background spectrum acquired earlier. The cell is then chilled in a -20 °C freezer for two days before the IR spectrum of the sample at -20 °C is acquired against the CCl_4 background spectrum. More water or aqueous acid solutions could be added in the same manner. All additions of extra water or acid solutions are performed at room temperature. All acquired spectra are then graphed using Origin Lab 9.0.

2.4 Theoretical Methods[†]

Calculations were performed on a Parallel Quantum Solutions Linux box using the Parallel Quantum Solutions (PQS) suite of programs.[41] Density functional theory (DFT) with the hybrid method B3LYP was chosen since it has been reported to give trustworthy results for many water cluster studies,[42,43] specifically for predicting energies and spectra for gas-phase

[†] This section along with all other theoretical calculations are credited to Dr. David J. Anick.

water clusters $(H_2O)_n$ and for $X(H_2O)_n$ clusters, where X is an ion or a polar solute, when a triple-ζ basis is employed.[44-53] The triple-ζ basis includes both polarizations and diffuse functions. Diffuse basis functions, used in the PQS programs, caused overlap problems when applied on the aromatic ring which then led to nonconvergence of the self-consistent field. This is not to say that the diffuse basis functions caused this problem, since the causation was never identified, but since diffuse functions are usually not necessary for aromatic optimization, the B3LYP with a "mixed basis" was adopted. The "mixed basis" consisted of 6-311++G(d,p) on the water molecules and S and O atoms of the sulfonyl group but also consisted of 6-311G** on the aromatic ring and the methyl group of pTSA. The mixed basis is denoted 6-311[++]G(d,p), which is the method used for all calculations in this report.

Calculated IR frequencies of the clusters were generated with the harmonic approximation and were scaled by 0.965[54] prior to comparison with experimental results. Free energies at -20°C and 1 atm were calculated using standard formula, which does not adequately account for the free rotation (treated as low-frequency vibration) of the methyl group. This treatment has minimal effect on the zero point energy (ZPE), but could have a significant effect on the calculated entropy. Methods for calculating rotations are complex. To minimize errors, the principal results of this approach are the free energy differences, which then approximately cancels errors.

Ab initio molecular dynamics (AIMD) studies were also ran for the di- and trihydrate $(pTSA)\bullet(H_2O)_2$ and $(pTSA)\bullet(H_2O)_3$. Each run was of the NVE type (fixed moles (N), volume (V), and energy (E)) starting at the global minimum with kinetic energy added at random to approximate -20°C. In this case, NVE simulates dynamics for a single isolated cluster with no solvent, moving under its B3LYP –computed potential conserving total energy. In these runs,

kinetic energy is defined as the total kinetic energy divided by $\frac{k_B(3N_{at}-6)}{2}$ where ($3N_{at} - 6$) is the number of degrees of freedom. The NVE method was employed as a compromise since it requires less computation time than a highest-quality simulation including solvent molecules filling out a periodic box along with a thermostat. Runs used a step size of 0.5 fs and lasted at least 12 ps after a 1 ps equilibration period.

3: Small (pTSA)•$(H_2O)_n$ Clusters (n ≤ 10)

3.1 Experimental Results

The gas-phase IR spectrum of water is complex because water is an asymmetric rotor, but it is simplified in CCl_4 since water exists as monomers in the CCl_4 matrix. The isolated monomers' vibrations and rotations can be modeled as a pseudo prolate top[1] having free rotations about its symmetry axis and quenched rotations about the other two orthogonal axes. A typical water spectrum in CCl_4 shows two fundamental vibrations in the free –OH stretching region: the symmetric and asymmetric stretches at 3617 and 3709 cm^{-1}, respectively (Figure 1.1). The rotational wings resulted from the water's rotation about the symmetry axis accompanies the asymmetric stretch. These features are labeled in figure 3.1 (pure water spectrum shown in reference 1 and Figure 1.1). These features are redshifted relative to gas-phase water due to the dielectric constant of CCl_4 (2.2379). Monitoring changes in these features give insights to the molecular bonding interactions of molecules in the matrix, in this case water and pTSA. For example, the presence of a weak hydrogen bond acceptor restricts the rotation of water monomer about its symmetry axis, which leads to the collapse of the rotational wings. On the other hands, a strong interaction gives redshifted stretch bands and removes equivalence of the two O–H stretches.[55] Additionally, interaction with the oxygen atom lone pair enhances the symmetric

stretch oscillator strength (hence enhances the intensity of the symmetric stretch peak) relative to the asymmetric stretch.[56-61] The results reported in this chapter is reproduced from reference 62.

a) (pTSA)•(H₂O)ₙ

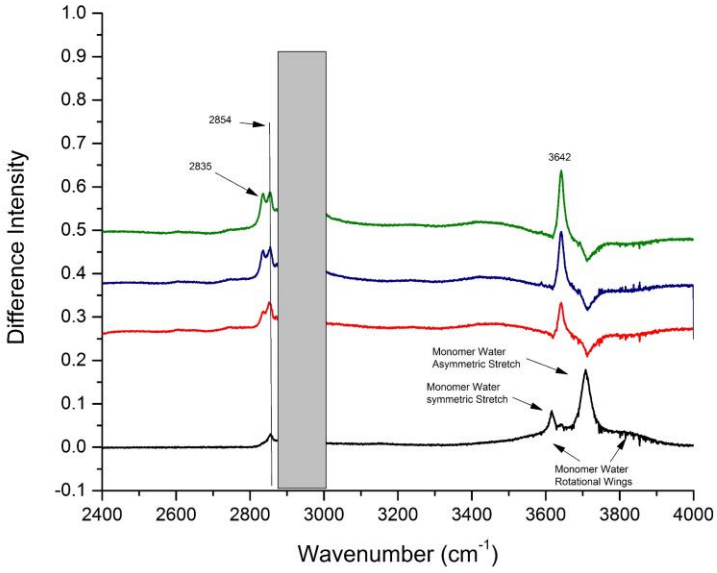

Figure 3.1 – Infrared spectra of pTSA·H_2O in CCl_4: injected solution mole ratio acid:water 1:6 at room temperature (black line) and -20 °C (red line). Adding 14, and 28 μL water and cooling to – 20 °C (acid to water mole ratio 1:6, 1:8, 1:10) (red, blue, and green, respectively; spectra offset for clarity). At 1:6, the injected water is more than 20 times that of saturated neat water. The grey region is inaccessible due to hydrocarbons in CCl_4. The low intensity peak at 2854 cm-1 is also an impurity. All spectra are difference spectra subtracting the room temperature, nominally dry CCl_4 spectrum.

The presence of acid in the CCl_4-water system alter the IR spectrum (Figure 3.1). The stock solutions used for the spectra in Figure 3.1 have the acid:water ratio of 1:6 (black at room temperature, red at -20 °C), 1:8 (blue), and 1:10 (green). At 1:6, the water concentration present in CCl_4 is more than 20 times the saturated amount of neat water in CCl_4 (7.5 mM).[1] The symmetric and asymmetric stretch of water are visible at room temperature in Figure 3.1 along with an additional peak at 3642 cm^{-1}.

The spectrum changes when the sample is cooled to -20 ℃. The water monomers peaks diminish significantly, shown by the "negative" asymmetric stretch. Since the sample is taken against the "dry" CCl_4 background, the "negative" peak indicates that the concentration of monomer water after the cooling process is less than at room-temperature in the presence of acid. This is consistent with the dehydrating capacity of sulfuric acid and its derivatives, meaning monomer water molecules are hydrogen bonding to each other and to the acid molecule. The small but broad band from 3000-3550 cm^{-1} is further evidence for this interpretation, since this band signifies hydrogen bonding. The 3642 cm^{-1} peak enhances as the temperature is cooled and increases further as more water is added. Additionally, a new peak appears at 2835 cm^{-1} and also increases in intensity as more water is added at -20 °C. This peak is red of the impurity peak at 2854 cm^{-1}, which is a hydrocarbon impurity that appears in all spectra including the CCl_4 solution without acid-water addition. This impurity peak, along with the grey-out region from 2900-3000 cm^{-1}, appears in both 99.5% and 99.9% CCl_4 solutions from Sigma-Aldrich, although less intense in 99.9% solution, which is characteristic of impurities (See Appendix). The impurities peaks are discussed in more details in chapter 5. Changes from cooling are entirely reversible: reheating and recooling the sample produce the same spectra. Therefore, within this acid:water ratio ($n \leq 10$), the 2835 cm^{-1} and 3642 cm^{-1} cannot be distinctly observed at room temperature.

b) $(pTSA)\bullet(D_2O)_n$ and $(pTS^{-}Na^{+})\bullet(H_2O)_n$

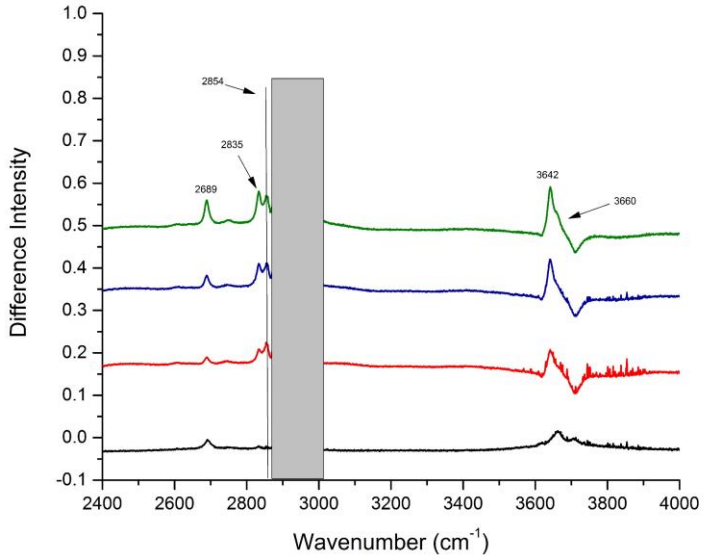

Figure 3.2 – Substitution of D_2O for H_2O to dissolve the acid monohydrate. In CCl_4 at room temperature (black line) and at -20 °C with increasing D_2O (red, blue, and green, respectively). Spectra are difference spectra subtracting the room temperature, nominally dry CCl4 spectrum. Note that pTSA is a monohydrate, hence there are three ordinary hydrogen atoms per acid anion. Mole ratios acid ordinary water to heavy water are 1:1:5 (red), 1:1:7 (blue), and 1:1:9 (green). Spectra are offset for clarity.

To further aid in the identification of the 2835 and 3642 cm^{-1} resonances, D_2O[31,32,63] and the salt version of pTSA, sodium p-toluenesulfonic acid (pTS^-Na^+), were used. $pTSA•H_2O$ was dissolved in D_2O using the same method. D_2O stretches are redshifted by $\sqrt{1/2}$ relative to normal water (Figure 3.2). Normal OH modes remain from the normal hydrogen bond of the monohydrate to the acid. Peaks blue of the 3550 cm^{-1} appears broader than the corresponding peaks in normal water (Figure 3.1 and 3.2). The monomer normal water peaks are less intense in Figure 3.2 than in Figure 3.1, consistent with using D_2O to dissolve the acid rather than H_2O. Due to deuterium substitution, the 3600-3800 cm^{-1} region is that of the OH resonances of the HOD species. The OD stretch of this species is at 2689 cm^{-1}.

The purpose for using the salt experiment is to test whether the 2835 and 3642 cm^{-1} are acid-water resonances. Since pTS^-Na^+ is the salt version, the lack of both aforementioned

resonances would be adequate evidence to conclude that they are indeed acid-water peak. The salt-water solutions were prepared in the same way and their spectra are displayed in Figure 3.3. The salt lacks the acid OH on the sulfonyl group, hence fewer features were observed in Figure 3.3. At room temperature, the water monomer peaks are present with lower intensity than in the corresponding acid experiment despite higher water concentration in the stock solution. The 2854 cm^{-1} peak is more intense in the salt. The reason for this enhancement is discussed in chapter 5. Since the 2835 cm^{-1}, 3642 cm^{-1}, and the broad hydrogen bonded region from 3000-3550 cm^{-1} features are absent in the salt experiment, they are concluded to be acid-water features.

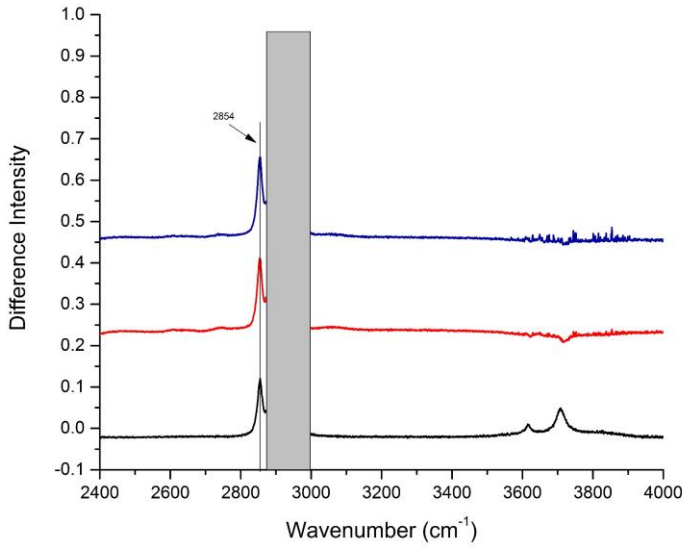

Figure 3.3. Infrared spectra of pTS-Na+ and water in CCl_4 at room temperature (black) and at -20 °C with 0 and 10 μL added water (salt to water mole ratios 1:20, 1:21; (red and blue, respectively)). Spectra are difference spectra subtracting the room temperature, nominally dry CCl_4 spectrum. Note absence of the 2835 cm^{-1} peak (the sharp peak at 2854 cm^{-1} is the impurity mentioned above).

3.2 Computational Results[‡]

a) Low Energy Clusters

Table 3.1 gives the lowest energy structure found at -20 °C for each n, $1 \leq n \leq 12$, and others found within 2 kcal•mol^{-1} of the lowest. This is given in terms of the free energy of formation from widely separated pTSA and nH$_2$O units, denoted as ΔG^{253}. Unionized clusters are named pTSA.WnX where X is a letter. Ionized clusters are named pTS–.H+WnX. Only the lowest energy structure is listed for isomers having one or more "DA" (single donor-acceptor) water molecules having a free H with two possible orientations. Similarly, only the lowest structure is listed when several local minima occur with respect to rotation around the C–CH$_3$ or the C–S bonds. Table 3.1 also lists the calculated electronic energy of formation $\Delta E°$ as well as ΔG^{0K} (defined as $\Delta E° + \Delta ZPE$). There are three clusters whose energy lies beyond the 2 kcal•mol^{-1} limit but are of interests due to occurring in the AIMD simulation or having a water molecule that donates into the aromatic ring are also included in Table 3.1.

[‡] This section along with all other theoretical calculations are credited to Dr. David J. Anick.

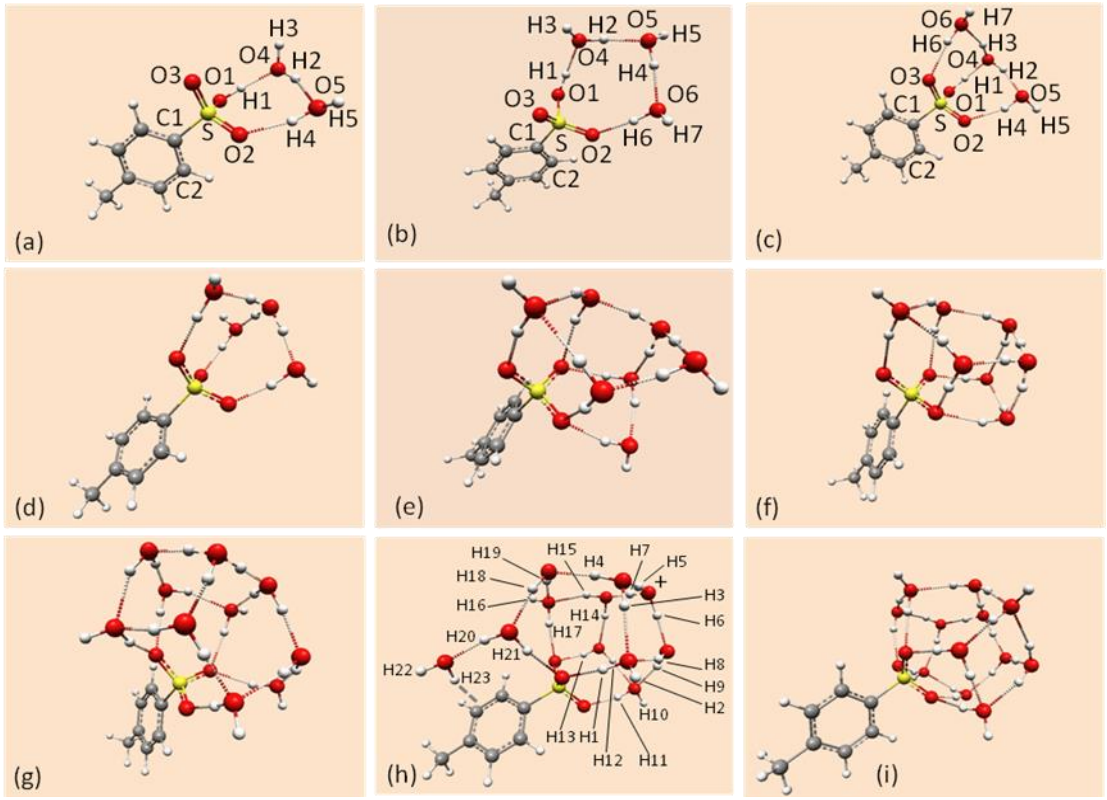

Figure 3.4 – A selection of the optimized (pTSA)(H2O)n clusters listed in Table . (a) pTSA.W2A (b) pTSA.W3A (c) pTSA.W3B (d) pTS−.H+W4A (e) pTS−.H+W7A (f) pTS−.H+W7D (g) pTS−.H+W10A (h) pTS−.H+W11X (i) pTS−.H+W12A.

Table 3.1 – Selected cluster binding energy (kcal·mol-1) via B3LYP/6-311[++]G(d,p), including electronic energy, ZPE-corrected electronic energy (denoted ⊿G0K), and free energy at 253 K.

CLUSTER	ΔE^{o}	ΔG^{0K}	ΔG^{253}	CLUSTER	ΔE^{o}	ΔG^{0K}	ΔG^{253}
pTSA.W1	-11.64	-9.10	-2.04	pTS−.H+W7B	-85.89	-66.97	-13.76
				pTS−.H+W7C	-87.10	-67.48	-13.57
pTSA.W2A	-24.25	-19.40	-5.50	pTS−.H+W7D	-87.73	-67.87	-13.38
				pTS−.H+W7E	-86.33	-66.49	-12.16
pTSA.W3A	-35.70	-28.50	-7.56				
pTSA.W3B	-35.93	-28.84	-6.93	pTS−.H+W8A	-100.02	-77.84	-16.16
pTSA.W3C	-35.47	-28.03	-6.30	pTS−.H+W8B	-98.00	-75.97	-14.70
pTSA.W3D	-31.00	-24.55	-4.55				
pTS−.H+W3A	-35.14	-28.36	-6.11	pTS−.H+W9A	-112.26	-87.28	-17.66
				pTS−.H+W9B	-111.80	-86.72	-17.27
pTS−.H+W4A	-48.70	-38.56	-8.91	pTS−.H+W9C	-112.30	-87.55	-16.75
pTS−.H+W4B	-48.56	-38.66	-8.82	pTS−.H+W9D	-112.74	-87.47	-16.68
pTSA.W4A	-46.60	-37.09	-8.24	pTS−.H+W9E	-110.38	-85.50	-16.19
pTSA.W4B	-45.14	-35.74	-7.80	pTS−.H+W9X	-104.96	-80.79	-12.21
pTSA.W4C	-45.89	-36.22	-7.39				
				pTS−.H+W10A	-123.48	-95.85	-19.04
pTS−.H+W5A	-59.34	-47.01	-10.49	pTS−.H+W10B	-122.89	-95.34	-18.52
pTS−.H+W5B	-60.51	-47.48	-9.70	pTS−.H+W10C	-123.16	-95.32	-18.29
pTS−.H+W5C	-59.32	-46.24	-8.83	pTS−.H+W10D	-122.37	-94.93	-17.77
pTS−.H+W5D	-61.46	-47.39	-8.74	pTS−.H+W10E	-119.92	-92.95	-17.59
pTSA.W5A	-57.93	-46.14	-9.58				
pTSA.W5B	-56.28	-44.76	-8.91	pTS−.H+W11A	-136.05	-105.69	-20.92
				pTS−.H+W11B	-135.44	-105.03	-19.98
pTS−.H+W6A	-75.37	-58.21	-11.86	pTS−.H+W11C	-134.85	-104.48	-19.86
pTS−.H+W6B	-70.70	-55.34	-11.82	pTS−.H+W11X	-128.97	-99.38	-15.92
pTS−.H+W6C	-74.28	-57.47	-11.06				
				pTS−.H+W12A	-148.03	-114.86	-22.33
pTS−.H+W7A	-86.60	-67.41	-13.82	pTS−.H+W12B	-148.10	-114.68	-22.02

Selected clusters from Table 3.1 are illustrated in Figure 3.4. The coordinates for these clusters can be found in xyz format in the Appendix. Clusters with the letter "A" are local minima. Breaking an H-bond could result in greater binding energy in some cases. For instance, "pTS⁻H+W7A" and "pTS⁻H+W7D" fall into this category (Figure 3.4e,f): one H-bond in Figure 3.4f is broken in 3.4e. From Table 3.1, the electronic and free energy of 3.4f is lower at 0K, but 3.4e is lower at 253K since the entropy gained from the breaking of that bond lowers the free energy more than the lost enthalpy raises it. Global minima for clusters with $n \geq 8$ have an outer surface consisting of the Eigen ion and DDA waters (Figure 3.4g,i for n = 10 and n = 12, respectively) besides the DAA waters that donate to the negatively charged O atoms of the sulfonyl group. This picture is consistent of the "hydrophobic water"[64-66] that tends to repel other similar surfaces or free water.

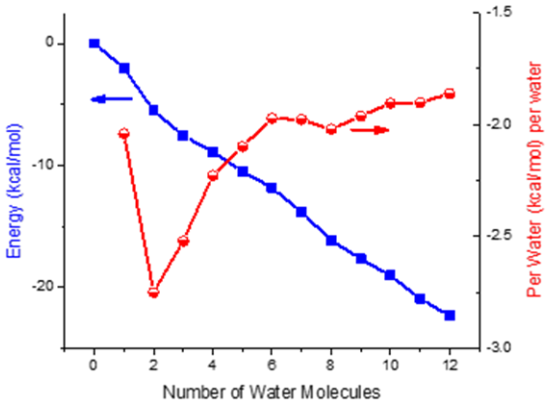

Figure 3.5 – Cluster binding energy as a function of the number of water molecules (blue line/symbols). Note the larger stabilization gain from n =1 to n = 2 than any other step, shown dramatically in the binding energy per water plot (right axis, red line/symbols).

Free energy of formation of the lowest energy clusters shown in Table 3.1 is graphed in Figure 3.5 for each *n* as a function of *n*. A large gap in binding energy of 3.5 kcal•mol^{-1} occurs between the mono- and dihydrate. Subsequent water molecules additions have a consistent binding energy of ~1.7 kcal•mol^{-1}. The result is a "kink" at $n = 2$ due to a slope change. Enhanced binding per water for $n = 2$ is emphasized by the per molecule binding energy, shown in Figure 3.5. Stabilization at $n = 2$ implies that the "preferred" number of water per acid molecule is two, meaning the population of the pTSA dihydrate is expected to be overrepresented in a system with populations of various (pTSA)•$(H_2O)_n$ clusters. This interpretation is similar to the situation that causes the $n = 21$ to be a "magic number" among the $H^+(H_2O)_n$ clusters.[38,67-69] Details of the source of this unusual binding energy is under investigation.

Note that the binding energies in Table 3.1 are much smaller at 253K than at 0K due to entropy contribution to water cluster free energy near ambient temperature, which is a known phenomenon as discussed by Shields et al.[70] for solute-free $(H_2O)_n$ clusters with $2 \leq n \leq 10$. In Shields' Table 8, ΔE_e, ΔE_0, and $\Delta G_T°$ (T = 10, 200, 298) notations correspond to ΔE^0, ΔE^{0K}, and ΔG^T (T = 253) in this report. For $(H_2O)_n$ clusters, Shields et al. found that binding energies become significantly smaller at 200 K than at 0 K and positive at 298 K, meaning small water clusters are unstable at 298 K and evaporate over time to dissociate to water monomers. ΔG^{253} values in Table 3.1 are negative, thus the pTSA-water clusters are predicted to be stable at 253 K. It is also found that the entropy term greatly affects both the absolute and relative binding energies (i.e., relative ordering for a fixed *n*) of pTSA-water clusters.

b) Identification of the 2835 and 3642 cm^{-1} Resonances

2835 cm^{-1}. After 150 (pTSA)•$(H_2O)_n$ cluster optimizations and frequency calculations, we reasoned that the identity of this peak was either somewhere among the OH stretch signals already computed or from an OH stretch with a local bonding environment that is similar to one computed. (The exact frequency of an OH stretch is extremely sensitive to its donor types (DA, DAA, etc.) and (if H-bonded) of its acceptor.[71-74])

Modes in the range of 2835 ± 15 cm^{-1} are called "matches" and in the range of 2835 ± 10 cm^{-1} are "strong matches." In total, 28 matches are found, 12 of which are strong matches ranging from 2830 to 2845 cm^{-1} and are the O-H stretch of the sulfonic acid H donating to the O of a water molecule in pTSA.W2A, the dihydrate. This stretch is seen in various dihydrate clusters because there are separate optimizations for the pTSA.W2A where either toluene is rotated or the direction of the free H atom is flipped. The other 16 matches occur in clusters with $n \geq 5$ and are the threefold symmetric stretch of a H_3O^+ embedded in an Eigen ion. Since the Eigen ion is known to have a very broad signal experimentally, even at cryogenic temperature, so the idea of the existence of an Eigen ion at ambient energy can be ruled out. Therefore, the 2835 cm^{-1} is tentatively assigned the S–O–H--- O of the dihydrate. As described above in Figure 3.5 and Table 3.1, the dihydrate has an unusually strong binding energy and is likely to be overrepresented, thus its signal is predicted to be unexpectedly strong. This assignment of the 2835 cm^{-1} to the S–O–H--- O stretch is thus consistent with the binding energy calculation. The other O–H stretch of the two water molecules in the dihydrate were either low intensity free O–H bonds or water-water H-bonds, which are too broad at 253 K to be distinctly detected. The full predicted IR spectrum of the dihydrate is included in the Appendix.

3642 cm^{-1}. The same approach is taken for the 3642 cm^{-1} signal, which resulted in 37 matches. One match is the free O–H stretch of dry pTSA at 3645 cm^{-1}, but it was ruled out because it would imply that pTSA, which exists as the monohydrate, lost *all* its water to the CCl_4 solvent. Fourteen of the matches are from bonds of a DDA water to one O of the SO_3^-. These bonds are strained (large H–O–O angle), or coupled with other stretches, or both. The 3642 cm^{-1} for the range of DDA---O–S stretches is on the blue end of the specified range and is expected to occur only if the H---O distance is unusually long or if the frequency is altered by strong coupling, or both. These bonds are one of the weakest and intermittently break and reform at -20 °C, making them poor candidates for the narrow signal observed in the experimental data. Eight other matches are strained and long DDA-DAA bonds, seven are DDA---DDAA or DDAA---O–S are also dismissed as weak and/or strained, thus unlikely to generate a strong, narrow peak.

Finally, there are six strong matches ranging from 3641 to 3651 cm^{-1} and are the water donating to the benzene ring, denoting π-OH. The benzene π-OH resonance has been reported to be at 3660 cm^{-1} and is expected to be redshifted about 20 cm^{-1} when attached with an electron withdrawing group,[75] such as the sulfonate substituent. An earlier work[62] hypothesized that the mechanism for the formation of the π-OH is through a "spillover" mechanism. Water H-bonded more favorably with the sulfonyl group than the benzene ring, and thus attempts at H_2O---benzene interaction optimizations resulted in water being ripped away to form bonds at the sulfonyl group. Thus, one way for water to reach the benzene ring in pTSA is for the cluster at the sulfonyl group to get relatively big, then some water molecule *could* spillover and interacts with the benzene ring, forming something like a scorpion tail in Figure 3.4h. The predicted number of water molecules needed for this mechanism to occur was between 16 and 20.

More recent computational results did not support this hypothesis. The energy of the "spillover" clusters are not the global minima in terms of binding energy for a given *n*. Thus, a second hypothesis was proposed. Ionic liquids could exist in aqueous solution as totally dissociated ions or as ionic pairs: molecularly dispersed or forming parts of aggregates. In this sense, pTSA was found to be forming aggregates in aqueous solutions.[76] On a molecular level, this means that the water cluster on pTSA could be a multi-acid cluster. This picture would allow some water molecules to come in contact with the benzene ring of another pTSA molecule while bonding with the sulfonyl group of a pTSA molecule. Since pTSA are bulky groups, it is predicted that the number of water needed for this to occur would need to be large, similarly predicted in the first hypothesis, although the exact number remains to be explored. Thus, the 3642 cm^{-1} is assigned the π-OH interaction of a water to a benzene ring for a "large, multi-acid cluster" with unspecified size or geometry.

Since the "matching" method compares the gas-phase computation results to the liquid-phase experimental observations, one could ask whether solvent interaction, in this case CCl_4, could alter the frequencies significantly. The features of dangling H atoms exposed to the CCl_4 are redshifted by 35 to 50 cm^{-1} according to both experimental and theoretical result and is shown in the monomer's symmetric and asymmetric stretches. Since all dangling H's in all clusters in this calculation resonate at least 90 cm^{-1} bluer than 3642 cm^{-1}, solvent effect cannot be the explanation.

c) AIMD Results

NVE AIMD runs for the dihydrate pTSA.W2A and trihydrates pTSA.W3B were performed in the gas-phase. The pTSA.W2A and pTSA.W3B data were collected for 12.2 ps and the pTSA.W3A for 20.3 ps following a 1 ps equilibration interval. Temperature for the dihydrate based on kinetic energy was 268 ± 26 K. From Figure 3.4a, the O1—O4 H-bond remained intact throughout while the O4—O5 H-bond present during 98.1% of the snapshots. Following Kumar's geometric criteria[77] for O_D-H*---O_A to be deemed H-bonded,[§] the O5—O2 bond broke and reformed several times. Starting at 2.84 ps, it remained severed for 55 ps and become attached to O3 via H4 instead of bonding via H4 to O2 when reformed. This pattern persists for the rest of the run. Overall, an H-bond was present from O5 to either O2 or O3 during 93.2% of snapshots (98.1% if $\beta_{cut} = 40°$). The dangling H's flips often.

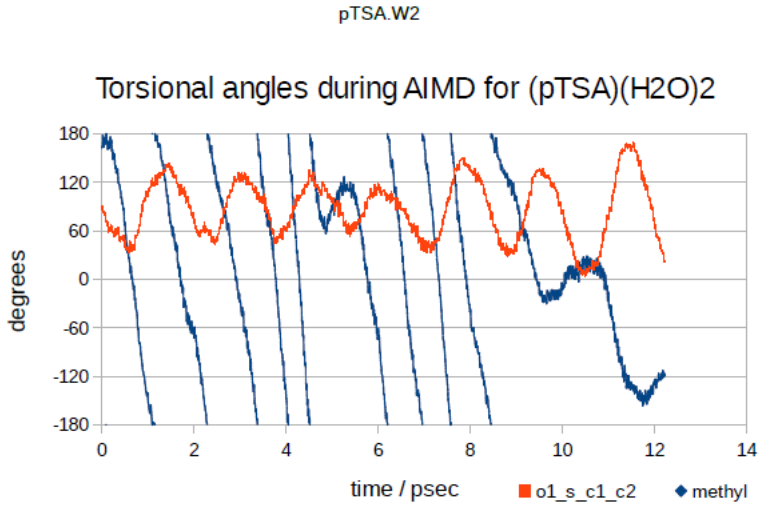

Figure 3.6 – Evolution of the torsional angles – measuring internal rotations – during the AIMD run. The methyl group (blue) spins freely. In contrast, there is no net rotation about the S-O bond.

[§] d(H*, O_A) < 2.5 Å, d(O_D, O_A) < 3.4, and β = angle(H*-O_D-O_A) < $\beta_{cut} = 30°$.

Figure 3.6 shows the instantaneous torsional angles, measuring internal rotations of the methyl (blue) and sulfonic (red). The methyl group spun freely (180° to -180°, making a 360° rotation) completing almost 10 net revolutions during the run. On the contrary, no net rotation was observed for the S—C bond but only mere oscillation across a mean position of ~90°. The transition state for rotation about the S—C has $\Delta G^{ts253} = 3.1$ kcal•mol^{-1} and occurs at orientations of -6° and 174° for the O1—S—C1—C2 dihedral angle. The dihedral angle of the optimized geometry is 81°.

The trihydrate run (pTSA.W3A) lasted for 20.36 ps and temperature 241 ± 29 K revealed a fairly stable bonding pattern. From Figure 3.4b, the O1—H1---O4 bond stays connected for the entire run and O4—H2---O5 was present for 99.9% of snapshots (100.0% if $\beta_{cut} = 35°$). An H-bond from O5 to O6 appeared in 98.0% of snapshots, which flipped once from using H4 to H5 midway through the simulation. The bond from O6 to O2 flipped from using H6 to H7 at 17.3 ps and "walked" to an O6—H6---O3 bond at 19.5 ps then "walked" back to O6—H7---O2 at 20.3 ps right before the run completion.

From 2.3 to 3.6 ps, an additional OS—H5---O3 H-bond formed, turning the structure to that of pTSA.W3C and the system also became topologically pTSA.W3C during 19.9 to 20.1 ps when an O5—H4---O2 bond occurred. Comparing the total of 1.5 ps of the additional bond with the 18.8 ps without it yields a ratio of 12.5 favoring pTSA.W3A over pTSA.W3C. This result is consistent with the ratio predicted in Table 3.1. The ΔG^{253} difference between pTSA.W3A and pTSA.W3C of 1.26 kcal•mol^{-1} equals 2.5 kT and predicts an occurrence ratio of 12.2. Although other trihydrate topologies including the pTSA.W3B would also occur in a long enough run, but the barriers to interchange are higher and were not overcome in this limited simulation.

Another simulation with the similar parameters were performed starting with the pTSA.W3B topology (Figure 3.4c) at 238 ± 23 K. This topology shows less bond stability than the pTSA.W3A and the From Figure 3.4c, the O1—H1---O4 bond was only intact for 6 fs when β crested at 31.2°. H1 "almost" transferred once when d(O1,H1) surged briefly to 1.17 Å. The O5 side was more stable during the run: an O4—H2---O5 bond (respectively, an O5—O2 bond via either H4 or H5) was present in 88.9% (respectively 84.9%) of snapshots. This percentage rose to 98.1% (respectively, 93.3%) when β_{cut} was raised to 40°, suggesting similar behavior to the dihydrate. The O6 water, on the other hand, is freer than the ones described above. The O4—H3---O6 bond was present for 69.2% and 76.0% for β_{cut} = 40° (47.0%, respectively). The configuration topology match the cluster pTSA.W3D, a high energy cluster, 43.2% of the time with the entire final 3.5 ps when the O6 water appeared to swing wildly on the end of the O4—O6 bond and remained far removed from the sulfonate, matching the low-energy pTSA.W3B (Figure 3.4c) just 14.6% of the time. Similarly, with the dihydrate, the methyl group spun freely, whereas the S—O bond only slowly oscillated. The methyl group completed seven revolutions in this run within the first 4 ps, then 10 more in the reverse direction prior to the run completion. This result is consistent with a classical calculation of the moment of inertia around the C—C bond of the methyl group, yielding 1.31 THz as the frequency when rotational kinetic energy is 1/2kT.

Although bond rearrangements are expected to happen more slowly in solvent than in gas phase, the simulations described still provides relevant insights to the matrix: the AIMD run support the idea of the unusual stability of the dihydrate. While the trihydrate with the pTSA.W3A topology (with ~8% as pTSA.W3C) seems stable, this picture has the possibility to change bond directions if it turns to pTSA.W3B. When converted, the flanking waters (i.e. O5 or

O6) is held very loosely by the trihydrate that they could be prone to "evaporation" into the matrix monomer population at this temperature. Contrastingly, when a dihydrate cluster interacts with a monomer, the monomer may join the cluster for a while. The general picture is a dynamic equilibrium where water molecules are exchanged among $(pTSA)(H_2O)_n$ clusters via the monomer population. Investigations on how the dynamics may change once $n \geq 4$ and the cluster dissociates are in progress. Preliminary data on $n = 7$ cluster shows frequent interchange among top four geometries (Figure 3.4e,f) but no proton transfers that affect the embedded H_3O^+.

d) D and H Position Preferences in D_2O

When the system contains both ^1H and D in which these isotopes are allowed to freely distribute into the various available positions for H, a "positional isotope effect" can be observed. For example, the central H of the Zundel cation is 2.3 times more likely to be H than D at 80 K.[31] Another well documented phenomenon of the HOD monomer binding to benzene is its preferred orientation with the O—D making the H-bond.[78-80] A previous computational studies of the "positional isotope effects" for a large database of $(H_2O)_n$ clusters found that a J-shaped curved accurately predicted the ZPE of replacing a single position with D as a function of the O—H* distance in the optimized structure.[81] This study also shows that there exist mild cooperativity effects when replacing two H by D atoms on the same or adjacent water molecules. This cooperation is small, thus a reasonable approximation is that the effect of multiple substitution is additive.

The reported experiments involved addition of D_2O followed by observing the O—^1H stretch resonances. In these experiments, a few exchangeable H atoms are ^1H from the original pTSA monohydrate (3 ^1H atoms per acid molecule) and a small amount of adventitious water in "dry" CCl_4, but the remainder (10, 14, or 18 hydrogen atoms per acid molecule) is D. Thus, the

water clusters in these systems consist of mainly D_2O with some small number of H substitutions. To investigate the positional isotope effects on the results (or, perhaps, lack thereof), computation on the free-energy difference between the cluster with all D and the cluster with all H were performed in both the pTS-.H+W11X (Figure 3.4h) as a representation of a cluster having a H-bond to the benzene ring and for the dihydrate. The procedure for this computation is outlined in reference 81.

Table 3.2. For two clusters, calculated ZPE change and free energy change (at –20℃) from switching a single position from D to H, along with the Boltzmann probability for that position to be H when there is just one H in the cluster.

	ΔZPE (D→H)	ΔG^{253} (D→H)	prob
pTS.H+ W11X			
H1	2.152	2.205	0.042
H2	2.036	2.155	0.046
H3	2.179	2.238	0.039
H4	2.158	2.200	0.042
H5	1.978	2.009	0.062
H6	2.120	2.155	0.046
H7	2.038	2.069	0.055
H8	2.176	2.235	0.039
H9	2.173	2.231	0.040
H10	2.031	2.152	0.046
H11	2.163	2.214	0.041
H12	2.148	2.220	0.040
H13	2.145	2.217	0.041
H14	2.176	2.226	0.040
H15	2.180	2.238	0.039

	ΔZPE (D→H)	ΔG^{253} (D→H)	prob
pTS.H+ W11X			
H16	2.032	2.154	0.046
H17	2.156	2.213	0.041
H18	2.183	2.238	0.039
H19	2.168	2.235	0.039
H20	2.147	2.219	0.041
H21	2.157	2.222	0.040
H22	1.955	2.130	0.048
H23	2.007	2.142	0.047
pTSA.W2A			
H1	2.043	2.078	0.234
H2	2.152	2.211	0.179
H3	2.017	2.153	0.201
H4	2.145	2.214	0.179
H5	1.986	2.139	0.207

The results from this study is listed in Table 3.2: $\Delta ZPE(D \rightarrow H)$ is the effect of single D-to-H substitution at the indicated hydrogen while the $\Delta G^{253}(D \rightarrow H)$ is the calculated free-energy difference at -20 °C. After one ^1H substitution with a Boltzman distribution at -20 °C, the last column shows the probability of each position having the ^1H. Hydrogen labels are the same as in Figure 3.4a,h. Without the positional isotope effect, these probabilities would be 1/23 = 0.043 and 1/5 = 0.2 for the two-water clusters.

These results are consistent with the theory in reference 81: positions in short H-bonds associated with the Eigen cation have the smallest substitution energy, followed by dangling H atoms, and lastly those in H_2O—H_2O H bonds. Figure 3.4h shows the H_3O^+ with a "+" sign with its three hydrogens H5, H6, and H7. The benzene-bonding H is H23, which is one of the more favored positions to be ^1H in the cluster overall. When the temperature is at -20 °C, the effect is small, thus it is only ~10% more likely to be ^1H than pure chance prediction. As for the dihydrate, the sulfonic acid is 30% more likely to be ^1H than the other bonding H atoms (H2 and H4). This result is uncertain for it is suspected that many pTSA molecules never dissociate in the low-water environment and those that becomes a dihydrate may keep the protium atom that they started with. For pTSA.W2A, a Boltzmann distribution may determine ^1H and D at H2 through H5, but not at H1.

3.3 Implications of the 3642 and 2835 cm^{-1} resonances

The experimental results of the aforementioned systems – pTSA-$(H_2O)_n$, pTSA-(H_2O)-$(D_2O)_{n-1}$, and pTS^-Na^+-$(H_2O)_n$ – along with the theoretical results support the existence of at least two structures in the CCl_4 matrix: a dihydrate with two water molecules interacting with the nonionized acid giving rise to the 2835 cm^{-1} and the other a large water cluster d—OH donating into the π ring giving rise to the 3642 cm^{-1}. Both of these resonances grow with addition of

water, suggesting a source consisting of relatively dry acid. Since the amount of water in this system is beyond the saturation point of water in CCl_4, there must be many water-water bonds. Thus, the method for assigning these resonances is as follows. The most intense water resonances are expected to be the Zundel and Eigen associated, but they are known to be very broad. Additionally, the nonhydronium water—water bonds are not observed because they are also known to be very broad under ambient thermal conditions. For nonwater-water interactions in these systems, the SO—H—OH_2 stretch is overrepresented, high-intensity, and is at the right frequency matching the resonance observed at 2835 cm^{-1}. Similarly, the water—π resonance is known[82] and would redshifts about -20 cm^{-1} with an electron withdrawing substituent such as the sulfonate[75] to be at the right frequency (3642 cm^{-1}) and to be narrower than water—water bands. Thus, this section focuses on discussing these two resonances and the smaller 3660 cm^{-1} shoulder. Then, the section concludes with a possible three-structure model: the dihydrate, the multiwater single-acid cluster π donation, and a relatively dry acid source that is consistent with observations.

a) 2835 cm^{-1}

Strong evidence presented in this studies support the assignment of this peak as an acid resonance. Experimentally, this resonance is not observed in the salt solution even though it contains many times more water in the system than in the acid solution. Since it is only present in the acid system, the possible assignment of this peak to any C—H stretching resonances of the toluene group or any hydrocarbon impurities is eliminated. Additional experimental observations narrow potential assignments: the frequency is unaffected by added water or with substitution of D_2O for H_2O to dissolve the acid, and the intensity increased with added H_2O and D_2O. Therefore, the associated structure must be stable.

The AIMD simulations of the dihydrate structure (Figure 3.4a) supports the claimed stability of this structure at -20 °C. Consistently, both the acid and salts[61] show that a two-water structure is IR-observable. When only two water molecules bind with the acid, a five-member ring is formed, thus stabilizing the dihydrate. Comparing the calculated binding energy of pTSA-$(H_2O)_n$ isomers at -20 °C for n = 1-12 (Table 3.1 and Figure 3.5), the dihydrate structure is preferred over other cluster sizes from n = 1-12 on a per water basis. Thus, there is strong experimental and theoretical evidence of the dihydrate existence in the acid solution.

Furthermore, the 2835 cm^{-1} resonance also increases in intensity when using D_2O to dissolve the acid monohydrate relative to the intensity gain using normal water. This observation suggests that the 2835 cm^{-1} is site specific in both normal water and D_2O. Absence of H/D exchange in the D_2O system does not make the ionization impossible at various points in the process as long as the H never departs from the S—O—H---O H-bond in which it starts.

b) 3642 and 3660 cm^{-1} Shoulder

Similarly, there is strong experimental and theoretical evidence that supports the assignment of the 3642 cm^{-1} resonance. This peak and the broad hydrogen bonded feature are not detected in the salt system, thus it must be associated with the acid system. Comparing the 3642 cm^{-1} resonance in normal and D_2O water, one could see that it is somewhat more intense in the normal water system than in deuterated system. The broad resonance is also more intense and structured in normal water. The broad feature from 3000-3550 cm^{-1} is non-detectable in the salt but noticeable in the acid, which is could be explained from the stronger polarization of the water by the acid.

The strongest d-OH resonances in this system is one donating into the aromatic π cloud, consistent with the π cloud polarizing OH bond, thus enhancing the oscillator strength. There is

ample precedent for this assignment,[82-90] especially the 4 cm^{-1} wide benzene—water stretch at 3642 cm^{-1} for n = 5 reported by Pribble and Zwier.[82] The assignment to a sulfonate donating OH resonance is eliminated since the intensity grows with n. Formation of this cluster is reversible as indicated by its disappearance on warming and reappearance in recooling, consistent with the weak OH—π bond.

The 3660 cm^{-1} shoulder is assigned the d-OH of the HOD water. A 3660 cm^{-1} resonance was observed previously in a CCl_4 matrix for mixed isotope water.[91] The heavy water system shows a larger 3660 cm^{-1} peak due to the contribution of both the d-OH of the cluster and of the HOD monomers. Consistently, the d-OD of this species is observed at 2689 cm^{-1} that grows with added D_2O.

c) A Possible Model Tying the 3642 and 2835 cm^{-1}

The assignments above – 2835 cm^{-1} to the dihydrate and 3642 cm^{-1} to the OH-π of a larger water cluster – suggest that there are at least two species existing simultaneously in the solution. Consider, then, a model with a multi-acid hydrated cluster reservoir, breaking into smaller units as water is added. The size and nature of the units show an interesting aspect of the CCl_4 matrix, since injection of neat water only results in monomers but larger clusters could exist when aqueous acid solutions are injected. The existence of the dihydrate (2:1 water/acid) in a 6:1 water/acid injected solution would require the existence of some units with larger water/acid ratios. This bimodal distribution is consistent with the asymmetric fission model of a water-organic droplet argued by Donaldson, Tuck, and Vaida[92,93] based on thermodynamics. The unexpected stability of the dihydrate is likely the driving force for its separation from the multi-acid multi-water cluster. Alternately, various sizes units may initially separate, then exchange with the monomer population, as suggested by the AIMD run of the trihydrate pTSA.W3B,

which then leads to an equilibrium distribution among cluster sizes in which dihydrates dominates for aforementioned reasons. The stability of the 2835 cm^{-1} resonance suggests that the H stays with the sulfonate and does not exchange with D. Additions of water to the pool caused more dihydrates detachments, increasing the 2835 cm^{-1} peak. D_2O is more efficient in this mechanism, thus the larger 2835 cm^{-1} enhancement with D_2O addition.

The larger-water clusters are somewhat of a mystery, as there are multiple possible interpretations of them. Previous work[62] mentioned that it could be a larger cluster detachment from the multi-acid multi-water cluster reservoir as a single acid multi-water cluster with a "scorpion tail" d-OH—π feature causing the 3642 cm^{-1}. Recent computational studies could not find a low energy cluster like one described above as *n* increases, therefore the existence of this cluster is not supported. Another model could be the shedding of a larger multi-acid cluster with a d-OH from a water molecule of one pTSA-$(H_2O)_n$ donating to the π ring of another pTSA-$(H_2O)_n$ cluster, resulting in the 3642 cm^{-1} resonance. Yet the 3642 cm^{-1} could also be the d-OH—π from the multi-acid multi-water reservoir. Although there are equivocal pictures on the structure of the larger acid cluster, it is unambiguous that the 3642 cm^{-1} is the result of the d-OH—π resonance. Polarization from the donation increases the oscillator strength and a slight bias for a d-OH instead of a d-OD in the mixed isotope system coupled with enhanced couple splitting with D_2O leads to a nearly isotope independent growth of the 3642 cm^{-1} resonance. Additional tuning of experimental methods are currently being conducted in order to elucidate the complete spectrum of pTSA-$(H_2O)_n$ without impurities. This spectrum could provide more information about the system as a whole as well as the structure of the larger acid cluster.

4: Large (pTSA)•$(H_2O)_n$ Clusters (n ≥ 20)

An interesting question to ask about this system is if this type of bimodal distribution would persist at lower acid concentration (more water than acid). Another question is whether the H of the SO—H---OH_2 bond would exchange when dissolve with larger amount of D_2O and how much D_2O is needed. It is also of interest to study larger water clusters near the "magic" number n = 21, since it has interesting stability properties that could provide insights into clathrate hydrates formation mechanisms. Furthermore, most gas hydrates are big water clusters ($n \geq$ 20),[29] therefore it makes sense to go toward this direction for this project. This chapter discusses the findings of large pTSA•$(H_2O)_n$ and pTSA•$(D_2O)_n$ clusters and promising new leads at 3420 and 1717 cm^{-1}.

4.1 Experimenta Results of Large H_2O and D_2O Clusters Spectra

a) 1:26 pTSA-H_2O and 1:1:25 pTSA-H_2O-D_2O

Figure 4.1 shows the 1:26 pTSA•(H_2O) solution in CCl_4. The method for this experiment is the same as described above. There are some notable new features about this spectrum. First, the 2835 cm^{-1} and the 3642 cm^{-1} are not only present, but also extremely intense and sharp even at room temperature. The 3642 cm^{-1} also seems like it has saturated. Several new features appear: a small "bump" at 3420 cm^{-1}, a broad H-bonded band at 3500 cm^{-1}, and some new features that overlap with the hydrocarbon impurities (covered but are discussed in Chapter 5).

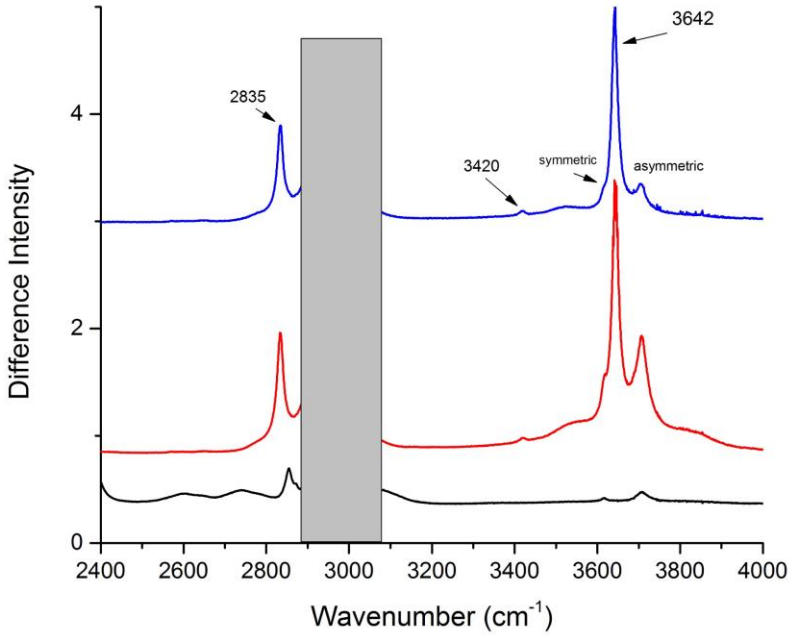

Figure 4.1 - Infrared spectra of pTSA and water in CCl_4 at room temperature (red) and at -20°C (blue). Spectra are difference spectra subtracting the room temperature, nominally dry CCl_4 spectrum. The black line is CCl_4 against cell background spectrum at room temperature, showing adventitious water. Note the intense 2835 cm^{-1} and 3642 cm^{-1} peaks along with the 3420 cm^{-1} bump. Spectra are offset for clarity.

The intense and sharp 2835 cm^{-1} and 3642 cm^{-1} peaks are consistent with the previous small clusters studies. Previous studies show that both the 2835 and 3642 cm^{-1} increase with increasing water concentration, thus these high intensity peaks are consistent with the trend. Nevertheless, it is quite unexpected that their intensities are this high. They imply large populations of both the dihydrate and d-OH—π clusters, both stable at room temperature and -20 °C. They also answer the question that the bimodal distribution persists at this acid/water ratio.

The 3420 cm^{-1} and 3500 cm^{-1} are H-bonded features. The 3420 cm^{-1} implies the existence of the hydronium ion in solution. The vibrational feature of the hydronium ion is known to be

broad and has not been observed at ambient energy conditions. Thus, the 3420 cm^{-1} feature is an important insight and is discussed in more details in Section 4.2. The overlapping features observed at the hydrocarbon impurities region are discussed in Chapter 5.

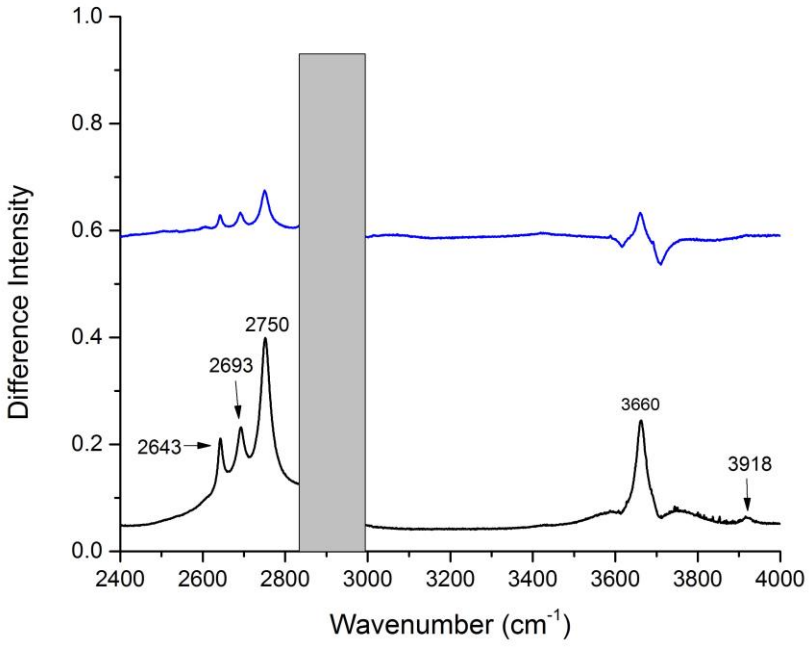

Figure 4.2 - Infrared spectra of pTSA and D_2O in CCl_4 at room temperature (black) and at -20 °C (blue). Spectra are difference spectra subtracting the room temperature, nominally dry CCl_4 spectrum. Spectra are offset for clarity.

Figure 4.2 shows the 1:1:25 (pTSA)-(H_2O)-(D_2O)$_{25}$ experiment. Two familiar resonances appear at 2693 and 3660 cm^{-1}, the OD and OH stretch of the HOD species, respectively. Additionally, the 2643 and 2750 cm^{-1} resonances are also observed. These are the symmetric and asymmetric stretches of the D_2O species. No H_2O monomer features, beside its rotational wings, are observed in the OH-stretching region. This observation shows that enough D_2O have been added to exchange virtually all H_2O species to the HOD species with D_2O monomers leftover. When the system is cooled down to -20 °C, the 2835 and 3642 cm^{-1}, which are the SO—H---OH_2 stretch of the dihydrate and the OH---π stretch of a bigger cluster, are not observed. This

observation shows that the H in SO—H---OH_2 that is responsible for the 2835 cm^{-1} had exchanged to become the D species. The same could be said about the 3642 cm^{-1}: its absence shows that the responsible H donation had become D. This is consistent with the model proposed in chapter 3.

A new feature shows up in this spectrum at 3918 cm^{-1}. This feature is assigned to be the first overtone of the S—O—D---OD_2 of the deuterium analogue of dihydrate, further evidence that deuterium exchange occurs at this acid-water-deuterium ratio. The lack of an O—D---π feature implies that it is less favorable for the OD stretch to donate into the π ring. More experimental and theoretical work must be done to elucidate this phenomenon.

b) Experimental Results for the 1:51 pTSA-H_2O Cluster

Figure 4.3 shows the spectra for the 1:51 pTSA-H_2O experiment against room temperature CCl_4 background. The sample was taken at room temperature (black line) and -20 °C (red line). Per usual, the symmetric stretch, asymmetric stretch, and the rotational wings are observed at the free OH stretching region at room temperature. Several new observations are also observed in this experiment. The 3420 cm^{-1}, like the 1:26 pTSA-H_2O experiment, is also observed here at both temperatures, accompanies by a 3480 cm^{-1} feature. When this sample is cooled to -20 °C, a very broad and structured H-bonded band is observed from 3000-4000 cm^{-1}. The 3420 and 3480 cm^{-1} features ride on this broad band at -20 °C. The monomer symmetric and asymmetric stretches decreased significantly, but did not disappear completely. This observation signals the loss of monomers to the H-bonded cluster and also that the cluster is at its equilibrium size and thus some monomers are left over. The 2835 cm^{-1} and 3642 cm^{-1} can be observed, but they are very weak and can only be seen as shoulders and not sharp, distinct peaks.

The well-structured H-bonded feature is typical of the existence of large water clusters[94-96] and ice.[97,98] This large cluster is likely to have multiple hydration layer with 3- and 4-coordinate water, and perhaps this is the reason that the 3642 cm^{-1} is quenched: there are many different d-OH on this cluster, thus multiple ways for the d-OH—π to interact which then leads to a broad distribution and therefore resulted in broader resonances instead of a sharp peak.

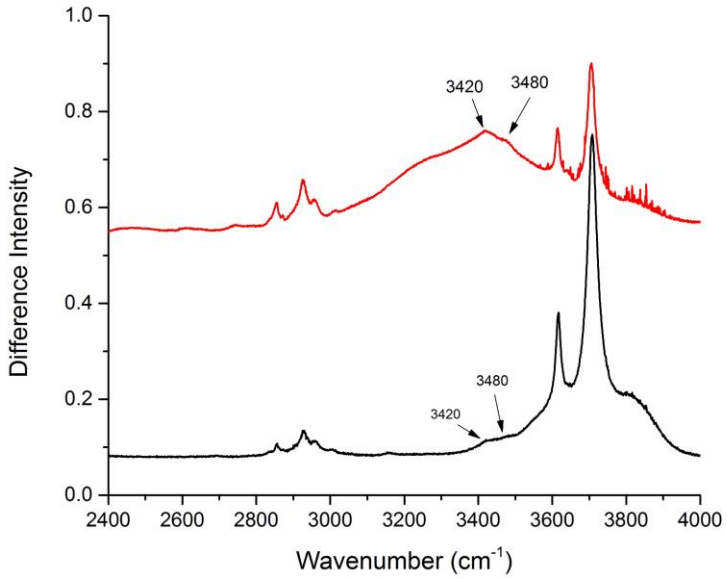

Figure 4.3 – Infrared spectra of the 1:51 pTSA-H_2O sample against room temperature CCl_4 spectrum. The sample was taken at room temperature (black line) and at -20 °C (red line). The features from 2850-3000 $cm^{-1}$are hydrocarbon impurities, which are discussed in more details in Chapter 5. Spectra are offset for clarity.

The lack of the 2835 cm^{-1} and 3642 cm^{-1} as well as the appearance of a much more intense H-bonded structure signify that the distribution of water clusters in this system no longer follows the bimodal theory proposed above. This result answers the question: does the bimodal distribution persists in bigger cluster system presented earlier in the chapter. It was determined, by experimental results, that this distribution persists at 1:26 pTSA:H_2O ratio. At 1:51, the bimodal distribution collapses, giving rise to a large cluster with multi-hydration layers. The

threshold ratio at which this bimodal distribution collapsed and the structure as well as geometry of this multi-hydration cluster are still unknown. Experimental data with acid:water ratio between 1:26 and 1:51 are needed to see whether there is a pattern of gradient (i.e. a slow decrease of the 2835 and 3642 cm^{-1} and a slow increase of the H-bonded band) or a sudden collapse at specific acid:water ratio. Theory could then be applied once a clear pattern, or lack thereof, could be established. Nevertheless, some observations from this experiment are consistent behaviors of larger clusters ($n \geq 20$): the 3420 cm^{-1} "bump" and the 1717 cm^{-1} sharp peak.

4.2 A Promising Lead for Observing the H_3O^+ at Ambient Energy: 3420 cm^{-1} and 1717 cm^{-1}

3420 cm^{-1}. The small "bump" at 3420 cm^{-1} is analogous to previous studies of salt ions and water in CCl_4.[61] A small "bump" is also observed in this study at 3440 cm^{-1} and is assigned the water-water bond of a dimer induced by the cation. With only a 20 cm^{-1} difference and in the H-bond region, the 3420 cm^{-1} is probably the water-water bond, but whether it is of the dihydrate or not is unclear. A similar peak at around 3450 cm^{-1} is shown in the predicted spectrum of the dihydrate (see Appendix), which is the d-OH donating to one of the =O on the sulfonate group.

The region between 3400 and 3450 cm^{-1} have shown up in multiple SFG studies on ice[99,100] and spectroscopic studies on aqueous ionic solutions,[101,102] to name a few. Despite the multiple reports, few have given a definitive assignment on this feature. On the SFG study of the prism face of ice,[99] Bisson and Shultz reported and assigned a resonance at 3415 cm^{-1} to three coordinate water that has only a single donor to the 4-coordinate water in the bottom half of the top bilayer. Gopalakrishman *et al.*[102] reasoned that the increase of the 3450 cm^{-1} resonance in a salt ionic solution is from the increased ordering of the interfacial water molecules under the influence of a local weak electric field induced by dianions in aqueous Na_2SO_4 and $(NH_4)_2SO_4$

and/or an increase in the interfacial depth. Shultz and Allen *et al.*[101] reported the same 3450 cm^{-1} in acidic solutions, claiming that its enhancement is caused by a short range polar ordering due to the negative ion at the interface.

The 3420 cm^{-1} resonance falls in this range and is consistent with the aforementioned studies. It is only observed when the acid/water ratio decreases (more water than acid), similar to the "bulk" amount of water in ice and aqueous solutions. The aforementioned studies observed the 3400-3450 cm^{-1} features at the water/air interface, which is a water/hydrophobic interface, analogous to that of water/CCl_4 interface. Therefore, there is precedent to assigning the 3420 cm^{-1} feature as the 3-coordinate water molecules with a single H donating to a 4-coordinate water molecules at or near the interface.

This interpretation provides insights into the structure of the acid/water cluster. First, for the above interpretation to work, the cluster size has to be quite large, which is consistent with the acid/water ratio used for both aforementioned experiments (1:26 and 1:51 pTSA:H_2O). Second, increased ordering induced by the local electric field of the anion would require that the pTSA molecule in the cluster be ionized. According to theoretical calculations, as mentioned above, the acid proton would be ionized when n = 8. Although the exact threshold is experimentally unknown, the ratios of acid:water in the large cluster experiments are much larger than 8, thus the acid is expected to be ionized. Therefore, the interpretation that this peak was caused by the increased ordering due to the local electric field of the anion is consistent.

Enhanced ordering of the water on the interfacial surface could also be caused by the hydronium ion on the exterior. The hydronium ion is amphiphillic[66] with three covalently bonded hydrogen to the oxygen and one lone pair. In a bulk water solution, it is pushed to the exterior, similar to the hydrophobic effect.[64,65] It has a solvation asymmetry, donating all three hydrogen

atoms when H-bonded to other water molecules while not accepting any H-bond, which in turns caused increased ordering of the water molecules in its vicinity. Thus, the rise of the 3420 cm^{-1} could have been caused by the water molecule in the vicinity of the hydronium ion in the water/CCl_4 interface.

The above interpretations of the 3420 cm^{-1} give us a simple picture: water is sandwiched between the ionized pTSA molecule and the H_3O^+. This is consistent with the findings in Bisson and Shultz's studies of salts in CCl_4[61] as well as our theoretical results. The 3420 cm^{-1} also confirms the existence of the hydronium in solution and that the acid is ionized at 26 water to 1 acid solution. The threshold at which the acid is ionized is still experimentally unknown, although theoretical calculation suspected that ionization of pTSA occurs at $n = 8$.

1717 cm^{-1}. Figure 4.4 shows the 1717 cm^{-1} resonance for the 1:26 and 1:51 (pTSA)•$(H_2O)_n$ experiments. The 1717 cm^{-1} for the 1:26 experiment is quite intense – to the point of saturation in the spectrum. The same peak for the 1:51 experiment is less intense, although is still quite sharp. Both are observed at room temperature and at -20 °C and are not observed in the small cluster experiments discussed in Chapter 3.

This 1717 cm^{-1} peak is quite promising, for it falls in the region where bending modes of water in different bonding environment exist. Notably, resonances assigned to be the bending mode of the hydronium ion have been reported in the region between 1700 and 1800 cm^{-1}.[103] Since this resonance only is only observed in bigger clusters, it is consistent with the picture provided above from the interpretation of the 3420 cm^{-1} where the hydronium ion is on the interface of water/CCl_4. Preliminary calculations suspect that this resonance might be due to the coupling of the stretching and bending motion of the Zundel cation. Many obstacles, both

computationally and experimentally, are still needed to be overcome before a definitive assignment of this peak.

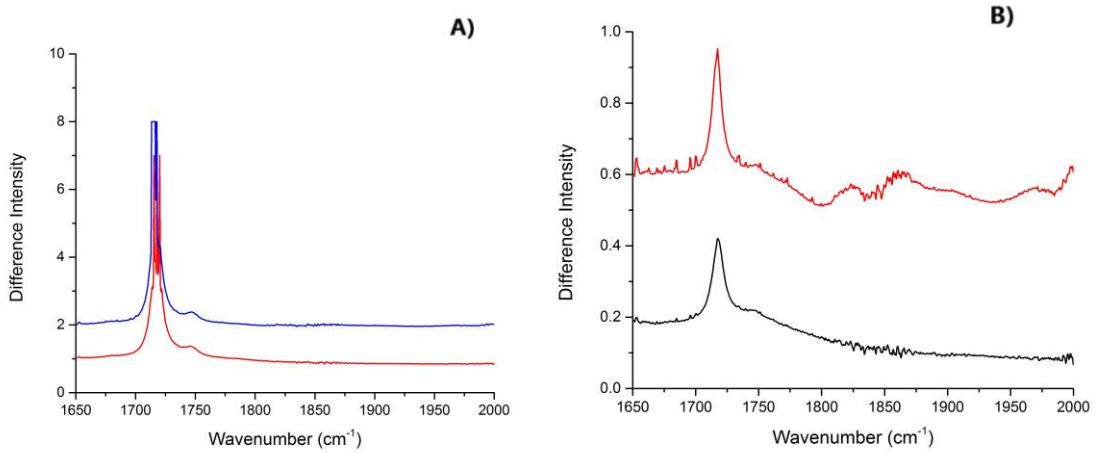

Figure 4.4 – A) The 1717 cm^{-1} peak of pTSA-H_2O with ratio 1:26 against room temperature CCl_4 background spectrum. The sample was taken at room temperature (red line) and at -20°C (blue line). B) The 1717 cm^{-1} peak of pTSA-H_2O with ratio 1:51 against room temperature CCl_4 background spectrum. Notice the different scales of A and B and that the 1717 cm^{-1} in A is much more intense than in B. The reason for this is under investigation. Spectra are offset for clarity.

Experimentally, the region from 1650 to 2000 cm^{-1} is where some unknown absorption features from CCl_4 are observed. These features could be seen in the cold spectrum of the 1:51 (Figure 4.4b), and they could be from the CCl_4 absorption or from hydrocarbon impurities. Therefore, "cleaning" this region would be ideal for more information. Computationally, the bending mode of the hydronium ion has not been studied extensively in the literature, thus it is difficult to claim any particular bending mode to be responsible for this feature. Additionally, due to the bimodal distribution nature of this system, it is impossible to know the size and structure of this cluster that is responsible for the 1717 cm^{-1}. Thus, more experimental data are needed. For example, CsOH could be added to test whether the 1717 cm^{-1} is indeed a feature of an acidic species. CsOH is a base, thus is expected to balance the positive charge from the acid. Cs^+ is a large and polarizable cation, thus is not suspected to be interacting with the system

significantly. If the 1717 cm^{-1} diminished after the introduction of CsOH, then it could indeed be concluded to be an acidic feature. The 1717 cm^{-1} is quite promising, for if it is a feature caused by the hydronium or Zundel cation, it would be the first time it is observed at ambient energy conditions.

5: Hydrocarbon Impurities

Hydrocarbon impurities are inherent in CCl_4, probably residues from its synthesis. Their features range from 2800-3100 cm^{-1}. Although these residues are minimal – CCl_4 use in the experiments above are 98.5% and 99.9% pure – their resonances can be seen in IR spectroscopy. Other methods besides FTIR have been used, namely H-NMR and C-NMR, without prevail. This section shows their FTIR features, some attempts of identifying them, and their implications in the presence of pTSA.

5.1 Hydrocarbon Impurities Experimental Spectra and What They Are Not

Figure 5.1 shows typical hydrocarbon impurities vibrational resonances from 2800-3000 cm^{-1} (black line). A Lorentzian deconvolution of this spectrum shows at least five resonances: 2854 cm^{-1}, 2872 cm^{-1}, 2903 cm^{-1}, 2926 cm^{-1}, and 2958 cm^{-1}. These peaks could be from one molecule with multiple C—H stretches or multiple molecules with different C—H stretches. According to the U.S. National Library of Medicine,[104] CCl_4 is synthesized by reacting carbon disulfide with chlorine and a catalyst, chlorination of hydrocarboms (namely CH_4), or pyrolysis of perchloroethane (C_2Cl_6). The first reaction does not produce any hydrocarbon, but the second and third reactions do. They are shown below.

(1) $$CH_4 + 2Cl_2 \rightarrow CCl_4 + H_2$$

$$\textbf{Side Products: } CHCl_3, CH_2Cl_2, CH_3Cl$$

(2) $C_2Cl_6 + Cl_2 \rightarrow 2CCl_4$

Side Products: $C_2HCl_5, C_2H_2Cl_4, \ldots, CH_5Cl$

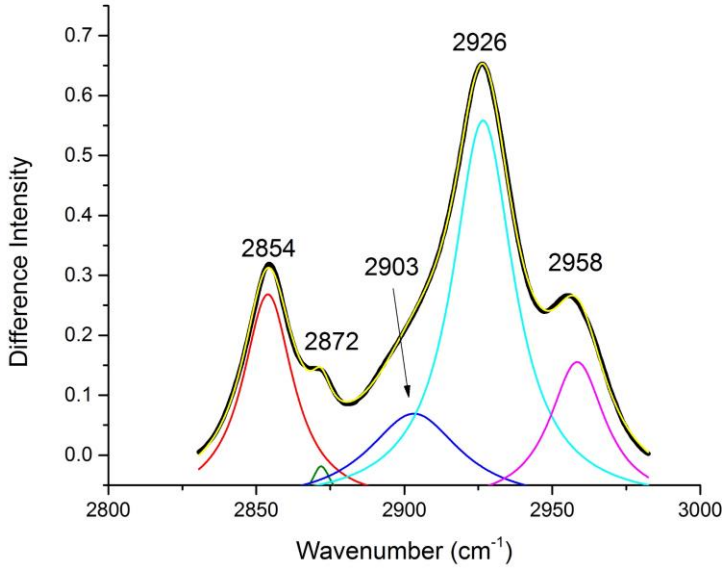

Figure 5.1 – Experimental FTIR spectrum of typical CCl_4 hydrocarbon impurities resonances (black line). Lorentzian fits deconvolution shows at least 5 resonances combined to form an excellent cumulative spectrum (yellow).

Although the second reaction does not produce hydrocarbon side products directly, the perchloroethane that was used for the reaction could have contained some side products. The first reaction produces the side products chloroform ($CHCl_3$), dichloromethane (DCM, CH_2Cl_2), and Chloromethane (CH_3Cl). These side products are easy to investigate: chloromethane is a gas at room temperature (boiling point -24.2 °C), therefore is not expected to be in solution. Chloroform and DCM are common solvents, thus were injected to CCl_4 solution with the same procedure as described above. Their peaks are shown in Figure 5.2. One C—H stretch peak is observed for chloroform at 3017 cm^{-1} and two for DCM (symmetric, 2982 cm^{-1}, and asymmetric,

3049 cm^{-1}), as expected. These peaks, although are within the region, are not the exact peaks of the impurities. Therefore, they are ruled out.

The side products of the second reaction are more complicated, as they are more numerous. A literature search[105] or their resonances in CCl_4 as well as some pilot theoretical calculations show that indeed they are within the region, but no matches were found. Although the search for the identity(ies) of the hydrocarbon impurity(ies) was unsuccessful, it is confirmed that they are indeed hydrocarbon impurities, since they are within the hydrocarbon impurities region. Since the motivation for this project was to observed pTSA's role in promoting gas hydrate formation, it is important to observe how the impurity peaks are affected by the addition of pTSA and water and what those effects imply.

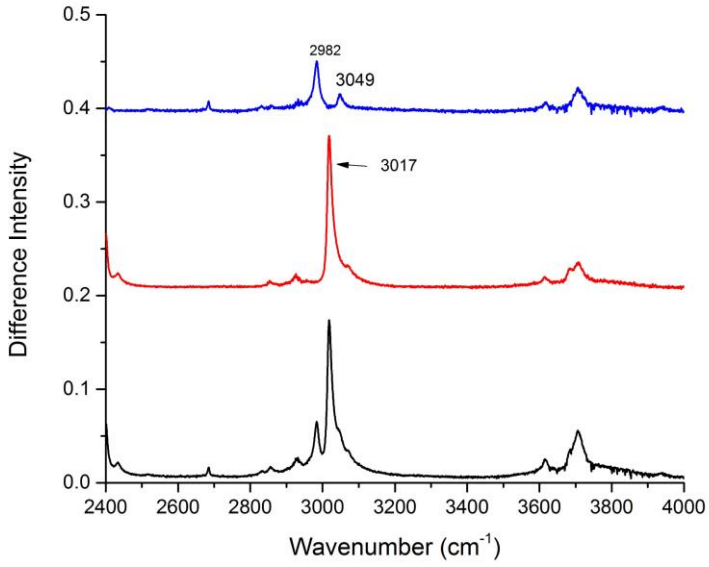

Figure 5.2 – FTIR spectra of DCM and chloroform against room temperature CCl_4 (black line), of only chloroform (red line), and of only DCM (blue line). Spectra were taken at room temperature

5.2 Implications of the Hydrocarbon Impurities in the Presence of pTSA

Figure 5.3a and 5.3b show the deconvoluted experimental spectra of the room temperature and cooled 1:6 pTSA/water from 2800-3200 cm^{-1}. These features were covered in Figure 3.1 for clarity. The features in Figure 5.3a are the same as the impurities features in Figure 5.1. Comparing Figure 5.3b to Figure 5.1, one could see that there are some subtle differences. The most obvious one is the 2835 cm^{-1}, as discussed above. A small shoulder (cyan line) also seem to occur at 2894 cm^{-1}. Perhaps the most pronounced differences are observed in the deconvolution of the peaks at the hydrocarbon stretches in the 1:26 experiment, shown in Figure 5.3c. These peaks are intense and sharp as well as being at completely different frequency than the impurities peaks, save the 2953 cm^{-1} resonance. These resonances did not show up in previous experiments with only water, but shows up here after pTSA is added. Thus, there are reasons to believe that perhaps these are either pTSA-water cluster peaks or pTSA-water-hydrocarbon related peaks. The 2835 cm^{-1}, although are closed in frequency to these resonances, can be classified as not an impurity because it changes with the addition of water, whereas the impurities resonances only change with the initial addition of pTSA-water cluster. A method of cleaning the CCl_4 solution using TiO_2 is currently underway. Removing the hydrocarbon impurities would elucidate the spectrum more, thus provide more insight into the solvation mechanism of pTSA and water.

The increase in intensity of these hydrocarbon impurities resonances in the presence of pTSA is consistent with Gnanendran and Amin works[16,17] on pTSA as a hydrate promoter as mentioned in the earlier chapters. They claim that pTSA improves the efficiency of gas hydrate formation by solubilizing more nonpolar gases (CH_4, for example) into the solution, thereby increasing the hydrate storage capacity. They also claim that the anionic species is more efficient at this task.[16] This is also observed in the experimental data: the impurities peak for the salt

experiment at 2854 cm^{-1} (Figure 3.3) is sharper and more intense than the ones in the other two experiments where pTSA and not $Na^{+}pTS^{-}$ was used.

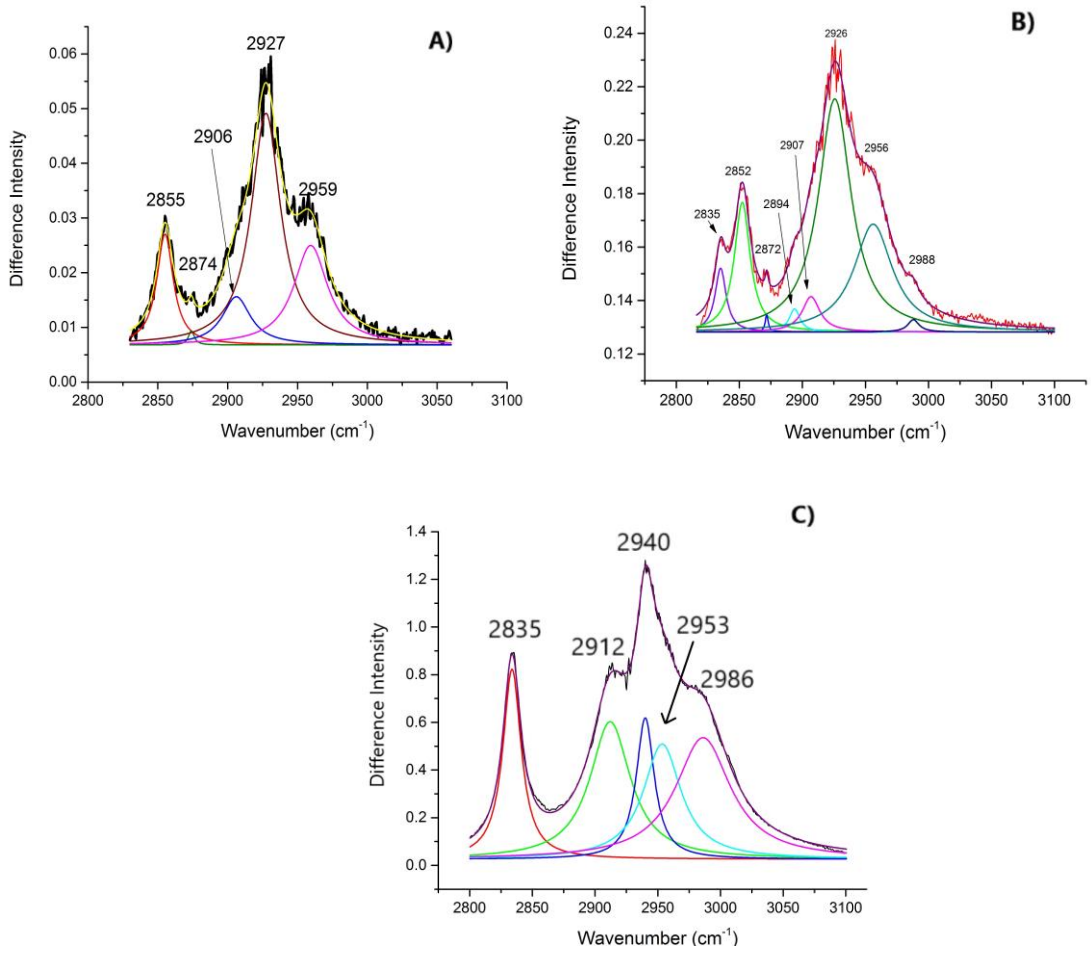

Figure 5.3 – A) Experimental data of the black line (room temperature 1:6 pTSA:water against CCl_4 background) covered by the gray bar in Figure 3.1. B) Experimental data of the red line (-20 °C 1:6 pTSA:water against CCl_4 background) covered by the gray bar in Figure 3.1. C) Experimental data of the black line (room temperature 1:26 pTSA:water against CCl_4 background) covered by the gray bar in Figure 4.1. All three spectra are deconvoluted by Lorentzian fits.

Consider a system where the hydrocarbon impurities concentration is high enough so that they phase separated to another layer not in the CCl_4 solution and only a small, saturated amount is left. This small, saturated amount gave the original peaks, which would be canceled out from

the background subtraction. The addition of pTSA, then, solubilizes more hydrocarbon impurities from the phase separated layer, bringing more of them into the CCl_4 solution, thus increase the intensity of the impurities resonances. The anionic species is more efficient at this, therefore more impurities are solubilized and thus the peaks are sharper. To test this hypothesis, SFG could be use to determine if an interface between some hydrocarbon and CCl_4. This interpretation is a promising insight, since it shows pTSA potential as a gas hydrate promoter. Eventually, perhaps gas hydrate formation mechanism could be studied using this system by employing a known hydrocarbon, such as methane.

6: Summary and Future Works

Natural gas hydrate is a potential new technology that could be used to remove CO_2 from the atmosphere or as a medium for gas storage and transport. Current manufacturing methods of natural gas hydrates are not cost efficient, since gas hydrates require a high pressure and low temperature environment to form. Even then, the production rate is too slow. Therefore, gas hydrate promoters, which increase the production rate thereby improve cost-effectiveness, are of great interests. Among the promoters, pTSA have been studied on a macroscopic level and concluded to be more efficient than surfactants.[16,17] This project studies pTSA's solvation mechanism in water on a molecular level using a CCl_4 matrix and FTIR spectroscopy in an attempt to give some insights into how pTSA works as a gas hydrate promoter.

Since water exists as monomers in CCl_4,[1] only the symmetric and asymmetric stretches as well as the rotational wing about the symmetry axis can be observed at the free-OH stretching region. Monitoring this picture after adding a molecule of interest could give insight into the molecule's interaction with water. Experimental results for pTSA small clusters ($n \leq 10$) found a

few new features arising at -20 °C: 2835 cm^{-1} resonance, 3642 cm^{-1} resonance, and a small but structured H-bonded region. Through complex computational methods, the 2835 cm^{-1} is assigned the SO—H---OH_2 of the dihydrate species where the acidic proton is not yet ionized. The 3642 cm^{-1} is assigned the OH---π. The cluster that is responsible for the 3642 cm^{-1} is expected to be large ($n \geq 12$), although the specific size and geometry of this cluster is unknown. This cluster could also be a multi-acid multi-water cluster. The existence of both the dihydrate and larger cluster give rise to the possible asymmetric fission model proposed by Donald, Tuck, and Vaida.[92,93]

A study of larger cluster ($n \geq 20$) also contains the above features with some new features: a small "bump" at 3420 cm^{-1} and a sharp peak at 1717 cm^{-1}. The region between 3400 and 3450 cm^{-1} has been observed in many SFG and ice studies[99,100] as well as in aqueous solutions[61,101,102]. It is assigned in these studies to be the feature of a 3-coordinate water on the top layer at the air-liquid interface donating to the second layer of the water H-bonded system with one weak H-bond. The rise of this resonance is caused by an increased in ordering of the water H-bonded network caused by the local electric field of the anion. The increase in ordering could also be caused by having the hydronium ion at the interface.[66] The hydronium ion is amphiphilic, thus have an asymmetric solvation mechanism. Therefore, the water around the hydronium can only accepts H-bond donated by it. The water in its vicinity then becomes a 3-coordinate water (DDA) and donate to the bottom half layer at the interface. Thus, the existence of this peak is evidence that the hydronium is in the solution, meaning the acid is ionized.

The 1717 cm^{-1} is also another piece of potential evidence for the existence of the hydronium in solution. The bending mode of the hydronium ion has been reported to be from 1700 to 1800 cm^{-1},[103] although not at ambient energy condition. If the 1717 cm^{-1} is indeed the

bending mode of the hydronium ion, then this study would be the first to report a hydronium feature at ambient energy condition. Unfortunately, the bending mode of the hydronium ion is difficult to model computationally. Furthermore, the structure, size, and geometry of the big cluster, where the hydronium ion supposedly exist, are still unknown. Therefore, more experimental and computational results are needed for definitive assignments. Nonetheless, the 3420 cm^{-1} and 1717 cm^{-1} give rise to a little glimpse into what the large cluster looks like: water is sandwiched between the anionic pTS^- species and the cationic hydronium ion. This picture is consistent with the works done on ionic salts reported by Bisson and Shultz,[61] where they observed a similar feature at 3440 cm^{-1}.

Some efforts have been given to identify the hydrocarbon impurities that give rise to the features from 2850-3000 cm^{-1}. Although the conclusion was not definitive, the behaviors of these features show pTSA's potential as a promoter. Gnanendran and Amin reported that pTSA, a hydrotrope, is more efficient than surfactants as a gas hydrate promoter because it can solubilize more hydrophobic species, thus increase the storage capacity of gas hydrate.[16,17] They also reported that the anionic species is more efficient at this task. Since the experiments were done with background subtractions, an increase in intensity of the hydrocarbon impurities peaks after the addition of pTSA means that more of those molecules are brought into solution as a result of adding pTSA. This increase is especially more intense in the salt experiment. Thus, there is reason to believe that there is another layer of hydrocarbon impurities on or below CCl_4, and pTSA solubilize them into solutions. This result is consistent with Gnanendran and Amin's works and is promising for future works with hydrocarbon-pTSA-water systems.

A project is currently being developed to clean CCl_4 of the hydrocarbon impurities with TiO_2. This work takes precedent, since more information could be extracted at that region. After

CCl_4 is cleaned, an experiment could be conducted where a hydrocarbon of interest is introduced to the solution so that its molecular interactions with pTSA-water could be elucidated. This experiment has the potential to impact the petroleum industry, since the promoter-hydrate formation mechanism is still lacking. An experiment where CsOH is added to a system where the 1717 cm^{-1} appears could be performed. CsOH is a base, and Cs^+ is polarizable since it is a big ion therefore is not expected to interact with the system. If the 1717 cm^{-1} is quenched after the addition of CsOH, then it is indeed an acidic feature. Another interesting experiment could be to study pTSA-water in CCl_4 at the interface using SFG. This could potentially give more insight to the orientation of pTSA-water clusters at the interface with CCl_4, and perhaps give more information on the hydronium features at the interface.

Appendix

1. Spectra of CCl_4 at room temperature and at -20 °C - Figure S 1
2. Spectra of CCl_4 with no acid-water: both 99.5% and 99.9% pure - Figure S 2
3. Selected clusters from Table I and illustrated in Figure 4 coordinates - Table S 1
4. Predicted stretch spectrum of the dihydrate - Figure S 3
5. A preliminary look at the case of *n*=7 water finds frequent interchange among the top four geometries (see Figures 4(e), 4(f)) but no proton transfers that affect the embedded H_3O^+.

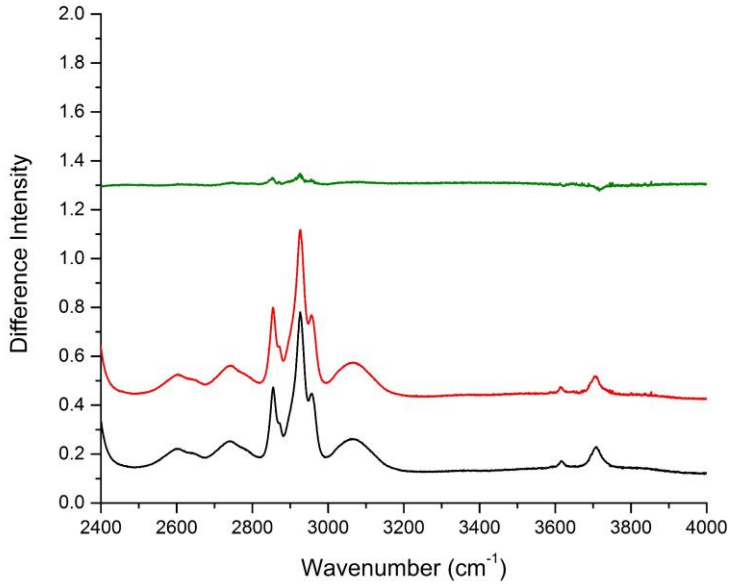

Figure S 2. 99.5% pure CCl_4 at room temperature (black line) and -20 °C (red line) along with the difference spectrum (green line).

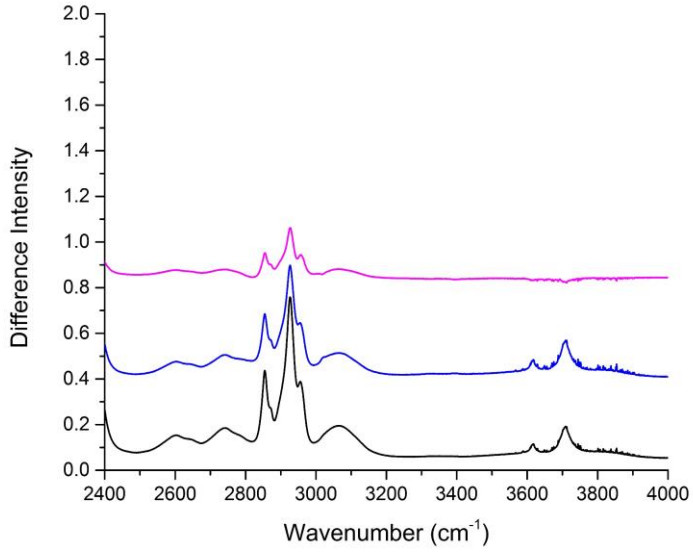

Figure S 1. 99.5% pure CCl_4 (black line), 99.9% pure CCl_4 (blue line), and the difference between the two (magenta line) at room temperature.

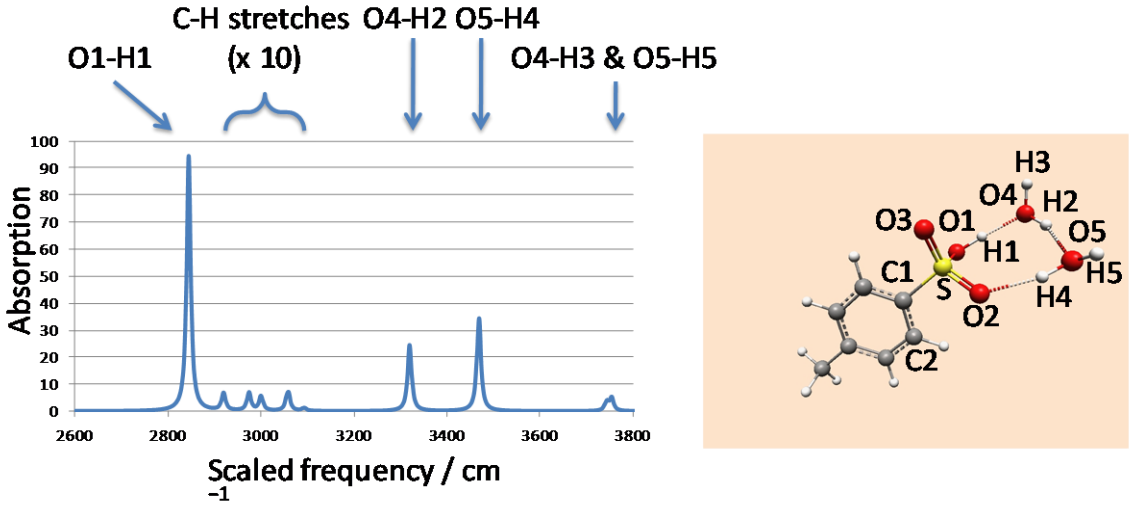

Figure S 3: Stretch region of predicted IR spectrum of $(pTSA)(H_2O)_2$. Computed frequencies are scaled by 0.965. Though plotted here as if all peaks have width 10 cm^{-1} at half-height, we propose that the water-O stretches at 3320 and 3469 cm^{-1} are not seen experimentally because they are substantially broader than the (S-)O1-H1 stretch at 2844 cm^{-1}. Figure 4(a), containing the labeling of O's and H's, is reproduced here for the reader's convenience.

Table S 1: Atomic coordinates in xyz format for all clusters listed in Table 3.1

22

pTSA.W1

c	2.299258	-0.165678	-0.362763
c	1.565039	-0.231573	0.826572
h	2.085338	-0.217096	1.778121
c	0.177151	-0.319187	0.812870
h	-0.383270	-0.382409	1.736834
c	-0.484035	-0.338709	-0.412119
c	0.217805	-0.278606	-1.613842
h	-0.316102	-0.308778	-2.554976
c	1.604384	-0.190416	-1.578027
h	2.155913	-0.142747	-2.510860
c	3.805872	-0.101591	-0.339756
h	4.237374	-1.101772	-0.454423
h	4.190303	0.514779	-1.155441
h	4.173869	0.309418	0.602229
s	-2.269551	-0.428296	-0.455030
o	-2.722930	1.127561	-0.424035
o	-2.676026	-0.963732	-1.738764
o	-2.736518	-1.042721	0.796065
h	-3.069109	1.353925	0.479271
o	-3.668971	1.218118	2.113840
h	-3.610266	0.248375	2.106879
h	-4.575529	1.441136	2.347354

25

pTSA.W2A

c 3.127038 -0.176552 -0.212190

c 2.363780 -0.022151 0.952158

h 2.863448 0.120776 1.904230

c 0.975401 -0.049665 0.911681

h 0.389487 0.060527 1.815223

c 0.343188 -0.231245 -0.316204

c 1.071106 -0.389127 -1.491356

h 0.555177 -0.537121 -2.431367

c 2.460498 -0.359286 -1.428434

h 3.034666 -0.480316 -2.340595

c 4.633925 -0.176099 -0.149602

h 5.012470 -1.182359 0.060115

h 5.072320 0.148958 -1.095173

h 4.999627 0.481997 0.641500

s -1.437893 -0.264915 -0.393427

o -1.743928 1.308565 -0.382285

o -1.953951 -0.850181 0.856974

o -1.865026 -0.855006 -1.655657

h -2.731584 1.487362 -0.253289

o -4.305037 1.687532 0.048273

h -4.602059 0.977046 0.662001

h -4.910702 1.686067 -0.699060

o -4.558521 -0.429651 1.727716

h -3.658423 -0.756304 1.533697

h -5.135007 -1.198853 1.735072

28

pTSA.W3A

c 3.713522 -0.361455 -0.279360

c	2.831550	-0.069020	-1.326465
h	3.211457	0.011524	-2.339205
c	1.475581	0.128383	-1.092352
h	0.798793	0.369232	-1.902007
c	0.998089	0.029294	0.211688
c	1.849133	-0.252185	1.276594
h	1.456749	-0.304605	2.284159
c	3.202394	-0.443974	1.020978
h	3.872694	-0.655969	1.846981
c	5.177934	-0.602159	-0.548427
h	5.795159	-0.291969	0.297344
h	5.368838	-1.666918	-0.720758
h	5.515180	-0.061161	-1.434853
s	-0.738260	0.277786	0.537702
o	-1.295662	-1.186922	0.243627
o	-1.262500	1.206090	-0.479070
o	-0.940128	0.616668	1.943447
h	-2.258107	-1.299244	0.573006
o	-3.719122	-1.488093	1.057049
h	-4.389280	-0.917213	0.602603
h	-3.845542	-1.360712	2.002728
o	-5.420673	0.186913	-0.168671
h	-5.962000	-0.088073	-0.914171
h	-4.910170	0.975766	-0.466950
o	-3.800501	2.230837	-0.921585
h	-3.842419	3.099294	-0.510654
h	-2.882707	1.917885	-0.793378

28

pTSA.W3B

c	3.553727	-0.156419	0.000000
c	2.838353	-0.178309	1.202984
h	3.375423	-0.162883	2.145174
c	1.448930	-0.220932	1.214211
h	0.898556	-0.247635	2.145800
c	0.768075	-0.239468	0.000000
c	1.448930	-0.220932	-1.214211
h	0.898556	-0.247635	-2.145800
c	2.838353	-0.178309	-1.202984
h	3.375423	-0.162883	-2.145174
c	5.061769	-0.141235	0.000000
h	5.458565	-1.162191	0.000000
h	5.455341	0.363073	-0.884884
h	5.455341	0.363073	0.884884
s	-1.013666	-0.270982	0.000000
o	-1.352509	1.273739	0.000000
o	-1.479065	-0.880726	1.255895
o	-1.479065	-0.880726	-1.255895
h	-2.397153	1.434814	0.000000
o	-4.090446	-0.197973	2.133167
h	-3.208945	-0.590714	1.997912
h	-4.186010	-0.054569	3.078825
o	-3.854247	1.532238	0.000000
h	-4.164417	1.035420	0.786124
h	-4.164417	1.035420	-0.786124
o	-4.090446	-0.197973	-2.133167
h	-3.208945	-0.590714	-1.997912
h	-4.186010	-0.054569	-3.078825

28

pTSA.W3C

c	3.597551	-0.136939	-0.033033
c	2.859308	-0.836272	0.928622
h	3.377809	-1.427421	1.675604
c	1.470010	-0.782999	0.949658
h	0.901349	-1.314227	1.702004
c	0.814572	-0.015605	-0.008965
c	1.518315	0.699089	-0.974958
h	0.986694	1.304355	-1.698053
c	2.906514	0.632427	-0.977021
h	3.462258	1.191895	-1.721669
c	5.102678	-0.225323	-0.065572
h	5.427167	-1.028639	-0.735767
h	5.548907	0.703032	-0.428269
h	5.511755	-0.438280	0.923989
s	-0.965388	0.060880	-0.003027
o	-1.408263	1.313510	-0.625309
o	-1.444929	-0.219221	1.360040
o	-1.312951	-1.165626	-0.954294
h	-2.305745	-1.175045	-1.221572
o	-4.070134	0.544425	2.086919
h	-3.144389	0.249714	2.006790
h	-4.123718	1.052594	2.901220
o	-4.391995	1.290074	-0.587843
h	-3.523896	1.699745	-0.719617
h	-4.450050	1.162409	0.380079
o	-3.798639	-1.107053	-1.603308

h -4.159298 -0.236017 -1.280720

h -4.385495 -1.795482 -1.275928

28

pTSA.W3D

c 2.789409 2.333818 0.543405

c 1.735798 1.982123 1.395413

h 1.526225 2.593042 2.266956

c 0.953060 0.860234 1.147513

h 0.146892 0.584267 1.815289

c 1.229570 0.080891 0.027628

c 2.271753 0.401416 -0.837400

h 2.474160 -0.227722 -1.694748

c 3.042408 1.528434 -0.572699

h 3.855299 1.784213 -1.243946

c 3.653767 3.534378 0.838526

h 4.006896 4.006590 -0.080827

h 3.112403 4.282553 1.421082

h 4.537092 3.242969 1.417040

s 0.235392 -1.363941 -0.312811

o -0.989998 -0.693728 -1.078463

o -0.249722 -1.906680 0.970779

o 0.974082 -2.254026 -1.198532

h -1.823101 -1.303953 -1.111590

o -2.476428 -3.564545 1.178440

h -2.254410 -4.500081 1.199536

h -1.630253 -3.084479 1.267451

o -3.060965 -2.189398 -1.113875

h -3.050969 -2.769358 -0.321736

h -3.925974 -1.745824 -1.156365

o -5.529657 -0.832023 -1.401576

h -5.930361 -0.852558 -2.276791

h -5.622366 0.073386 -1.087699

28

pTS-.H+W3A

c 3.560577 -0.127283 -0.040154

c 2.853870 -0.189736 1.165682

h 3.397972 -0.212230 2.103980

c 1.463438 -0.225973 1.185304

h 0.918916 -0.285414 2.118784

c 0.770778 -0.198314 -0.021299

c 1.445259 -0.137829 -1.237976

h 0.888504 -0.129349 -2.166275

c 2.834971 -0.101547 -1.236940

h 3.364582 -0.054412 -2.182567

c 5.069147 -0.120568 -0.052193

h 5.461581 -1.142023 -0.103433

h 5.458420 0.422958 -0.915748

h 5.473036 0.340303 0.851717

s -1.016819 -0.199207 -0.011852

o -1.417866 1.274986 -0.066362

o -1.457946 -0.814793 1.266869

o -1.470853 -0.909378 -1.234351

o -3.982434 -0.080109 2.022213

h -3.082468 -0.465821 1.908936

h -4.079303 0.149317 2.951013

o -3.852310 1.499703 -0.057906

h -4.077306 0.997374 0.782529

h -2.746973 1.493679 -0.072397

h -4.102851 0.909055 -0.833719

o -3.986016 -0.190681 -2.043665

h -3.091608 -0.580111 -1.907243

h -4.596297 -0.922595 -2.172948

31

pTS-.H+W4A

c 4.029641 0.050271 -0.001018

c 3.313914 -0.042414 1.197695

h 3.851432 -0.086316 2.139266

c 1.923495 -0.082349 1.206157

h 1.374480 -0.166240 2.135250

c 1.236028 -0.027570 -0.002988

c 1.921002 0.064488 -1.211300

h 1.369508 0.093744 -2.142293

c 3.311553 0.103178 -1.200678

h 3.847177 0.173607 -2.141724

c 5.538663 0.059742 -0.001934

h 5.934900 -0.959528 -0.067268

h 5.933277 0.618952 -0.853120

h 5.935081 0.506543 0.912477

s -0.558230 -0.014268 -0.000539

o -0.976584 1.417616 0.104867

o -0.976519 -0.812619 1.191497

o -0.977233 -0.630354 -1.296137

o -3.479057 -1.104882 1.987134

h -2.509852 -1.035888 1.765308

h -3.586769 -0.806537 2.895135

o -3.475774 2.240100 -0.044807

h -2.504653 2.016223 0.008553

h -3.582403 2.889224 -0.746463

o -3.473349 -1.204550 -1.933968

h -2.504991 -1.036547 -1.767873

h -3.572664 -2.143212 -2.119068

o -4.620127 -0.019856 -0.004384

h -4.244363 -0.446200 0.853844

h -4.238543 0.936604 -0.061403

h -4.239039 -0.550962 -0.800217

31

pTS-.H+W4B

c 3.931820 -0.731404 -0.421498

c 2.998535 -1.588747 -1.012622

h 3.343146 -2.399061 -1.646475

c 1.632799 -1.424638 -0.800627

h 0.913114 -2.096848 -1.249531

c 1.194566 -0.386583 0.015004

c 2.100362 0.482251 0.619016

h 1.742467 1.276349 1.261861

c 3.460385 0.304103 0.394523

h 4.168098 0.979415 0.863920

c 5.412205 -0.935290 -0.629842

h 5.615433 -1.450106 -1.571127

h 5.948013 0.016610 -0.639116

h 5.838469 -1.542562 0.176099

s -0.561402 -0.134567 0.265410

o	-0.728957	0.327683	1.664887
o	-1.234103	-1.426817	-0.045057
o	-0.961720	0.940623	-0.727131
o	-3.690978	-1.402882	-1.159540
h	-2.816741	-1.583518	-0.735421
h	-3.790734	-2.022552	-1.887966
o	-3.363047	1.155753	-1.317404
h	-2.328086	1.120384	-1.094375
h	-3.645658	0.185828	-1.352194
h	-3.838045	1.624950	-0.543994
o	-4.452913	2.257984	0.717759
h	-3.952038	1.975106	1.530348
h	-4.557899	3.212833	0.766592
o	-2.962172	1.425303	2.751230
h	-2.124350	1.040093	2.403054
h	-3.290570	0.800308	3.404217

31

pTSA.W4A

c	4.042125	0.038675	-0.001049
c	3.318806	0.838430	0.891833
h	3.849981	1.479744	1.586763
c	1.928790	0.832462	0.900897
h	1.372297	1.462119	1.583217
c	1.255719	0.012226	-0.000651
c	1.943824	-0.789207	-0.907205
h	1.398174	-1.404181	-1.611165
c	3.333966	-0.767661	-0.899578
h	3.876798	-1.384262	-1.607734

c 5.550072 0.030877 0.018783

h 5.922601 -0.729415 0.713750

h 5.960942 -0.196919 -0.966848

h 5.949931 0.994062 0.342286

s -0.526903 -0.010802 0.005374

o -0.803125 -1.150505 1.061798

o -0.997465 -0.427259 -1.324084

o -1.015371 1.279522 0.514969

h -1.818026 -1.333980 1.248027

o -3.222743 -1.657600 1.523566

h -3.880439 -1.107030 0.991509

h -3.502771 -1.629808 2.443390

o -4.791175 -0.156987 0.079720

h -4.547349 -0.295193 -0.857161

h -4.560250 0.773888 0.270923

o -3.603482 -0.485685 -2.426194

h -2.670302 -0.471183 -2.146819

h -3.692589 -1.235037 -3.021833

o -3.641959 2.307733 0.714702

h -2.703568 2.052832 0.654928

h -3.726510 3.130141 0.223887

31

pTSA.W4B

c 4.230237 -0.454267 -0.133676

c 3.513260 0.124246 -1.186693

h 4.026079 0.375139 -2.108931

c 2.153525 0.393162 -1.071165

h 1.605139 0.855451 -1.881558

c	1.503859	0.076106	0.118019
c	2.190562	-0.492270	1.188191
h	1.671745	-0.709733	2.113140
c	3.549154	-0.751784	1.052991
h	4.090807	-1.186472	1.886203
c	5.698407	-0.767884	-0.277876
h	6.224641	-0.658262	0.672828
h	5.841707	-1.800396	-0.614334
h	6.176165	-0.114534	-1.010549
s	-0.244880	0.400044	0.286214
o	-0.904035	-0.955770	-0.221590
o	-0.586135	1.464015	-0.667704
o	-0.573124	0.587493	1.700131
h	-1.626053	-1.282269	0.446207
o	-2.643030	-1.665654	1.488453
h	-3.580912	-1.454831	1.247752
h	-2.435274	-1.125511	2.260702
o	-5.153108	-0.979702	0.841435
h	-5.764576	-1.589528	0.419458
h	-5.237586	-0.120283	0.364112
o	-3.051977	2.313451	-1.653913
h	-2.193686	2.050470	-1.267237
h	-2.945423	2.225855	-2.605508
o	-5.326990	1.386471	-0.466457
h	-5.700943	2.147319	-0.012787
h	-4.507554	1.709926	-0.905857

31

pTSA.W4C

c	3.925307	-0.824580	-0.458835
c	3.240246	0.084554	-1.272498
h	3.765519	0.579496	-2.082070
c	1.894250	0.365989	-1.064247
h	1.363880	1.062765	-1.700683
c	1.228234	-0.275596	-0.024292
c	1.879067	-1.188151	0.802389
h	1.337855	-1.682767	1.598722
c	3.224888	-1.452500	0.578580
h	3.739324	-2.160089	1.219847
c	5.377042	-1.146132	-0.710859
h	5.883615	-0.327579	-1.225681
h	5.908548	-1.344753	0.222368
h	5.472044	-2.039092	-1.338032
s	-0.496158	0.082294	0.254136
o	-1.126002	-1.106498	0.847541
o	-1.088843	0.611019	-0.980996
o	-0.386345	1.230169	1.338773
h	-1.249185	1.786867	1.465280
o	-2.418584	2.701596	1.739452
h	-2.251626	3.632953	1.565027
h	-3.294271	2.487741	1.312488
o	-4.686369	2.156350	0.491040
h	-5.474353	1.867263	0.959912
h	-4.516047	1.483744	-0.220337
o	-3.993176	0.323304	-1.343567
h	-4.029016	-0.566486	-0.940847
h	-3.045549	0.479334	-1.480214
o	-3.703482	-2.039208	0.139214

h -2.814834 -1.834598 0.482359

h -3.665977 -2.947406 -0.173970

34

pTS-.H+W5A

c 4.468412 -0.130471 0.082669

c 3.750525 -0.043204 1.279450

h 4.285507 -0.013233 2.222990

c 2.359108 -0.001529 1.285199

h 1.805865 0.051239 2.214134

c 1.673786 -0.050774 0.075395

c 2.362248 -0.144770 -1.131633

h 1.813049 -0.203729 -2.062694

c 3.751981 -0.184992 -1.118882

h 4.289218 -0.266972 -2.058207

c 5.977481 -0.146367 0.081806

h 6.369200 -0.779506 -0.717829

h 6.377693 0.861433 -0.074042

h 6.373340 -0.513196 1.031109

s -0.119273 0.052391 0.068644

o -0.567458 -0.473245 1.387061

o -0.571966 -0.783374 -1.086976

o -0.454971 1.497355 -0.119773

o -2.809022 -0.575409 -2.448956

h -1.934890 -0.664749 -1.974522

h -3.032676 -1.440941 -2.802871

o -2.804239 2.651313 -0.213899

h -1.891745 2.252827 -0.123629

h -2.704955 3.472059 -0.705570

o -2.849189 -1.653924 2.143255

h -2.005046 -1.210602 1.880987

h -2.672468 -2.598420 2.112190

o -4.988124 -0.598555 1.031665

h -4.200658 -1.025982 1.473700

h -5.544288 -0.238449 1.728812

o -4.343370 0.811370 -0.988647

h -3.783864 0.209872 -1.610020

h -4.628365 0.274092 -0.163772

h -3.750846 1.608445 -0.697144

34

pTS-.H+W5B

c 4.449152 -0.253818 0.093546

c 3.728491 -0.571157 1.248205

h 4.260936 -0.847203 2.152286

c 2.336113 -0.540032 1.261852

h 1.777307 -0.791412 2.154049

c 1.657602 -0.184687 0.101624

c 2.348178 0.136952 -1.065300

h 1.805179 0.405650 -1.962693

c 3.736770 0.100814 -1.059554

h 4.277729 0.352048 -1.965973

c 5.956568 -0.318382 0.076802

h 6.300795 -1.279982 -0.319245

h 6.381728 0.464973 -0.555047

h 6.371658 -0.209021 1.080727

s -0.132324 -0.113340 0.112209

o -0.600403 -0.789062 -1.134246

o -0.465837 1.362253 0.084722

o -0.593483 -0.773668 1.357940

o -3.338299 -1.274163 1.449266

h -2.363971 -1.228729 1.540833

h -3.478539 -1.554987 0.530450

o -4.150590 1.217632 1.804586

h -3.912746 0.247454 1.761225

h -4.121616 1.484165 2.728134

o -2.774616 2.244589 -0.087372

h -3.298498 1.920940 0.727831

h -1.783780 1.874503 -0.026877

h -3.228128 1.851136 -0.896525

o -3.130110 -1.513875 -1.493519

h -3.209982 -2.301254 -2.041183

h -2.157319 -1.325467 -1.410498

o -3.964646 1.026460 -2.069856

h -3.769386 0.065045 -1.982195

h -4.913935 1.115624 -2.196203

34

pTS-.H+W5C

c 4.453865 0.466203 -0.226856

c 3.819652 0.262155 1.004226

h 4.413434 0.223040 1.911525

c 2.440504 0.106252 1.087491

h 1.955647 -0.062385 2.040603

c 1.681883 0.157697 -0.079135

c 2.283668 0.359109 -1.317472

h 1.677207 0.384312 -2.213773

c	3.665247	0.511956	-1.381242
h	4.137238	0.667822	-2.345660
c	5.954480	0.601056	-0.309010
h	6.428827	-0.381330	-0.409294
h	6.254359	1.199010	-1.172206
h	6.362176	1.070374	0.589079
s	-0.101027	0.006275	0.021239
o	-0.608183	1.402466	0.310959
o	-0.386162	-0.921310	1.148301
o	-0.574927	-0.483078	-1.302186
o	-2.418206	-2.689267	1.257897
h	-1.655154	-2.061728	1.249471
h	-2.064841	-3.531047	0.955447
o	-4.561694	1.016189	1.410558
h	-4.355326	0.975948	2.349677
h	-4.634368	0.089573	1.092715
o	-2.919965	2.021688	-0.379699
h	-3.533589	1.779715	0.376358
h	-1.933331	1.823733	-0.067723
h	-3.099021	1.303868	-1.106318
o	-3.193883	0.042366	-1.949446
h	-2.266318	-0.280587	-1.906542
h	-3.716966	-0.599653	-1.436226
o	-4.489196	-1.447063	0.155684
h	-3.754681	-1.995044	0.549196
h	-5.261349	-2.018315	0.092360

34

pTS-.H+W5D

c	4.204375	0.272620	-0.006562
c	3.453331	0.274374	1.175117
h	3.963305	0.280443	2.132764
c	2.063557	0.267130	1.145728
h	1.489605	0.259440	2.063717
c	1.411772	0.257975	-0.085555
c	2.131103	0.257500	-1.276806
h	1.605598	0.241895	-2.223046
c	3.522020	0.264659	-1.227399
h	4.085061	0.263229	-2.154805
c	5.712288	0.248523	0.038199
h	6.145006	0.700134	-0.856893
h	6.093582	0.785489	0.909573
h	6.083563	-0.780292	0.099575
s	-0.379512	0.310388	-0.136176
o	-0.789261	1.730729	0.053603
o	-0.855985	-0.545469	1.014252
o	-0.788676	-0.249856	-1.454921
o	-3.517007	-0.057926	-1.841027
h	-2.537585	-0.133133	-1.906695
h	-3.665249	0.844443	-1.501409
o	-4.121755	-1.575983	0.086294
h	-3.929259	-1.008049	-0.769986
h	-3.362497	-2.243532	0.181550
h	-3.977740	-0.902927	0.860151
o	-3.484512	0.171373	1.823766
h	-2.514795	0.035484	1.810025
h	-3.617229	1.033398	1.386485
o	-3.412292	2.244335	-0.132606

h -3.680196 3.166835 -0.186679

h -2.423187 2.229096 -0.096704

o -1.982909 -2.954635 0.513534

h -1.530336 -3.504910 -0.133044

h -1.394181 -2.182780 0.695980

34

pTSA.W5A

c 4.460746 0.506360 -0.191526

c 3.863270 0.028530 0.980280

h 4.478956 -0.178608 1.848937

c 2.491480 -0.187289 1.054009

h 2.032220 -0.564676 1.958495

c 1.707982 0.083605 -0.064148

c 2.270859 0.559418 -1.245393

h 1.645133 0.754780 -2.106834

c 3.644245 0.766884 -1.298463

h 4.088958 1.137135 -2.215857

c 5.953525 0.707016 -0.269258

h 6.452881 -0.217911 -0.577465

h 6.214892 1.478699 -0.996079

h 6.367596 0.995032 0.699302

s -0.057377 -0.160636 0.027213

o -0.573949 1.256829 0.421445

o -0.324755 -1.131286 1.099691

o -0.551645 -0.518347 -1.320416

h -1.610845 1.505589 0.122578

o -2.614583 -2.661459 1.630530

h -1.791329 -2.156795 1.491845

h -2.369750 -3.589825 1.583798

o -4.813862 1.101282 1.362378

h -4.844421 1.106005 2.323021

h -4.868627 0.155089 1.073055

o -2.844064 1.852524 -0.259845

h -3.541452 1.690983 0.431888

h -3.104763 1.301194 -1.023509

o -3.185629 -0.289431 -2.044702

h -2.238356 -0.514348 -1.926309

h -3.378657 -0.367333 -2.984096

o -4.667489 -1.359749 0.274468

h -4.007354 -1.913468 0.738175

h -4.283836 -1.175794 -0.597210

34

pTSA.W5B

c 4.510079 -0.197939 -0.032567

c 3.784204 -0.954543 0.894102

h 4.312719 -1.574900 1.609822

c 2.393852 -0.926968 0.916030

h 1.834209 -1.507375 1.638171

c 1.723998 -0.129010 -0.006620

c 2.415789 0.637091 -0.941505

h 1.874246 1.257048 -1.644539

c 3.804884 0.594474 -0.946619

h 4.350168 1.187375 -1.673007

c 6.018194 -0.211486 -0.028182

h 6.420938 -0.055393 -1.031135

h 6.410364 0.587173 0.610709

h 6.407364 -1.157507 0.353494

s -0.059555 -0.097752 -0.003270

o -0.505516 1.220397 -0.480314

o -0.529403 -0.519495 1.325413

o -0.379054 -1.200934 -1.075358

h -1.404715 -1.333937 -1.319031

o -3.044783 -1.233630 2.375492

h -2.149060 -0.984322 2.083837

h -3.190890 -0.779483 3.210046

o -2.748782 -1.582336 -1.722709

h -3.469397 -1.341296 -1.048029

h -2.926476 -2.478238 -2.024667

o -2.715276 2.945052 -0.392203

h -1.970793 2.318459 -0.459255

h -2.439831 3.603409 0.252228

o -5.169393 1.719718 -0.190165

h -4.320011 2.205178 -0.272407

h -5.730134 2.038664 -0.902914

o -4.526410 -0.959134 0.033138

h -4.148482 -1.058561 0.929828

h -4.833048 -0.029798 -0.037815

37

pTS-.H+W6A

c 4.575628 -0.431328 0.000000

c 3.858610 -0.444013 1.201523

h 4.395128 -0.436518 2.144506

c 2.467967 -0.469187 1.211295

h 1.918860 -0.491667 2.143870

c	1.781720	-0.480301	0.000000
c	2.467967	-0.469187	-1.211295
h	1.918860	-0.491667	-2.143870
c	3.858610	-0.444013	-1.201523
h	4.395128	-0.436518	-2.144506
c	6.084368	-0.437072	0.000000
h	6.469335	-1.462667	0.000000
h	6.484917	0.062614	-0.884630
h	6.484917	0.062614	0.884630
s	-0.011213	-0.444759	0.000000
o	-0.426295	1.006102	0.000000
o	-0.444619	-1.126800	1.251536
o	-0.444619	-1.126800	-1.251536
o	-2.912911	-0.883063	-2.246942
h	-2.004568	-1.096465	-1.913810
h	-3.085169	-1.476647	-2.984511
o	-2.244881	1.902695	-1.909713
h	-1.437605	1.679006	-1.397382
h	-2.486472	1.067932	-2.349199
o	-2.912911	-0.883063	2.246942
h	-2.004568	-1.096465	1.913810
h	-3.085169	-1.476647	2.984511
o	-4.536405	-0.374051	0.000000
h	-4.075289	-0.734404	-0.784165
h	-4.075289	-0.734404	0.784165
o	-3.924092	2.105712	0.000000
h	-3.295650	2.135277	0.820221
h	-4.289685	1.140840	0.000000
h	-3.295650	2.135277	-0.820221

o -2.244881 1.902695 1.909713

h -2.486472 1.067932 2.349199

h -1.437605 1.679006 1.397382

37

pTS-.H+W6B

c 4.844910 -0.058942 -0.210842

c 4.148573 -0.523193 0.907278

h 4.700151 -0.893911 1.764952

c 2.755067 -0.524067 0.941961

h 2.215008 -0.890501 1.805388

c 2.049732 -0.054978 -0.159483

c 2.718282 0.409251 -1.291743

h 2.156489 0.760426 -2.148276

c 4.106747 0.403398 -1.309048

h 4.628292 0.760303 -2.191375

c 6.353695 -0.036641 -0.236438

h 6.740533 -0.385908 -1.197339

h 6.732399 0.979715 -0.083832

h 6.775281 -0.667498 0.548455

s 0.254137 -0.028279 -0.123234

o -0.136732 1.418878 -0.123403

o -0.158290 -0.736147 1.118521

o -0.186103 -0.715654 -1.375195

o -4.376802 -1.491675 1.566730

h -3.645605 -0.959099 2.011089

h -5.129185 -1.535939 2.162990

o -2.442058 -1.866389 -2.001484

h -1.574535 -1.431376 -1.755709

h -2.294449 -2.816540 -1.975490

o -2.348029 2.377161 0.881083

h -1.474391 2.061290 0.505798

h -2.200322 3.265741 1.219953

o -4.210844 1.704616 -0.954071

h -3.553237 2.041478 -0.295515

h -4.000908 2.123642 -1.794578

o -4.446697 -0.866300 -0.870530

h -4.482494 -1.131882 0.127071

h -4.369650 0.143170 -0.941524

h -3.624329 -1.311418 -1.328053

o -2.434631 -0.038274 2.504305

h -1.585113 -0.357764 2.127360

h -2.504890 0.873307 2.174226

37

pTS-.H+W6C

c 4.276233 0.460444 0.168700

c 3.520694 0.051900 1.270970

h 4.025209 -0.270289 2.175622

c 2.128194 0.051297 1.232619

h 1.545778 -0.268551 2.086903

c 1.483717 0.464897 0.071901

c 2.210720 0.880244 -1.043418

h 1.696087 1.199726 -1.941137

c 3.598471 0.874576 -0.986042

h 4.166356 1.198854 -1.851881

c 5.784193 0.436266 0.206520

h 6.172990 -0.446758 -0.311872

h 6.208101 1.314875 -0.285839

h 6.157114 0.407639 1.231958

s -0.307861 0.520307 0.017341

o -0.712626 1.947420 0.119679

o -0.794409 -0.295725 1.179248

o -0.710969 -0.078523 -1.301554

o -3.525511 0.229095 -1.622518

h -2.557964 0.136953 -1.735546

h -3.642918 1.126654 -1.260566

o -4.103912 -1.343858 0.329017

h -3.945709 -0.786355 -0.518353

h -3.305097 -2.019125 0.406950

h -3.957659 -0.671507 1.086636

o -3.425056 0.451202 2.050143

h -2.458849 0.310840 2.023578

h -3.557607 1.307426 1.602898

o -3.339785 2.525365 0.086920

h -3.590314 3.452889 0.035835

h -2.352908 2.488706 0.078256

o -2.040156 -2.756056 0.604671

h -1.638067 -3.022157 -0.250885

h -1.443902 -2.054138 0.934873

o -0.841137 -2.782979 -1.846146

h -0.637266 -1.827213 -1.794030

h -0.084177 -3.214343 -2.251453

40

pTS-.H+W7A

c 4.648204 0.413359 0.604882

c	3.869973	1.491455	0.176998
h	4.311796	2.480393	0.118953
c	2.532730	1.322573	-0.177165
h	1.931664	2.161405	-0.503389
c	1.967328	0.055156	-0.097622
c	2.719561	-1.040695	0.326009
h	2.264504	-2.021409	0.387879
c	4.050598	-0.853078	0.673684
h	4.637130	-1.703836	1.005065
c	6.095275	0.597284	0.990138
h	6.260146	0.331481	2.038835
h	6.747206	-0.042286	0.387839
h	6.416809	1.630829	0.851757
s	0.262796	-0.195696	-0.596074
o	-0.346052	-1.112918	0.426069
o	0.278531	-0.810174	-1.948955
o	-0.380094	1.161345	-0.595941
o	-2.736249	-2.422295	-0.493871
h	-1.892166	-2.105879	-0.120113
h	-2.650167	-2.270946	-1.450963
o	-1.461924	-0.326957	2.821416
h	-0.973526	-0.699061	2.056857
h	-0.905527	-0.457779	3.594389
o	-2.144919	1.933463	1.435369
h	-1.971583	1.246500	2.115875
h	-1.404032	1.823733	0.804175
o	-4.113563	1.361970	-0.029244
h	-3.352501	1.621531	0.640488
h	-3.660766	1.321049	-0.950959

h -4.440508 0.421920 0.202198

o -2.735958 1.266944 -2.184732

h -2.707247 0.415458 -2.662001

h -1.833769 1.369139 -1.821367

o -2.100367 -1.346451 -3.099829

h -1.159407 -1.224818 -2.828301

h -2.093527 -1.725244 -3.984251

o -4.801730 -1.056951 0.441678

h -5.076381 -1.369098 1.308784

h -4.052286 -1.641419 0.135436

40

pTS-.H+W7B

c 4.454441 -0.471129 1.201147

c 3.682169 0.648557 1.515826

h 4.113596 1.446004 2.111261

c 2.363982 0.765227 1.076407

h 1.770002 1.637287 1.316727

c 1.813427 -0.256119 0.312122

c 2.562132 -1.385731 -0.020820

h 2.125237 -2.171590 -0.624446

c 3.872329 -1.484454 0.425537

h 4.456406 -2.361620 0.166625

c 5.881972 -0.595599 1.673091

h 6.174721 0.256841 2.288224

h 6.023129 -1.503992 2.266285

h 6.572419 -0.651727 0.825960

s 0.114581 -0.140588 -0.253922

o -0.643169 -1.233415 0.444291

o 0.136343 -0.339738 -1.727205

o -0.369763 1.221078 0.146397

o -2.219650 -1.006471 2.743503

h -1.810261 -1.248219 3.578772

h -1.569783 -1.207204 2.042313

o -2.719880 1.463516 1.663665

h -2.763438 0.640965 2.195413

h -1.810076 1.454076 1.304921

o -3.952603 1.817250 -0.511640

h -3.567788 1.613196 0.430760

h -3.210319 2.333316 -0.984639

h -4.039401 0.937699 -1.057202

o -1.864946 2.816397 -1.672783

h -1.774963 2.303477 -2.496651

h -1.169317 2.450935 -1.092178

o -1.689281 0.616429 -3.467066

h -0.977668 0.207586 -2.917568

h -1.432579 0.502321 -4.387266

o -3.976282 -0.236026 -1.997615

h -3.301445 -0.036959 -2.673671

h -3.678872 -1.075894 -1.577058

o -2.865236 -2.393201 -0.766006

h -2.034411 -2.077329 -0.355291

h -2.675755 -3.255151 -1.146223

40

pTS-.H+W7C

c 4.534610 -0.427781 1.202265

c 3.784771 0.733253 1.399583

h	4.237942	1.585197	1.894982
c	2.460860	0.821145	0.970933
h	1.881752	1.721997	1.126137
c	1.881974	-0.271678	0.337757
c	2.606406	-1.445636	0.126518
h	2.144108	-2.291181	-0.367668
c	3.922911	-1.514222	0.559791
h	4.487920	-2.426282	0.397076
c	5.967832	-0.522165	1.663884
h	6.292542	0.399865	2.148840
h	6.098989	-1.342014	2.376519
h	6.639972	-0.714509	0.822156
s	0.187084	-0.181954	-0.242427
o	-0.541490	-1.328769	0.392294
o	0.227259	-0.304482	-1.723511
o	-0.346166	1.146313	0.212766
o	-2.527507	-1.420931	2.265113
h	-2.371569	-1.826803	3.123206
h	-1.676570	-1.444805	1.777397
o	-2.770327	1.294522	1.609860
h	-2.896473	0.405874	1.995055
h	-1.840576	1.290590	1.302740
o	-3.882351	1.909231	-0.603264
h	-3.553990	1.639142	0.333685
h	-3.085948	2.389352	-1.028887
h	-3.998092	1.039044	-1.177325
o	-1.700853	2.806821	-1.649133
h	-1.611658	2.298863	-2.475914
h	-1.046655	2.400124	-1.046882

o -1.622854 0.597699 -3.458217

h -0.909798 0.192157 -2.907961

h -1.375057 0.462131 -4.378141

o -3.977650 -0.142723 -2.056821

h -3.264922 -0.008333 -2.710811

h -3.736768 -0.961920 -1.559060

o -3.081726 -2.237270 -0.559384

h -2.129033 -2.066464 -0.443529

h -3.408896 -2.253398 0.350376

40

pTS-.H+W7D

c 4.584269 0.859585 0.088992

c 3.829774 0.981262 1.263735

h 4.335968 1.140425 2.210214

c 2.443288 0.902878 1.240385

h 1.868618 0.993297 2.153691

c 1.795652 0.698643 0.022379

c 2.517177 0.577375 -1.160208

h 1.997015 0.416798 -2.095647

c 3.907159 0.657570 -1.116588

h 4.471822 0.561456 -2.037751

c 6.090732 0.924674 0.135487

h 6.514445 1.077314 -0.858661

h 6.432823 1.738522 0.779879

h 6.509317 -0.004771 0.535777

s 0.003640 0.658531 -0.018998

o -0.478334 2.061336 0.061004

o -0.429877 -0.143901 1.176825

o -0.375329 -0.000958 -1.312763

o -3.155300 0.488913 2.005555

h -2.190548 0.396277 1.912610

h -3.374063 1.264958 1.463063

o -3.136313 2.549393 -0.037711

h -3.421085 3.468461 -0.044152

h -2.151622 2.551091 0.012943

o -3.046925 0.617551 -2.097494

h -3.293656 1.347955 -1.497571

h -2.074488 0.557252 -2.018722

o -3.674251 -1.780694 -1.465923

h -3.542751 -0.795501 -1.725840

h -2.754962 -2.211748 -1.600483

h -3.840616 -1.831079 -0.432027

o -1.249394 -2.649668 -1.568810

h -1.086592 -2.988563 -0.669823

h -0.762782 -1.800335 -1.588694

o -1.133753 -2.765521 1.267928

h -0.775382 -1.846975 1.305611

h -0.650501 -3.280216 1.921752

o -3.874041 -1.935079 1.040330

h -3.070218 -2.418636 1.304278

h -3.758916 -1.037871 1.445424

40

pTS-.H+W7E

c 4.555538 0.847992 0.066776

c 3.797158 0.984580 1.236229

h 4.301152 1.125893 2.186565

c	2.408300	0.946288	1.202774
h	1.831594	1.052040	2.113116
c	1.762810	0.766606	-0.019284
c	2.489878	0.632954	-1.198292
h	1.971685	0.496038	-2.138532
c	3.880368	0.673680	-1.145209
h	4.447977	0.570083	-2.063891
c	6.063162	0.862297	0.118419
h	6.456351	-0.146629	0.284264
h	6.490257	1.230282	-0.816708
h	6.428120	1.493208	0.931736
s	-0.030476	0.788433	-0.079607
o	-0.485000	2.187285	0.047235
o	-0.489809	-0.049264	1.099075
o	-0.412332	0.154567	-1.383491
o	-2.978214	0.507330	2.126843
h	-2.033838	0.397501	1.866955
h	-2.983162	0.772694	3.051981
o	-3.337378	2.447900	-0.044750
h	-3.476874	1.926267	0.761923
h	-2.386940	2.658501	-0.010960
o	-3.123297	0.725794	-2.126780
h	-3.361394	1.398144	-1.437964
h	-2.147615	0.697973	-2.096138
o	-3.682497	-1.639125	-1.582879
h	-3.538302	-0.611505	-1.814198
h	-2.769647	-2.070242	-1.740747
h	-3.838117	-1.729827	-0.579825
o	-1.248107	-2.491525	-1.750588

h -1.060263 -2.864454 -0.870791

h -0.777908 -1.632790 -1.740821

o -1.040934 -2.700168 1.080356

h -0.713850 -1.770009 1.140698

h -0.505378 -3.226894 1.681608

o -3.793024 -1.930476 0.989038

h -2.957548 -2.395162 1.180346

h -3.712444 -1.086260 1.475519

43

pTS-.H+W8A

c 4.905338 -0.136598 0.172095

c 4.240151 0.805126 0.970441

h 4.809961 1.418729 1.660586

c 2.864397 0.971083 0.892640

h 2.362388 1.707699 1.507575

c 2.133998 0.182872 0.002597

c 2.765697 -0.757118 -0.802892

h 2.183486 -1.352629 -1.493969

c 4.148444 -0.909313 -0.711021

h 4.643108 -1.640789 -1.340993

c 6.402407 -0.297029 0.267279

h 6.760286 -1.097346 -0.382464

h 6.915261 0.625372 -0.022096

h 6.709441 -0.530418 1.291002

s 0.351951 0.377861 -0.069838

o 0.084388 1.834151 -0.192048

o -0.199398 -0.184802 1.208743

o -0.104504 -0.405381 -1.265423

o -1.617364 0.715448 -3.308025

h -1.149118 1.252086 -3.953263

h -0.948677 0.385503 -2.674940

o -3.749398 1.271957 -1.685698

h -3.059803 1.164084 -2.378200

h -3.385991 1.931400 -1.061952

o -2.368403 2.940523 0.121211

h -1.441201 2.641443 -0.033997

h -2.360756 3.902183 0.086934

o -2.444486 1.194276 2.425046

h -2.579142 1.936159 1.812046

h -1.578098 0.832663 2.167450

o -1.503020 -2.523696 1.703058

h -0.919095 -1.738267 1.592674

h -1.052420 -3.124602 2.304409

o -3.947763 -0.995312 1.853473

h -3.266847 -1.670861 2.020153

h -3.523417 -0.150773 2.146995

o -4.194921 -1.005174 -0.672892

h -4.174597 -0.959809 0.363628

h -3.391996 -1.584260 -0.926982

h -4.052413 -0.057935 -1.076266

o -2.068799 -2.411348 -1.074240

h -1.865144 -2.766401 -0.190295

h -1.333933 -1.790754 -1.252543

43

pTS-.H+W8B

c 4.304262 -1.050479 1.662325

c	3.607590	-2.020640	0.930545
h	4.130556	-2.905015	0.581799
c	2.256279	-1.872920	0.642638
h	1.726608	-2.626427	0.073279
c	1.586742	-0.736295	1.092671
c	2.250963	0.241936	1.825515
h	1.715045	1.118667	2.165396
c	3.605270	0.076994	2.103458
h	4.125080	0.839662	2.673499
c	5.778375	-1.208206	1.941646
h	6.043229	-2.255668	2.102992
h	6.375031	-0.846404	1.097247
h	6.080051	-0.640407	2.823993
s	-0.170825	-0.571874	0.775545
o	-0.885701	-1.441777	1.745278
o	-0.389745	-1.037263	-0.638168
o	-0.502270	0.877199	0.961745
o	-0.478480	0.025229	-3.117997
h	-0.346459	-0.325464	-2.202915
h	-0.175016	-0.669788	-3.711310
o	0.476882	2.642582	-3.073046
h	0.401668	3.131059	-3.897530
h	0.216650	1.718759	-3.259901
o	-0.904789	3.058456	-0.733862
h	-0.371813	3.049290	-1.557743
h	-0.536838	2.362083	-0.155089
o	-3.319258	2.326120	-0.908984
h	-2.350083	2.701051	-0.901448
h	-3.444388	1.913197	0.018137

h -3.349034 1.562267 -1.610086

o -3.289995 1.301698 1.446504

h -3.632951 0.401388 1.603812

h -2.322032 1.210310 1.538900

o -3.595957 -1.500702 1.710576

h -2.625334 -1.597003 1.853845

h -4.034506 -2.025369 2.387368

o -3.134671 -1.865818 -1.125484

h -2.179248 -1.805344 -0.947845

h -3.537690 -1.887312 -0.241573

o -3.295124 0.418548 -2.587751

h -3.397941 -0.435790 -2.099170

h -2.410133 0.349471 -2.988811

46

pTS-.H+W9A

c 4.900088 0.206307 1.265017

c 4.010458 1.281182 1.317369

h 4.385142 2.276465 1.530485

c 2.644258 1.100891 1.105364

h 1.957633 1.935741 1.156757

c 2.165309 -0.175432 0.835106

c 3.029708 -1.269727 0.780436

h 2.642950 -2.261480 0.581210

c 4.386383 -1.070486 0.994023

h 5.060065 -1.920249 0.954354

c 6.377221 0.400599 1.501708

h 6.963833 0.036512 0.653112

h 6.622117 1.452969 1.653817

h	6.708909	-0.152716	2.385650
s	0.413984	-0.432461	0.542414
o	-0.019848	-1.540852	1.429639
o	0.281425	-0.818583	-0.911312
o	-0.259948	0.868984	0.832796
o	-4.397737	0.729738	0.210810
h	-4.310330	-0.272154	0.080570
h	-3.794742	0.931081	1.000888
o	-3.950649	-1.828142	0.067812
h	-3.286657	-2.051999	-0.613170
h	-3.531768	-2.035496	0.924268
o	-2.476239	-1.885633	2.499384
h	-2.490731	-2.497835	3.241499
h	-1.545527	-1.847447	2.176903
o	-2.738222	0.958033	2.203090
h	-2.746352	0.067605	2.596185
h	-1.836526	1.045988	1.837671
o	-3.524553	1.884017	-1.773794
h	-2.669073	2.330496	-1.552373
h	-3.282931	1.242061	-2.485984
h	-4.029151	1.250470	-0.675974
o	-1.002462	2.754355	-1.212661
h	-0.493262	2.392783	-1.956798
h	-0.706512	2.223051	-0.452471
o	0.235866	0.895682	-3.052164
h	0.400644	0.270998	-2.311568
h	1.031036	0.904034	-3.593518
o	-2.494965	0.079793	-3.554054
h	-2.422890	-0.789396	-3.124918

h -1.573647 0.381772 -3.631479

o -1.898000 -2.190977 -1.844326

h -1.080947 -1.788204 -1.467495

h -1.653362 -3.072336 -2.144278

46

pTS-.H+W9B

c 4.914966 0.190526 1.244988

c 3.975907 0.852726 2.046740

h 4.318248 1.509635 2.839445

c 2.611513 0.689451 1.842549

h 1.894584 1.214619 2.461245

c 2.174004 -0.148272 0.817488

c 3.082654 -0.816527 0.003514

h 2.726207 -1.452545 -0.796129

c 4.446420 -0.639268 0.222578

h 5.155718 -1.152350 -0.417902

c 6.393241 0.356830 1.495080

h 6.724981 -0.297869 2.308120

h 6.978827 0.104388 0.609161

h 6.635563 1.382298 1.783667

s 0.413357 -0.400419 0.585893

o -0.046628 -1.336775 1.642882

o 0.251481 -0.959294 -0.794244

o -0.227551 0.955182 0.726467

o -4.338753 0.727548 0.024761

h -4.267270 -0.291117 -0.002218

h -3.748365 1.000882 0.806878

o -3.960708 -1.817327 0.146048

h -3.298089 -2.129010 -0.503219

h -3.555984 -1.947877 1.024770

o -2.546135 -1.643826 2.598209

h -2.587523 -2.193938 3.386585

h -1.602650 -1.626008 2.309981

o -2.728801 1.155074 2.009891

h -2.767810 0.316055 2.502358

h -1.817314 1.180855 1.654172

o -3.357705 1.668884 -2.048680

h -2.522264 2.136785 -1.851347

h -3.112175 0.958252 -2.701707

h -3.938762 1.139922 -0.877082

o -0.794787 2.635723 -1.362279

h -0.539629 3.544299 -1.174322

h -0.524216 2.097981 -0.583810

o 0.189015 0.600724 -3.240997

h 0.395499 0.041311 -2.473552

h 0.013478 1.467458 -2.843051

o -2.440658 -0.287671 -3.650516

h -2.406954 -1.116292 -3.145980

h -1.501190 -0.015240 -3.719540

o -1.909874 -2.398937 -1.676481

h -1.101802 -1.959089 -1.325188

h -1.652068 -3.297757 -1.905227

46

pTS-.H+W9C

c 5.008559 0.058962 1.322817

c 4.215140 1.208643 1.263279

h	4.673197	2.182636	1.398928
c	2.843316	1.128995	1.038459
h	2.231821	2.021466	1.007874
c	2.257046	-0.121034	0.867221
c	3.022030	-1.284663	0.923692
h	2.551025	-2.252331	0.804160
c	4.389605	-1.185430	1.148954
h	4.986460	-2.090267	1.194558
c	6.488201	0.152271	1.601428
h	6.685464	0.083203	2.676674
h	7.037318	-0.657477	1.116044
h	6.900686	1.101438	1.253274
s	0.498423	-0.247309	0.534765
o	-0.009971	-1.388159	1.336542
o	0.358889	-0.516191	-0.944436
o	-0.099835	1.069581	0.912242
o	-4.462538	0.250391	-1.479996
h	-3.903754	0.165541	-2.292138
h	-4.338539	-0.611719	-1.005650
o	-3.777693	-2.089611	-0.303461
h	-2.994273	-2.342544	-0.823049
h	-3.472949	-2.050242	0.619990
o	-2.545106	-1.702264	2.255378
h	-2.605900	-2.279411	3.022979
h	-1.596639	-1.677668	1.991047
o	-2.690018	1.132332	2.135081
h	-2.845646	0.190170	2.331337
h	-1.738389	1.173807	1.926146
o	-3.708104	2.099031	-0.065250

h -3.431268 1.723482 0.832423

h -2.857802 2.481172 -0.455589

h -4.061271 1.273514 -0.708616

o -1.346715 2.883074 -0.865349

h -1.046810 2.556588 -1.732559

h -0.792540 2.387770 -0.232156

o -0.264558 1.265900 -2.926288

h 0.089576 0.643349 -2.251036

h 0.455655 1.457147 -3.535035

o -2.676319 -0.216854 -3.488739

h -2.305933 -1.063940 -3.186886

h -1.912580 0.384883 -3.488420

o -1.441844 -2.340232 -1.965203

h -0.742785 -1.789492 -1.547193

h -1.022633 -3.168510 -2.218247

46

pTS-.H+W9D

c 5.009419 0.026256 1.302984

c 4.089843 0.554553 2.219982

h 4.451115 1.023230 3.129428

c 2.722849 0.489141 1.987304

h 2.023011 0.903856 2.702259

c 2.260335 -0.115947 0.818415

c 3.148104 -0.650180 -0.108003

h 2.771262 -1.112506 -1.010778

c 4.517028 -0.574152 0.142088

h 5.210519 -0.990457 -0.580714

c 6.492498 0.128223 1.559389

h	7.054957	-0.563636	0.929906
h	6.855624	1.139461	1.347441
h	6.731026	-0.090114	2.603310
s	0.491025	-0.225490	0.541007
o	-0.058516	-1.153021	1.563605
o	0.319504	-0.743936	-0.857080
o	-0.048263	1.166258	0.697460
o	-4.339388	-0.009074	-1.620649
h	-3.701113	-0.228379	-2.406168
h	-4.201254	-0.761589	-0.945512
o	-3.775020	-1.990830	-0.074040
h	-3.004565	-2.390981	-0.520834
h	-3.486845	-1.812375	0.843536
o	-2.623309	-1.330302	2.394491
h	-2.714706	-1.832928	3.209998
h	-1.663699	-1.330586	2.164804
o	-2.626850	1.531010	1.951027
h	-2.836436	0.642727	2.283464
h	-1.688284	1.469783	1.699318
o	-3.630703	2.139855	-0.507734
h	-3.399395	1.964511	0.437736
h	-2.819067	2.532607	-0.881043
h	-4.059218	0.894859	-1.180366
o	-0.977342	2.877013	-1.220439
h	-0.611692	3.764341	-1.148260
h	-0.545374	2.335245	-0.521212
o	-0.437261	0.819326	-3.149088
h	-0.008339	0.311137	-2.437894
h	-0.613780	1.681041	-2.735944

o -2.678525 -0.699807 -3.417011

h -2.310207 -1.528797 -3.064386

h -1.899993 -0.090389 -3.457640

o -1.500530 -2.632200 -1.632413

h -0.788635 -2.037970 -1.298319

h -1.099812 -3.498789 -1.753423

46

pTS-.H+W9E

c 4.889789 -0.437138 0.351762

c 4.188607 0.240215 1.357399

h 4.727349 0.632187 2.213457

c 2.812005 0.416019 1.283080

h 2.280440 0.935195 2.071065

c 2.121677 -0.095175 0.185344

c 2.790034 -0.776694 -0.827471

h 2.233685 -1.176534 -1.665246

c 4.169122 -0.942974 -0.734827

h 4.690872 -1.479977 -1.519939

c 6.387742 -0.598673 0.426693

h 6.707220 -1.552582 0.001243

h 6.891927 0.194874 -0.135342

h 6.744011 -0.547960 1.457387

s 0.347690 0.148074 0.077834

o 0.127204 1.617924 -0.123720

o -0.232260 -0.303278 1.382524

o -0.121533 -0.663375 -1.083554

o 0.021408 3.002585 -2.547087

h 0.821022 3.374335 -2.930003

h	0.282030	2.582064	-1.706657
o	-1.583213	0.749166	-3.181093
h	-1.092378	1.589892	-3.226020
h	-1.020371	0.185914	-2.624142
o	-3.765915	1.001736	-1.595084
h	-3.050530	0.928598	-2.278218
h	-3.429461	1.662703	-0.959459
o	-2.396549	2.720196	0.211243
h	-1.475276	2.412356	0.066056
h	-2.394836	3.666529	0.033311
o	-2.511674	1.077840	2.564139
h	-2.647775	1.815699	1.947006
h	-1.642572	0.721921	2.311586
o	-4.013130	-1.122931	1.995302
h	-3.338690	-1.793935	2.198489
h	-3.595112	-0.272641	2.277878
o	-4.227282	-1.227654	-0.545686
h	-4.225597	-1.142790	0.482834
h	-3.428277	-1.821186	-0.759408
h	-4.065568	-0.285538	-0.985244
o	-2.090827	-2.664678	-0.845110
h	-1.902108	-2.980290	0.056396
h	-1.350947	-2.056648	-1.039150
o	-1.551264	-2.645554	1.950806
h	-0.968443	-1.863876	1.827454
h	-1.112247	-3.223939	2.582174

46

pTS-.H+W9X

c	4.370311	-0.533749	0.962283
c	3.603593	0.182144	1.892004
h	4.101994	0.790873	2.639097
c	2.215411	0.130092	1.874988
h	1.633659	0.693646	2.593771
c	1.573248	-0.648143	0.912265
c	2.307002	-1.370600	-0.024020
h	1.791786	-1.973736	-0.760891
c	3.700916	-1.303997	0.005428
h	4.273453	-1.872517	-0.720150
c	5.877245	-0.489786	1.014543
h	6.252897	-1.088389	1.850792
h	6.321696	-0.885470	0.099573
h	6.240890	0.530917	1.157493
s	-0.222999	-0.743117	0.910780
o	-0.626969	-1.598744	2.054506
o	-0.599500	-1.337457	-0.409984
o	-0.707070	0.667419	1.079137
o	-3.285322	-2.344255	-0.476703
h	-2.314157	-2.253086	-0.461893
h	-3.535591	-2.351791	0.465679
o	-3.311915	-2.041300	2.355364
h	-3.586374	-2.645287	3.052161
h	-2.329846	-1.988318	2.392292
o	-3.457654	0.838684	2.015564
h	-3.667307	-0.074279	2.272387
h	-2.490974	0.833474	1.904123
o	-4.032148	1.709859	-0.510418
h	-3.991042	1.413730	0.430945

h -3.240684 2.270046 -0.613638

o -1.380794 2.811960 -0.472899

h -1.189696 3.614382 0.023586

h -1.046230 2.064218 0.072632

o -1.446404 -0.272150 -2.863335

h -0.983113 -0.644046 -2.088672

h -1.003572 0.597460 -3.031020

o -3.813175 -0.321565 -2.013695

h -3.946323 0.518437 -1.417299

h -2.867710 -0.246925 -2.455696

h -3.749246 -1.129330 -1.401646

o -0.160529 2.105014 -2.954458

h -0.535624 2.545314 -2.171846

h 0.780940 1.971878 -2.749845

o 2.537590 1.548314 -2.146503

h 3.282814 1.508146 -2.753950

h 2.656523 0.812030 -1.532834

49

pTS-.H+W10A

c 5.222075 -0.281363 1.053335

c 4.672279 0.350542 -0.071538

h 5.329899 0.814580 -0.799257

c 3.300056 0.391392 -0.275323

h 2.890280 0.877326 -1.152221

c 2.455830 -0.209403 0.659385

c 2.971600 -0.844496 1.782591

h 2.300195 -1.312666 2.490552

c 4.352736 -0.875665 1.970271

h	4.756832	-1.374043	2.844877
c	6.716547	-0.312913	1.256557
h	6.985182	-0.861790	2.160577
h	7.219002	-0.790306	0.410104
h	7.122325	0.699525	1.344373
s	0.679494	-0.134607	0.411882
o	0.075721	-1.029606	1.430759
o	0.426955	-0.583853	-0.996067
o	0.283718	1.303581	0.590112
o	-4.268157	-0.388192	-1.903004
h	-3.589711	-0.466182	-2.672259
h	-4.052898	-1.163836	-1.279454
h	-4.110792	0.514431	-1.376742
o	-3.866801	1.715527	-0.620921
h	-3.847422	1.562120	0.360278
h	-3.020277	2.155212	-0.834091
o	-1.294550	2.787560	-1.106149
h	-1.166077	3.723758	-0.921514
h	-0.710100	2.302536	-0.481460
o	-0.431407	1.033286	-3.214336
h	0.027340	0.522089	-2.524658
h	-0.743478	1.821225	-2.739406
o	-2.458047	-0.744437	-3.676942
h	-1.998677	-1.537508	-3.350763
h	-1.765995	-0.040032	-3.652629
o	-1.102812	-2.633389	-1.946598
h	-0.481768	-1.978452	-1.552518
h	-0.587456	-3.426272	-2.125151
o	-3.483639	-2.367957	-0.438143

h -2.658518 -2.645695 -0.879487

h -3.231556 -2.139920 0.478862

o -2.526459 -1.494268 2.052185

h -2.560774 -2.047622 2.839020

h -1.572058 -1.328806 1.869310

o -3.599710 1.200801 2.013696

h -3.334559 0.273025 2.131596

h -2.844495 1.721182 2.349121

o -1.189214 2.516187 2.613154

h -0.552770 2.058871 2.030131

h -0.737889 2.668527 3.447899

49

pTS-.H+W10B

c 5.008825 -0.002354 1.679372

c 4.111967 1.017452 2.015145

h 4.474781 1.900765 2.530184

c 2.759176 0.921048 1.703440

h 2.069344 1.713245 1.963824

c 2.294146 -0.213269 1.043937

c 3.163284 -1.246820 0.700717

h 2.790612 -2.125555 0.189233

c 4.511936 -1.132824 1.019847

h 5.189338 -1.937426 0.754200

c 6.477575 0.126069 1.998853

h 6.962457 -0.850825 2.047070

h 6.993165 0.712666 1.230851

h 6.633796 0.631889 2.954367

s 0.542550 -0.384170 0.688904

o	-0.021858	-1.323568	1.689741
o	0.456040	-0.937402	-0.705284
o	-0.043037	0.991411	0.794152
o	-1.652291	-2.417456	-1.647763
h	-0.871847	-1.936576	-1.286921
h	-1.321776	-3.260659	-1.973964
o	-3.086345	-0.453804	-3.182113
h	-2.546764	-1.199493	-2.863191
h	-2.438144	0.257376	-3.429307
o	-4.589616	0.048789	-1.227578
h	-4.009275	-0.099120	-2.085165
h	-4.379885	-0.742504	-0.623359
h	-4.274787	0.915383	-0.751434
o	-3.829601	-2.016143	0.129513
h	-3.073707	-2.337366	-0.397557
h	-3.491807	-1.896851	1.039295
o	-2.566091	-1.505353	2.585520
h	-2.645319	-2.044505	3.378654
h	-1.614571	-1.514205	2.328707
o	-2.518308	1.371039	2.271975
h	-2.725514	0.471801	2.575546
h	-1.607784	1.299599	1.936697
o	-3.748192	2.127369	-0.046603
h	-3.432654	1.901199	0.861842
h	-2.955636	2.487693	-0.486445
o	-1.142104	2.722561	-1.039295
h	-0.738010	3.587767	-0.917610
h	-0.660438	2.107011	-0.442559
o	-1.215306	1.434507	-3.621177

h -0.345548 0.992640 -3.654648

h -1.178196 1.984962 -2.820461

o 1.154276 -0.022520 -3.239276

h 2.082865 0.195873 -3.355032

h 1.048280 -0.319347 -2.314844

49

pTS-.H+W10C

c 5.210328 -0.004471 0.105569

c 4.485087 -0.093243 1.295515

h 5.013478 -0.156685 2.240597

c 3.091227 -0.106257 1.293973

h 2.534548 -0.185164 2.218407

c 2.415197 -0.030148 0.082387

c 3.113116 0.054747 -1.122973

h 2.578294 0.100379 -2.063644

c 4.500778 0.066939 -1.101919

h 5.044530 0.129164 -2.038820

c 6.718607 0.015287 0.107418

h 7.124074 -0.786500 -0.516452

h 7.098519 0.960463 -0.292472

h 7.118394 -0.106824 1.115304

s 0.620630 -0.007074 0.053092

o 0.207653 1.381924 -0.320650

o 0.171641 -0.379511 1.430377

o 0.201952 -1.005273 -0.980204

o -1.292436 2.270623 -2.460138

h -0.657274 2.011927 -1.757601

h -0.936095 3.059680 -2.880381

o	-1.500573	-0.463567	-3.254018
h	-0.797662	-0.646578	-2.607151
h	-1.534763	0.506734	-3.281152
o	-1.387622	-3.249744	-0.757320
h	-0.718642	-2.537960	-0.852875
h	-1.024597	-4.031055	-1.186335
o	-3.514314	-1.652487	-1.829347
h	-2.969090	-2.361897	-1.444017
h	-2.901339	-1.205218	-2.460626
o	-4.442995	0.005642	-0.131875
h	-4.088120	0.947252	-0.362395
h	-4.084030	-0.678316	-0.816288
h	-4.135222	-0.258301	0.816952
o	-3.529397	2.321838	-0.669720
h	-2.940529	2.355504	-1.444992
h	-2.965348	2.667130	0.063449
o	-1.641210	3.046371	1.174060
h	-1.711087	2.582389	2.024397
h	-0.882998	2.615765	0.743813
o	-1.508875	0.991313	3.152977
h	-0.825708	0.531356	2.619204
h	-1.200052	0.986262	4.064453
o	-3.640336	-0.664893	2.191918
h	-3.100445	0.010319	2.640536
h	-3.043364	-1.450470	2.154671
o	-1.669621	-2.553765	1.997144
h	-0.921779	-1.943839	1.879288
h	-1.682531	-3.059769	1.167865

49

pTS-.H+W10D

c	5.203390	0.037077	0.101058
c	4.489326	1.212940	-0.155819
h	5.027813	2.134145	-0.351990
c	3.098392	1.226687	-0.159006
h	2.551256	2.142102	-0.344139
c	2.408929	0.044331	0.097401
c	3.092004	-1.141011	0.357990
h	2.545006	-2.051007	0.570775
c	4.482919	-1.135156	0.356549
h	5.016867	-2.056764	0.562028
c	6.711566	0.044044	0.131429
h	7.078913	0.436773	1.085487
h	7.118370	-0.961595	0.010268
h	7.122153	0.675937	-0.659710
s	0.614996	0.037782	0.046001
o	0.175667	1.444067	0.240707
o	0.164642	-0.888149	1.131091
o	0.225431	-0.492443	-1.310991
o	-1.645741	3.000759	-1.405565
h	-0.921216	2.620616	-0.880811
h	-1.641390	2.460968	-2.212166
o	-1.265483	0.814536	-3.221619
h	-0.612379	0.403209	-2.613451
h	-0.863527	0.834414	-4.095622
o	-1.337693	-2.675140	-1.909382
h	-0.666226	-1.983665	-1.717300
h	-0.959096	-3.258597	-2.574232

o -3.438424 -0.768435 -2.262708

h -2.889032 -1.568813 -2.178243

h -2.856143 -0.137948 -2.724458

o -4.434376 0.122712 -0.005102

h -4.095721 1.126763 0.165756

h -4.071029 -0.223229 -0.880157

h -4.124595 -0.493307 0.756218

o -3.633666 2.433087 0.394499

h -3.046754 2.736649 -0.337954

h -3.049699 2.471349 1.189874

o -1.676470 2.370089 2.306826

h -1.692131 1.596689 2.894223

h -0.926561 2.189895 1.716051

o -1.418959 -0.289802 3.325618

h -0.752668 -0.506525 2.639134

h -1.073733 -0.618166 4.161760

o -3.617617 -1.419159 1.869391

h -3.048673 -0.981748 2.527736

h -3.046314 -2.140335 1.515463

o -1.676990 -3.102724 0.899476

h -0.942853 -2.473914 1.007250

h -1.702481 -3.249987 -0.059635

49

pTS-.H+W10E

c 4.791209 0.602407 -0.709590

c 4.178772 1.583312 0.079728

h 4.792449 2.309895 0.601597

c 2.794509 1.650358 0.202422

h	2.326571	2.420843	0.802138
c	2.008271	0.719079	-0.472668
c	2.588936	-0.268130	-1.265683
h	1.963964	-0.976201	-1.794904
c	3.975100	-0.319112	-1.376153
h	4.428622	-1.085472	-1.995675
c	6.290872	0.562158	-0.867323
h	6.647043	-0.455613	-1.039664
h	6.605848	1.168729	-1.723230
h	6.796244	0.956689	0.016578
s	0.224912	0.759739	-0.268176
o	-0.147162	2.179765	-0.056349
o	-0.081508	-0.087496	0.944398
o	-0.357094	0.164240	-1.509593
o	-2.072727	1.497761	-3.253848
h	-1.682600	2.096076	-3.896521
h	-1.339377	1.119477	-2.731216
o	-4.117774	1.651433	-1.434418
h	-3.480244	1.712080	-2.178274
h	-3.731986	2.196842	-0.721974
o	-2.658642	3.026787	0.569059
h	-1.728360	2.842107	0.305810
h	-2.718743	3.972350	0.737658
o	-2.473580	0.854985	2.467334
h	-2.672770	1.690388	2.012407
h	-1.589902	0.613001	2.145313
o	-3.940469	-1.279909	1.575871
h	-3.202434	-1.921122	1.530662
h	-3.536809	-0.488543	2.005001

o	-4.391603	-0.817169	-0.863465
h	-4.286564	-0.972205	0.164977
h	-3.585874	-1.286987	-1.283403
h	-4.324530	0.190013	-1.078576
o	-2.242719	-1.993610	-1.672226
h	-1.965878	-2.487570	-0.874192
h	-1.550882	-1.314990	-1.774503
o	-1.521163	-2.562674	0.949313
h	-0.994709	-1.741297	0.950939
h	-0.978705	-3.206215	1.454029
o	0.342393	-3.937573	2.463185
h	0.933153	-3.167736	2.600631
h	0.163752	-4.299104	3.336181
o	1.716595	-1.537484	2.583630
h	1.179726	-0.925883	2.044751
h	2.625867	-1.408417	2.298010

52

pTS-.H+W11A

c	4.119642	2.419013	2.173988
c	3.772658	1.797551	0.966894
h	4.481016	1.789644	0.145144
c	2.536723	1.184912	0.802301
h	2.291726	0.705263	-0.137285
c	1.627306	1.189529	1.859815
c	1.946179	1.794431	3.070477
h	1.229629	1.779316	3.881151
c	3.190678	2.403228	3.217678
h	3.441366	2.870886	4.163826

c	5.454130	3.105001	2.329460
h	5.424406	4.113458	1.902997
h	5.733845	3.200276	3.380286
h	6.246130	2.556981	1.813749
s	0.019081	0.414498	1.656098
o	-0.660402	0.496361	2.970465
o	0.260151	-0.998747	1.216920
o	-0.707995	1.195264	0.594519
o	-2.478440	0.313224	-3.287180
h	-2.002709	-0.329783	-3.847514
h	-1.783641	0.881426	-2.905189
o	-3.969410	-0.699804	-1.404229
h	-3.429784	-0.310044	-2.165151
h	-3.589698	-1.703045	-1.156052
h	-3.855622	-0.095207	-0.599121
o	-3.112979	-2.920877	-0.832390
h	-2.354317	-3.177068	-1.414513
h	-2.769053	-2.921921	0.096347
o	-2.075937	-2.704270	1.661682
h	-2.594387	-2.148292	2.266896
h	-1.219548	-2.248321	1.588708
o	-3.197329	-0.477797	3.153119
h	-3.652578	-0.414917	3.998241
h	-2.303100	-0.087790	3.275155
o	-3.539975	0.837293	0.645762
h	-3.671305	0.430720	1.521921
h	-2.598771	1.097795	0.638684
o	-0.309582	1.689256	-2.022510
h	-0.175646	2.636596	-2.129991

h -0.406344 1.533635 -1.052004

o 1.294696 -0.363875 -3.189688

h 1.441270 -0.969726 -2.439705

h 0.876028 0.426956 -2.803557

o 1.296732 -2.174468 -0.993543

h 2.032701 -2.723363 -0.703682

h 0.944709 -1.739916 -0.181438

o -0.713489 -1.504968 -4.543723

h -0.572352 -1.666510 -5.481596

h 0.114211 -1.089856 -4.184194

o -0.942138 -3.397038 -2.384849

h -0.150700 -3.090329 -1.909140

h -0.937783 -2.904580 -3.224037

52

pTS-.H+W11B

c 4.995129 1.722442 -1.712467

c 3.871331 2.541081 -1.557183

h 3.929048 3.587848 -1.836043

c 2.678444 2.040172 -1.044841

h 1.819916 2.686847 -0.915384

c 2.606419 0.697251 -0.684087

c 3.709267 -0.141502 -0.826371

h 3.641495 -1.179806 -0.527575

c 4.893062 0.377051 -1.339674

h 5.753575 -0.274653 -1.448551

c 6.294423 2.282044 -2.236126

h 6.934517 2.613303 -1.411297

h 6.852335 1.532325 -2.801379

h	6.125070	3.143298	-2.885522
s	1.059959	0.016818	-0.076973
o	1.411996	-1.090768	0.839940
o	0.307894	-0.476945	-1.289140
o	0.333787	1.149045	0.578867
o	-1.565538	0.867249	-2.768482
h	-0.800931	0.432834	-2.327394
h	-1.319208	1.000150	-3.689119
o	-1.719898	2.777309	-0.620709
h	-0.940155	2.335676	-0.241749
h	-1.825762	2.344735	-1.483591
o	-3.481923	1.859930	1.286894
h	-2.820095	1.753146	1.993424
h	-2.979541	2.291543	0.557746
o	-1.139691	1.392920	2.890868
h	-0.520931	1.272792	2.137722
h	-0.743854	2.057707	3.463607
o	-1.910313	-1.191301	3.856707
h	-1.146685	-1.739652	3.605700
h	-1.643024	-0.279533	3.647292
o	0.184201	-2.745894	2.636189
h	0.644921	-2.143980	2.011401
h	0.873364	-3.233729	3.097794
o	-1.982920	-3.807403	1.064978
h	-1.203778	-3.622693	1.617914
h	-1.723935	-3.535658	0.167661
o	-3.832051	-2.120805	2.159287
h	-3.277852	-2.817387	1.729880
h	-3.244891	-1.753402	2.865277

o -4.511708 -0.376173 0.553883

h -4.148399 -0.602719 -0.359196

h -4.125138 0.525191 0.848247

h -4.228124 -1.145075 1.259207

o -3.494369 -0.986974 -1.783156

h -2.999238 -0.272589 -2.224525

h -2.855417 -1.721922 -1.735512

o -1.248474 -2.723162 -1.493455

h -0.897757 -3.315915 -2.165842

h -0.588551 -2.001065 -1.385142

52

pTS-.H+W11C

c 5.177665 -0.050747 1.715967

c 4.464403 0.973944 1.082397

h 4.982949 1.876629 0.777298

c 3.099690 0.859444 0.841832

h 2.558561 1.666055 0.362581

c 2.434327 -0.299228 1.236507

c 3.117433 -1.334518 1.867569

h 2.580705 -2.222027 2.176482

c 4.482885 -1.201857 2.101655

h 5.015563 -2.007544 2.595806

c 6.650950 0.095016 2.005208

h 6.811378 0.466057 3.023164

h 7.169688 -0.862612 1.921862

h 7.124845 0.800670 1.320096

s 0.680615 -0.474596 0.892326

o 0.198238 -1.609840 1.717810

o	0.560356	-0.774090	-0.579063
o	0.040808	0.830000	1.243925
o	-3.395364	0.785083	-3.203130
h	-2.862469	0.037799	-3.562132
h	-2.742296	1.519628	-3.111931
o	-4.453952	0.248103	-1.016538
h	-4.017124	0.471312	-1.960628
h	-4.117078	-0.649060	-0.686469
h	-4.187087	0.968144	-0.333341
o	-3.529109	-2.031230	-0.179400
h	-2.755692	-2.344899	-0.686790
h	-3.261474	-2.084236	0.757759
o	-2.395904	-2.050999	2.420465
h	-2.500670	-2.749460	3.074005
h	-1.433991	-1.986276	2.222771
o	-2.457651	0.809991	2.799546
h	-2.625951	-0.144404	2.867785
h	-1.542685	0.860456	2.476527
o	-3.720840	2.011453	0.683284
h	-3.405135	1.595915	1.520348
h	-2.946993	2.513105	0.370183
o	-1.111502	2.982537	-0.014665
h	-0.764801	3.779721	0.398722
h	-0.625899	2.228356	0.386190
o	-1.319484	2.543265	-2.834386
h	-0.549371	1.970739	-2.990407
h	-1.236009	2.822287	-1.906405
o	0.686722	0.478047	-3.016372
h	1.582088	0.503240	-3.367469

h 0.748887 0.096855 -2.113766

o -1.564408 -1.132499 -3.954762

h -1.495400 -1.818898 -3.270246

h -0.741318 -0.624706 -3.860154

o -1.148348 -2.685068 -1.554443

h -0.484374 -2.083314 -1.147083

h -0.776377 -3.571742 -1.510487

52

pTS-.H+W11X

c 4.777166 -0.053042 1.633005

c 4.000886 1.092721 1.428322

h 4.473264 2.069444 1.442272

c 2.622021 1.005902 1.227310

h 2.022912 1.895619 1.084057

c 2.013582 -0.244302 1.222680

c 2.764102 -1.402590 1.424613

h 2.280065 -2.371366 1.426134

c 4.134593 -1.299331 1.625914

h 4.716551 -2.201087 1.784936

c 6.260221 0.045349 1.891402

h 6.811715 -0.727980 1.350837

h 6.655196 1.018447 1.594071

h 6.476151 -0.087378 2.956588

s 0.244949 -0.390518 0.925534

o -0.309190 -1.201169 2.038080

o 0.112902 -1.082307 -0.397925

o -0.287686 1.008144 0.893227

o -1.963319 -2.606748 -1.288141

h	-1.189206	-2.109624	-0.934980
h	-1.635070	-3.474941	-1.542942
o	-3.241997	-0.694142	-3.011124
h	-2.748614	-1.439333	-2.624189
h	-2.554348	-0.029559	-3.290866
o	-4.796216	-0.003484	-1.167196
h	-4.179558	-0.233094	-1.986942
h	-4.634420	-0.744464	-0.491688
h	-4.488894	0.892707	-0.746958
o	-4.152678	-1.970142	0.393802
h	-3.408767	-2.373649	-0.092148
h	-3.815906	-1.779564	1.291100
o	-2.902337	-1.283666	2.827557
h	-3.026942	-1.746012	3.662256
h	-1.941125	-1.330398	2.617072
o	-2.798621	1.559543	2.287287
h	-3.021602	0.686733	2.650897
h	-1.879402	1.459050	1.986672
o	-3.974471	2.152854	-0.112959
h	-3.682190	1.991837	0.816088
h	-3.167601	2.472521	-0.558584
o	-1.349192	2.625805	-1.085337
h	-0.912702	3.482151	-1.033480
h	-0.887932	2.040802	-0.445322
o	-1.319826	1.096078	-3.549432
h	-0.433811	0.678650	-3.495091
h	-1.327379	1.731832	-2.814997
o	1.064549	-0.190702	-2.942002
h	1.928763	0.231024	-2.810695

h 0.819580 -0.539513 -2.068237

o 3.638274 0.934826 -2.175828

h 4.439188 0.598353 -2.590121

h 3.774372 0.839713 -1.224527

55

pTS-.H+W12A

c 5.579711 -0.039769 0.065392

c 4.849410 0.180547 1.236793

h 5.373242 0.300369 2.178940

c 3.458562 0.244684 1.219782

h 2.901130 0.404803 2.133985

c 2.787560 0.084058 0.011351

c 3.488953 -0.139487 -1.172171

h 2.953529 -0.276971 -2.102724

c 4.876515 -0.200360 -1.135594

h 5.423022 -0.380129 -2.055540

c 7.086537 -0.107276 0.084219

h 7.442884 -1.061740 -0.314117

h 7.522014 0.684210 -0.533166

h 7.478873 0.002690 1.096406

s 0.999431 0.234235 -0.030735

o 0.680086 1.674775 -0.266270

o 0.508716 -0.236289 1.301388

o 0.532556 -0.631493 -1.160650

o -0.674191 3.469410 1.342976

h -0.076798 2.898826 0.814118

h -0.184273 4.272606 1.545240

o -2.879656 3.322597 -0.497661

h	-2.270435	3.515853	0.236724
h	-2.283843	3.209740	-1.274272
o	-0.954477	2.785008	-2.395203
h	-0.253959	2.493148	-1.788058
h	-1.147235	1.986760	-2.912938
o	-1.215650	0.025732	-3.177698
h	-0.549205	-0.224706	-2.500077
h	-0.944595	-0.392550	-4.000966
o	-3.729834	-0.488841	-1.969441
h	-2.912060	-0.300585	-2.466831
h	-3.645999	-1.415550	-1.668178
o	-4.338617	1.239140	-0.133186
h	-3.777285	2.083769	-0.271292
h	-4.115883	0.568863	-0.860961
h	-4.134010	0.807932	0.824752
o	-3.848596	0.236488	2.078624
h	-3.011406	0.593336	2.459809
h	-3.731677	-0.742936	2.033683
o	-3.324578	-2.431673	1.796522
h	-3.452189	-2.729319	0.879303
h	-2.383286	-2.591156	1.980566
o	-3.232909	-3.084594	-1.021508
h	-2.246616	-3.210224	-1.033384
h	-3.620932	-3.866298	-1.427090
o	-0.567920	-3.268863	-0.807053
h	-0.127614	-2.426794	-1.020373
h	-0.432313	-3.359493	0.152513
o	-0.434379	-2.732439	1.982650
h	0.025274	-3.102391	2.742812

h -0.040647 -1.848403 1.817888

o -1.420997 1.187777 2.913644

h -0.742542 0.680017 2.436544

h -1.261402 2.102954 2.630514

55

pTS-.H+W12B

c 5.570225 -0.084595 0.056668

c 4.795411 -0.647198 1.073272

h 5.281340 -1.171060 1.889210

c 3.405303 -0.543967 1.064991

h 2.811486 -0.971731 1.862269

c 2.784218 0.132628 0.021678

c 3.532152 0.708259 -1.006221

h 3.039173 1.245486 -1.807024

c 4.915273 0.594641 -0.980882

h 5.498746 1.045105 -1.777133

c 7.074885 -0.190490 0.069548

h 7.443927 -0.666608 -0.843625

h 7.537320 0.799507 0.127925

h 7.426753 -0.775704 0.920556

s 0.993698 0.249213 -0.026966

o 0.667326 1.666283 -0.369704

o 0.502351 -0.162785 1.315500

o 0.534218 -0.687928 -1.114100

o -0.710523 3.530093 1.145904

h -0.106853 2.937410 0.649777

h -0.218546 4.336658 1.329237

o -2.892474 3.298022 -0.705867

h	-2.291836	3.528276	0.025294
h	-2.287942	3.154428	-1.470805
o	-0.943119	2.675340	-2.549678
h	-0.263721	2.400431	-1.910997
h	-1.136645	1.854839	-3.031458
o	-1.191096	-0.112150	-3.186986
h	-0.532136	-0.332671	-2.492133
h	-0.917635	-0.573452	-3.986011
o	-3.727914	-0.569769	-1.974159
h	-2.907344	-0.408801	-2.474934
h	-3.618625	-1.460000	-1.560161
o	-4.326813	1.218643	-0.271273
h	-3.771643	2.065234	-0.436685
h	-4.090722	0.503317	-0.977614
h	-4.126797	0.843788	0.677626
o	-3.810017	0.318899	2.029976
h	-2.977761	0.698899	2.401943
h	-3.723781	-0.651728	2.105262
o	-3.313278	-2.456661	2.121308
h	-3.721628	-2.998225	2.804189
h	-2.330135	-2.556438	2.224276
o	-3.254842	-2.947351	-0.718938
h	-2.310526	-3.167003	-0.785018
h	-3.430660	-2.875851	0.236023
o	-0.353834	-3.262146	-0.704969
h	0.035394	-2.379316	-0.892073
h	0.179884	-3.908436	-1.177319
o	-0.639395	-2.689216	2.074619
h	-0.472762	-3.127519	1.222219

h	-0.215524	-1.820048	1.964096
o	-1.421655	1.342254	2.861436
h	-0.718881	0.814773	2.445227
h	-1.272020	2.236418	2.512703

Reference

1. Kuo, M.; Kamelamela, N.; Shultz, M. J., "Rotational Structure of Water in a Hydrophobic Environment: Carbon Tetrachloride," *J Phys Chem A* **2008**, *112*, 1214-1218. 10.1021/jp7097284
2. Makogon, Y. F.; Holditch, S. A.; Makogon, T. Y., "Natural Gas-Hydrates - a Potential Energy Source for the 21st Century," *J. Petrol. Sci. Eng.* **2007**, *56*, 14-31. 10.1016/j.petrol.2005.10.009
3. Kvenvolden, Keith A., "Methane Hydrate — a Major Reservoir of Carbon in the Shallow Geosphere?," *Chemical Geology* **1988**, *71*, 41-51. https://doi.org/10.1016/0009-2541(88)90104-0
4. Makogon, Y. F.; Holste, J. C.; Holditch, S. A., "Natural Gas Hydrates and Global Change," *Int Offshore Polar E* **1998**, 73-74.
5. Wuebbles, D. J.; Hayhoe, K., "Atmospheric Methane and Global Change," *Earth-Sci Rev* **2002**, *57*, 177-210. Pii S0012-8252(01)00062-9

Doi 10.1016/S0012-8252(01)00062-9
6. Brewer, P. G.; Friederich, C.; Peltzer, E. T.; Orr, F. M., "Direct Experiments on the Ocean Disposal of Fossil Fuel Co2," *Science* **1999**, *284*, 943-945. DOI 10.1126/science.284.5416.943
7. Liro, C. R.; Adams, E. E.; Herzog, H. J., "Modeling the Release of Co2 in the Deep Ocean," *Energ Convers Manage* **1992**, *33*, 667-674. Doi 10.1016/0196-8904(92)90070-D
8. Kojima, R.; Yamane, K.; Aya, I., "Dual Nature of Co2 Solubility in Hydrate Forming Region," *Greenhouse Gas Control Technologies, Vols I and Ii, Proceedings* **2003**, 825-830.
9. Lee, S.; Liang, L. Y.; Riestenberg, D.; West, O. R.; Tsouris, C.; Adams, E., "Co2 Hydrate Composite for Ocean Carbon Sequestration," *Environ Sci Technol* **2003**, *37*, 3701-3708. 10.1021/es026301l
10. Thomas, S.; Dawe, R. A., "Review of Ways to Transport Natural Gas Energy from Countries Which Do Not Need the Gas for Domestic Use," *Energy* **2003**, *28*, 1461-1477, Article. 10.1016/s0360-5442(03)00124-5
11. Sun, Z. G.; Wang, R. Z.; Ma, R. S.; Guo, K. H.; Fan, S. S., "Natural Gas Storage in Hydrates with the Presence of Promoters," *Energ Convers Manage* **2003**, *44*, 2733-2742. 10.1016/S0196-8904(03)00048-7
12. Gudmundsson, J.; Borrehaug, A., "Frozen Hydrate for Transport of Natural Gas," *Ngh '96 - 2nd International Conference on Natural Gas Hydrates, Proceedings* **1996**, 415-422.
13. Zhong, Y.; Rogers, R. E., "Surfactant Effects on Gas Hydrate Formation," *Chem Eng Sci* **2000**, *55*, 4175-4187. Doi 10.1016/S0009-2509(00)00072-5
14. Sun, Z. G.; Ma, R. S.; Wang, R. Z.; Guo, K. H.; Fa, S. S., "Experimental Studying of Additives Effects on Gas Storage in Hydrates," *Energ Fuel* **2003**, *17*, 1180-1185. 10.1021/ef020191m
15. Kang, S. P.; Lee, H., "Recovery of Co2 from Flue Gas Using Gas Hydrate: Thermodynamic Verification through Phase Equilibrium Measurements," *Environ Sci Technol* **2000**, *34*, 4397-4400. Doi 10.1021/Es001148l
16. Gnanendran, N.; Amin, R., "The Effect of Hydrotropes on Gas Hydrate Formation," *J. Petrol. Sci. Eng.* **2003**, *40*, 37-46. 10.1016/S0920-4105(03)00082-2

17. Gnanendran, N.; Amin, R., "Equilibrium Hydrate Formation Conditions for Hydrotrope-Water-Natural Gas Systems," *Fluid Phase Equilibr.* **2004**, *221*, 175-187. 10.1016/j.fluid.2004.04.013
18. Shultz, M. J.; Vu, T. H., "Hydrogen Bonding between Water and Tetrahydrofuran Relevant to Clathrate Formation," *J Phys Chem B* **2015**, *119*, 9167-9172. 10.1021/jp509343x
19. Kassner, J. L.; Hagen, D. E., "Clustering of Water on Hydrated Protons in a Supersonic Free Jet Expansion - Comment," *J Chem Phys* **1976**, *64*, 1860-1861. 10.1063/1.432330
20. Kebarle, P.; Haynes, R. N.; Collins, J. G., "Competitive Solvation of Hydrogen Ion by Water and Methanol Molecules Studied in Gas Phase," *Journal of the American Chemical Society* **1967**, *89*, 5753-5757. 10.1021/Ja00999a003
21. Kebarle, P.; Searles, S. K.; Zolla, A.; Scarboro.J; Arshadi, M., "Solvation of Hydrogen Ion by Water Molecules in Gas Phase. Heats and Entropies of Solvation of Individual Reactions - $H^+(H_2o)_{N-1}$ + $H_2o \rightarrow H^+(H_2o)_N$," *J. Am. Chem. Soc.* **1967**, *89*, 6393-6399. 10.1021/Ja01001a001
22. Schwarz, H. A., "Gas-Phase Infrared-Spectra of Oxonium Hydrate Ions from 2 to 5 M," *J Chem Phys* **1977**, *67*, 5525-5534. 10.1063/1.434748
23. Stace, A. J.; Moore, C., "Solvation of Hydrogen-Ions in Mixed Water Alcohol Ion Clusters," *Journal of the American Chemical Society* **1983**, *105*, 1814-1819. 10.1021/Ja00345a022
24. Wang, Q.; Hammes-Schiffer, S., "Hybrid Quantum/Classical Path Integral Approach for Simulation of Hydrogen Transfer Reactions in Enzymes," *J Chem Phys* **2006**, *125*. Artn 184102

10.1063/1.2362823
25. Pfaendtner, J.; Yu, X. R.; Broadbelt, L. J., "Quantum Chemical Investigation of Low-Temperature Intramolecular Hydrogen Transfer Reactions of Hydrocarbons," *J Phys Chem A* **2006**, *110*, 10863-10871. 10.1021/jp061649e
26. Sakaguchi, N.; Hirano, S.; Matsuda, A.; Shuto, S., "Radical Reactions with 2-Bromobenzylidene Group, a Protecting/Radical-Translocating Group for the 1,6-Radical Hydrogen Transfer Reaction," *Org. Lett.* **2006**, *8*, 3291-3294. 10.1021/ol061162o
27. Haji-Akbari, Amir; Debenedetti, Pablo G. , "Perspective: Surface Freezing in Water: A Nexus of Experiments and Simulations," *J. Chem. Phys.* **2017**, *147*, 060901:1-11. 10.1063/1.4985879
28. Zhang, Zhengcai; Guo, Guang-Jun, "The Effects of Ice on Methane Hydrate Nucleation: A Microcanonical Molecular Dynamics Study," *Phys. Chem. Chem. Phys.* **2017**, *19*, 19496-19505. 10.1039/C7CP03649C
29. Sloan, E. D.; Koh, C. A., *Clathrate Hydrates of Natural Gases* Third Edition ed. (CRC Press, 2008) Vol. 119 pgs. 701 Translated by.
30. Biswas, R.; Carpenter, W.; Fournier, J. A.; Voth, G. A.; Tokmakoff, A., "Ir Spectral Assignments for the Hydrated Excess Proton in Liquid Water," *J Chem Phys* **2017**, *146*. 10.1063/1.4980121
31. Devlin, J. P.; Severson, M. W.; Mohamed, F.; Sadlej, J.; Buch, V.; Parrinello, M., "Experimental and Computational Study of Isotopic Effects within the Zundel Ion," *Chemical Physics Letters* **2005**, *408*, 439-444. 10.1016/j.cplett.2005.04.087
32. Kaledin, M.; Wood, C. A., "Ab Initio Studies of Structural and Vibrational Properties of Protonated Water Cluster H_7o^{3+} and Its Deuterium Isotopologues: An Application of Driven Molecular Dynamics," *J. Chem. Theory Comput.* **2010**, *6*, 2525-2535. 10.1021/ct100122s
33. Kulig, W.; Agmon, N., "Both Zundel and Eigen Isomers Contribute to the Ir Spectrum of the Gas-Phase $H_9o_4^+$ Cluster," *J Phys Chem B* **2014**, *118*, 278-286. 10.1021/jp410446d
34. Wolke, C. T.; Fournier, J. A.; Dzugan, L. C.; Fagiani, M. R.; Odbadrakh, T. T.; Knorke, H.; Jordan, K. D.; McCoy, A. B.; Asmis, K. R.; Johnson, M. A., "Spectroscopic Snapshots of the Proton-Transfer Mechanism in Water," *Science* **2016**, *354*, 1131-1135. 10.1126/science.aaf8425
35. Fournier, J. A.; Wolke, C. T.; Johnson, C. J.; Johnson, M. A.; Heine, N.; Gewinner, S.; Schollkopf, W.; Esser, T. K.; Fagiani, M. R.; Knorke, H.; Asmis, K. R., "Site-Specific Vibrational Spectral Signatures of

Water Molecules in the Magic $H_3O^+(H_2O)_{20}$ and $Cs^+(H_2O)_{20}$ Clusters," *Proc. Natl. Acad. Sci. USA* **2014**, *111*, 18132-18137. 10.1073/pnas.1420734111
36. Fournier, J. A.; Wolke, C. T.; Johnson, M. A.; Odbadrakh, T. T.; Jordan, K. D.; Kathmann, S. M.; Xantheas, S. S., "Snapshots of Proton Accommodation at a Microscopic Water Surface: Understanding the Vibrational Spectral Signatures of the Charge Defect in Cryogenically Cooled $H^+(H_2O)_{N=2-28}$ Clusters," *J Phys Chem A* **2015**, *119*, 9425-9440. 10.1021/acs.jpca.5b04355
37. Headrick, J. M.; Diken, E. G.; Walters, R. S.; Hammer, N. I.; Christie, R. A.; Cui, J.; Myshakin, E. M.; Duncan, M. A.; Johnson, M. A.; Jordan, K. D., "Spectral Signatures of Hydrated Proton Vibrations in Water Clusters," *Science* **2005**, *308*, 1765-1769. 10.1126/science.1113094
38. Shin, J. W.; Hammer, N. I.; Diken, E. G.; Johnson, M. A.; Walters, R. S.; Jaeger, T. D.; Duncan, M. A.; Christie, R. A.; Jordan, K. D., "Infrared Signature of Structures Associated with the $H^+(H_2O)(N)$ (N=6 to 27) Clusters," *Science* **2004**, *304*, 1137-1140. 10.1126/science.1096466
39. Chemistry, Physical and theoretical. McQuarrie, Donald A.; Simon, John D., *Physical Chemistry : A Molecular Approach* (University Science Books, Sausalito, Calif., 1997) pgs. xxiii, 1270 p. Translated by 0935702997 (acid-free paper).
40. Chemistry, Inorganic Textbooks. Atkins, P. W.; Shriver, D. F., *Inorganic Chemistry* 4th ed. (W.H. Freeman, New York, 2006) pgs. xxi, 822 p. Translated by 0716748789.
41. Chemistry, Turnkey Computational, "Pqs Ab Initio Version 4.0 Released," **2011**.
42. Becke, A. D., "Density-Functional Thermochemistry .3. The Role of Exact Exchange," *J Chem Phys* **1993**, *98*, 5648-5652. 10.1063/1.464913
43. Lee, C. T.; Yang, W. T.; Parr, R. G., "Development of the Colle-Salvetti Correlation-Energy Formula into a Functional of the Electron-Density," *Phys. Rev. B* **1988**, *37*, 785-789. 10.1103/PhysRevB.37.785
44. Anick, D. J., "Comparison of Hydrated Hydroperoxide Anion $(Hoo^-)(H_2O)_N$ Clusters with Alkaline Hydrogen Peroxide $(Hooh)(Oh^-)(H_2O)_{N-1}$ Clusters, N=1-8, 20: An *Ab Initio* Study," *J Phys Chem A* **2011**, *115*, 6327-6338. 10.1021/jp110558y
45. Bryantsev, V. S.; Diallo, M. S.; van Duin, A. C. T.; Goddard, W. A., "Evaluation of B3lyp, X3lyp, and M06-Class Density Functionals for Predicting the Binding Energies of Neutral, Protonated, and Deprotonated Water Clusters," *J. Chem. Theory Comput.* **2009**, *5*, 1016-1026. 10.1021/ct800549f
46. Ganesan, A.; Dreyer, J.; Wang, F.; Akola, J.; Larrucea, J., "Density Functional Study of Cu^{2+}-Phenylalanine Complex under Micro-Solvation Environment," *J. Mol. Graph. Model.* **2013**, *45*, 180-191. 10.1016/j.jmgm.2013.08.015
47. Gao, B.; Wyttenbach, T.; Bowers, M. T., "Protonated Arginine and Protonated Lysine: Hydration and Its Effect on the Stability of Salt-Bridge Structures," *J Phys Chem B* **2009**, *113*, 9995-10000. 10.1021/jp903307h
48. Lambrecht, D. S.; Clark, G. N. I.; Head-Gordon, T.; Head-Gordon, M., "Exploring the Rich Energy Landscape of Sulfate-Water Clusters So_4^{2-} $(H_2O)(N$=3-7): An Electronic Structure Approach," *J Phys Chem A* **2011**, *115*, 11438-11454. 10.1021/jp206064n
49. Lee, H. M.; Tarkeshwar, P.; Kim, K. S., "Structures, Energetics, and Spectra of Hydrated Hydroxide Anion Clusters," *J Chem Phys* **2004**, *121*, 4657-4664. 10.1063/1.1779566
50. Momany, F. A.; Appell, M.; Willett, J. L.; Bosma, W. B., "B3lyp/6-311++G** Geometry-Optimization Study of Pentahydrates of Alpha- and Beta-D-Glucopyranose," *Carbohyd Res.* **2005**, *340*, 1638-1655. 10.1016/j.carres.2005.04.020
51. Ramondo, F.; Bencivenni, L.; Caminiti, R.; Pieretti, A.; Gontrani, L., "Dimerisation of Urea in Water Solution: A Quantum Mechanical Investigation," *Phys Chem Chem Phys* **2007**, *9*, 2206-2215. 10.1063/b617837e

52. Senthilkumar, L.; Umadevi, P.; Nithya, K. N. S.; Kolandaivel, P., "Density Functional Theory Investigation of Cocaine Water Complexes," *J. Mol. Model.* **2013**, *19*, 3411-3425. 10.1007/s00894-013-1866-0
53. Smith, A.; Vincent, M. A.; Hillier, I. H., "Mechanism of Acid Dissociation in Water Clusters: Electronic Structure Studies of $(H_2o)_Nhx$ (*N* = 4, 7; X = Oh, F, Hs, Hso_3, $Ooso_2h$, $Ooh{\cdot}So_2$)," *J Phys Chem A* **1999**, *103*, 1132-1139. 10.1021/Jp984216n
54. National Institute of Standards and Technology, Precomputed Vibrational Scaling Factors; **2016**, http://cccbdb.nist.gov/vibscalejust.asp.
55. Shultz, M. J.; Vu, T. H.; Meyer, B.; Bisson, P., "Water: A Responsive Small Molecule," *Accounts Chem. Res.* **2012**, *45*, 15-22. 10.1021/ar200064z
56. Vaden, T. D.; Lisy, J. M.; Carnegie, P. D.; Pillai, E. D.; Duncan, M. A., "Infrared Spectroscopy of the $Li^+(H_2o)Ar$ Complex: The Role of Internal Energy and Its Dependence on Ion Preparation," *Phys Chem Chem Phys* **2006**, *8*, 3078-3082. 10.1039/b605442k
57. Vaden, T. D.; Forinash, B.; Lisy, J. M., "Rotational Structure in the Asymmetric Oh Stretch of $Cs^+(H_2o)Ar$," *J Chem Phys* **2002**, *117*, 4628-4631. 10.1063/1.1503310
58. Vaden, T. D.; Weinheimer, C. J.; Lisy, J. M., "Evaporatively Cooled $M^+(H_2o)Ar$ Cluster Ions: Infrared Spectroscopy and Internal Energy Simulations," *J Chem Phys* **2004**, *121*, 3102-3107. 10.1063/1.1774157
59. Weinheimer, C. J.; Lisy, J. M., "Gas-Phase Cluster Ion Vibrational Spectroscopy of $Na^+(Ch_3oh)(2-7)$," *J. Phys. Chem.* **1996**, *100*, 15305-15308. 10.1021/Jp9621787
60. Weinheimer, C. J.; Lisy, J. M., "Vibrational Predissociation Spectroscopy of $Cs^+(H_2o)(1-5)$," *J Chem Phys* **1996**, *105*, 2938-2941. 10.1063/1.472160
61. Bisson, P.; Xiao, H.; Kuo, M.; Kamelamela, N.; Shultz, M. J., "Ions and Hydrogen Bonding in a Hydrophobic Environment: Ccl_4," *J Phys Chem A* **2010**, *114*, 4051-4057. 10.1021/jp9106712
62. Khuu, T.; Anick, D.; Shultz, M. J., "Matrix Isolation Spectroscopy: Aqueous P-Toluenesulfonic Acid Solvation," *J Phys Chem A* **2018**, *122*, 762-772. 10.1021/acs.jpca.7b08939
63. Max, J. J.; Chapados, C., "Isotope Effects in Liquid Water by Infrared Spectroscopy," *J Chem Phys* **2002**, *116*, 4626-4642. 10.1063/1.1448286
64. Chen, H. N.; Xu, J. Q.; Voth, G. A., "Unusual Hydrophobic Interactions in Acidic Aqueous Solutions," *J Phys Chem B* **2009**, *113*, 7291-7297. 10.1021/jp9025909
65. Zhou, X. Y.; Wang, C. L.; Wu, F. M.; Feng, M.; Li, J. Y.; Lu, H. J.; Zhou, R. H., "The Ice-Like Water Monolayer near the Wall Makes Inner Water Shells Diffuse Faster inside a Charged Nanotube," *J Chem Phys* **2013**, *138*, 204710:1-6. 10.1063/1.4807383
66. Petersen, M. K.; Iyengar, S. S.; Day, T. J. F.; Voth, G. A., "The Hydrated Proton at the Water Liquid/Vapor Interface," *J Phys Chem B* **2004**, *108*, 14804-14806, Letter. 10.1021/jp046716o
67. James, T.; Wales, D. J., "Protonated Water Clusters Described by an Empirical Valence Bond Potential," *J Chem Phys* **2005**, *122*, 134306:1-11. 10.1063/1.1869987
68. Wei, S.; Shi, Z.; Castleman, A. W., "Mixed Cluster Ions as a Structure Probe - Experimental-Evidence for Clathrate Structure of $(H_2o)_{20}h^+$ and $(H_2o)_{21}h^+$," *J Chem Phys* **1991**, *94*, 3268-3270. 10.1063/1.459796
69. Yang, X. L.; Castleman, A. W., "Large Protonated Water Clusters $H^+(H_2o)_N$ ($1\leq N>60$) - the Production and Reactivity of Clathrate-Like Structures under Thermal Conditions," *Journal of the American Chemical Society* **1989**, *111*, 6845-6846. 10.1021/Ja00199a056
70. Shields, Robert M.; Temelso, Berhane; Archer, Kaye A.; Morrell, Thomas E.; Shields, George C., "Accurate Predictions of Water Cluster Formation, $(H_2o)_{N=2-10}$," *J. Phys. Chem. A* **2010**, *114*, 11725-11737. 10.1021/jp104865w
71. Anick, D. J., "O-H Stretch Modes of Dodecahedral Water Clusters: A Statistical Ab Initio Study," *J Phys Chem A* **2006**, *110*, 5135-5143. 10.1021/jp055632s

72. Buck, U.; Ettischer, I.; Melzer, M.; Buch, V.; Sadlej, J., "Structure and Spectra of Three-Dimensional $(H_2o)_N$ Clusters, *N* = 8, 9, 10," *Phys. Rev. Lett.* **1998**, *80*, 2578-2581. 10.1103/PhysRevLett.80.2578
73. Sadlej, J., "Theoretical Study of Structure and Spectra of Cage Clusters $(H_2o)_N$, *N*=11,12," *Chemical Physics Letters* **2001**, *333*, 485-492. 10.1016/S0009-2614(00)01397-X
74. Sadlej, J.; Buch, V.; Kazimirski, J. K.; Buck, U., "Theoretical Study of Structure and Spectra of Cage Clusters $(H_2o)_N$, *N*=7-10," *J Phys Chem A* **1999**, *103*, 4933-4947. 10.1021/Jp990546b
75. Barth, H. D.; Buchhold, K.; Djafari, S.; Reimann, B.; Lommatzsch, U.; Brutschy, B., "Hydrogen Bonding in (Substituted Benzene)·$(Water)_N$ Clusters with *N* <= 4," *Chemical Physics* **1998**, *239*, 49-64. 10.1016/S0301-0104(98)00306-1
76. Pierola, I. F.; Agzenai, Y., "Ion Pairing and Anion-Driven Aggregation of an Ionic Liquid in Aqueous Salt Solutions," *J Phys Chem B* **2012**, *116*, 3973-3981. 10.1021/jp212202b
77. Kumar, R.; Schmidt, J. R.; Skinner, J. L., "Hydrogen Bonding Definitions and Dynamics in Liquid Water," *J Chem Phys* **2007**, *126*, 204107:1-12. 10.1063/1.2742385
78. Gregory, J. K.; Clary, D. C., "Quantum Simulation of the Benzene-Water Complex," *Mol. Phys.* **1996**, *88*, 33-52. 10.1080/00268979650026587
79. Gutowsky, H. S.; Emilsson, T.; Arunan, E., "Low-J Rotational Spectra, Internal-Rotation, and Structures of Several Benzene-Water Dimers," *J Chem Phys* **1993**, *99*, 4883-4893. 10.1063/1.466038
80. Pribble, R. N.; Zwier, T. S., "Size-Specific Infrared-Spectra of Benzene-$(H_2o)_N$ Clusters (*N*=1 through 7) - Evidence for Noncyclic $(H_2o)_N$ Structures," *Science* **1994**, *265*, 75-79. 10.1126/science.265.5168.75
81. Anick, D. J., "Proton and Deuteron Position Preferences in Water Clusters: An *Ab Initio* Study," *J Chem Phys* **2005**, *123*, 244309:1-10. 10.1063/1.2139669
82. Pribble, R. N.; Zwier, T. S., "Probing Hydrogen-Bonding in Benzene-$(Water)_N$ Clusters Using Resonant Ion-Dip Ir Spectroscopy," *Faraday Dis.* **1994**, *97*, 229-241. 10.1039/Fd9949700229
83. Wang, H.; Agmon, N., "Protonated Water Dimer on Benzene: Standing Eigen or Crouching Zundel?," *J Phys Chem B* **2015**, *119*, 2658-2667. 10.1021/jp509004j
84. Prakash, M.; Samy, K. G.; Subramanian, V., "Benzene-Water (Bzw_n (*N*=1-10)) Clusters," *J Phys Chem A* **2009**, *113*, 13845-13852, Review. 10.1021/jp906770x
85. Miyazaki, M.; Fujii, A.; Ebata, T.; Mikami, N., "Infrared Spectroscopy of Hydrated Benzene Cluster Cations, C_6h_6-$(H_2o)_N^+$ (*N*=1-6): Structural Changes Upon Photoionization and Proton Transfer Reactions," *Phys Chem Chem Phys* **2003**, *5*, 1137-1148, Article. 10.1039/b210293e
86. Miyazaki, M.; Fujii, A.; Ebata, T.; Mikami, N., "Infrared Spectroscopy of Size-Selected Benzene-Water Cluster Cations $[C_6h_6$-$(H_2o)N]^+$ (*N*=1-23): Hydrogen Bond Network Evolution and Microscopic Hydrophobicity," *J Phys Chem A* **2004**, *108*, 10656-10660. 10.1021/jp045823f
87. Kim, K. S.; Tarakeshwar, P.; Lee, J. Y., "Molecular Clusters of Pi-Systems: Theoretical Studies of Structures, Spectra, and Origin of Interaction Energies," *Chem Rev* **2000**, *100*, 4145-4185. 10.1021/cr990051i
88. Hagemeister, F. C.; Gruenloh, C. J.; Zwier, T. S., "Resonant Ion-Dip Infrared Spectroscopy of Benzene-$(Water)_N$-$(Methanol)_M$ Clusters with *N*+*M*=4,5," *Chemical Physics* **1998**, *239*, 83-96. 10.1016/s0301-0104(98)00353-x
89. Gruenloh, C. J.; Carney, J. R.; Hagemeister, F. C.; Arrington, C. A.; Zwier, T. S.; Fredericks, S. Y.; Wood, J. T.; Jordan, K. D., "Resonant Ion-Dip Infrared Spectroscopy of the S_4 and D_{2d} Wafer Octamers in Benzene-$(Water)_8$ and $Benzene_2$-$(Water)_8$," *J Chem Phys* **1998**, *109*, 6601-6614. 10.1063/1.477346
90. Fredericks, S. Y.; Jordan, K. D.; Zwier, T. S., "Theoretical Characterization of the Structures and Vibrational Spectra of Benzene-$(H_2o)_N$ (*N*=1-3) Clusters," *J. Phys. Chem.* **1996**, *100*, 7810-7821. 10.1021/jp9535710

91. Vu, T. H.; Shultz, M. J., "Vibrating Hydroxide in Hydrophobic Solution: The Ion to Keep an Eye On," *Chemical Physics Letters* **2013**, *572*, 13-15. 10.1016/j.cplett.2013.04.038
92. Donaldson, D. J.; Tuck, A. F.; Vaida, V., "Spontaneous Fission of Atmospheric Aerosol Particles," *Phys Chem Chem Phys* **2001**, *3*, 5270-5273. 10.1039/B105215m
93. Donaldson, D. J.; Tuck, A. F.; Vaida, V., "The Asymmetry of Organic Aerosol Fission and Prebiotic Chemistry," *Origins Life Evol. Biosph.* **2002**, *32*, 237-245. 10.1023/A:1016575224538
94. Mizuse, Kenta; Mikami, Naohiko; Fujii, Asuka, "Infrared Spectra and Hydrogen-Bonded Network Structures of Large Protonated Water Clusters H+(H2o)N (N=20–200)," *Angewandte Chemie International Edition* **2010**, *49*, 10119-10122. doi:10.1002/anie.201003662
95. Fujii, Asuka; Mizuse, Kenta, "Infrared Spectroscopic Studies on Hydrogen-Bonded Water Networks in Gas Phase Clusters," *Int Rev Phys Chem* **2013**, *32*, 266-307. 10.1080/0144235x.2012.760836
96. Hamashima, Toru; Mizuse, Kenta; Fujii, Asuka, "Spectral Signatures of Four-Coordinated Sites in Water Clusters: Infrared Spectroscopy of Phenol−(H2o)N (∼20 ≤ N ≤ ∼50)," *The Journal of Physical Chemistry A* **2011**, *115*, 620-625. 10.1021/jp111586p
97. Zasetsky, A. Y.; Khalizov, A. F.; Earle, M. E.; Sloan, J. J., "Frequency Dependent Complex Refractive Indices of Supercooled Liquid Water and Ice Determined from Aerosol Extinction Spectra," *The Journal of Physical Chemistry A* **2005**, *109*, 2760-2764. 10.1021/jp044823c
98. Wieliczka, D. M.; Weng, S. S.; Querry, M. R., "Wedge Shaped Cell for Highly Absorbent Liquids - Infrared Optical-Constants of Water," *Appl. Optics* **1989**, *28*, 1714-1719, Article. 10.1364/ao.28.001714
99. Bisson, P. J.; Shultz, M. J., "Hydrogen Bonding in the Prism Face of Ice I-H Via Sum Frequency Vibrational Spectroscopy," *J Phys Chem A* **2013**, *117*, 6116-6125, Article. 10.1021/jp400129f
100. Wei, X.; Shen, Y. R., "Vibrational Spectroscopy of Ice Interfaces," *Appl Phys B-Lasers O* **2002**, *74*, 617-620. 10.1007/s003400200860
101. Gopalakrishnan, S.; Liu, D. F.; Allen, H. C.; Kuo, M.; Shultz, M. J., "Vibrational Spectroscopic Studies of Aqueous Interfaces: Salts, Acids, Bases, and Nanodrops," *Chem Rev* **2006**, *106*, 1155-1175. 10.1021/cr040361n
102. Gopalakrishnan, S.; Jungwirth, P.; Tobias, D. J.; Allen, H. C., "Air-Liquid Interfaces of Aqueous Solutions Containing Ammonium and Sulfate: Spectroscopic and Molecular Dynamics Studies," *J Phys Chem B* **2005**, *109*, 8861-8872. 10.1021/jp0500236
103. McCoy, A. B.; Guasco, T. L.; Leavitt, C. M.; Olesen, S. G.; Johnson, M. A., "Vibrational Manifestations of Strong Non-Condon Effects in the H3o+Center Dot X-3 (X = Ar, N-2, Ch4, H2o) Complexes: A Possible Explanation for the Intensity in the "Association Band'' in the Vibrational Spectrum of Water," *Phys Chem Chem Phys* **2012**, *14*, 7205-7214. 10.1039/c2cp24110b
104. National Institute of Health, Hsdb: Carbon Tetrachloride; **2018**, https://toxnet.nlm.nih.gov/cgi-bin/sis/search2/r?dbs+hsdb:@term+@rn+@rel+56-23-5.
105. Hasegawa, Y.; Tsusima, S.; Noro, J.; Kusakabe, S., "Relationship between Lewis Acidity of Organic Solvents and Europium(Iii) Extraction in a Synergistic System," *Solvent Extr Ion Exc* **2006**, *24*, 663-676. 10.1080/07366290600760748